Pyrido-imidazodiazepinones as a new class of reversible inhibitors of human kallikrein 7

Dominique P Arama, Feryel Soualmia, Vincent Lisowski, Jean-François Longevial, Elodie Bosc, Ludovic T Maillard, Jean Martinez, Nicolas Masurier, Chahrazade El Amri

PYRIDO-IMIDAZODIAZEPINONES AS A NEW CLASS OF REVERSIBLE INHIBITORS OF HUMAN KALLIKREIN 7

Dominique P. Arama,[a†] Feryel Soualmia,[b†] Vincent Lisowski,[a] Jean-François Longevial,[a] Elodie Bosc,[b] Ludovic T. Maillard,[a] Jean Martinez,[a] Nicolas Masurier,[a]* Chahrazade El Amri[b]*

[a] Institut des Biomolécules Max Mousseron, UMR 5247, CNRS, Université de Montpellier, UFR des Sciences Pharmaceutiques et Biologiques, 15 Avenue Charles Flahault, 34093 Montpellier Cedex 5, France

[b] Sorbonne Universités, UPMC Univ Paris 06, UMR 8256, B2A, Biological Adaptation and Ageing, Integrated Cellular Ageing and Inflammation, Molecular & Functional Enzymology, 7 Quai St Bernard, F-75005 Paris.

[†] These authors contributed equally to the work.

***Corresponding authors:** Nicolas Masurier. Tel: + (33) 4 11 75 96 42, Fax: + (33) 4 11 75 96 41, E-mail: nicolas.masurier@univ-montp1.fr; Chahrazade El Amri. Tel: + (33) 1 44 27 69 52, Fax: + (33) 44 27 51 40 , E-mail: chahrazade.el_amri@upmc.fr

ABBREVIATIONS USED

AMC, 7-amino-4-methylcoumarin; DCM, dichloromethane; DMEM, Dulbecco's Modified Eagle Medium; DMSO, dimethyl sulfoxide; EDCI, 1-Ethyl-3-(3-dimethylaminopropyl)carbodiimide hydrochloride; HOBt, hydroxybenzotriazole; IP, imidazo[1,2-*a*]pyridine; KLK5, kallikrein-related peptidase 5; KLK7, kallikrein-related peptidase 7; KLK8, kallikrein-related peptidase 8; KLK14, kallikrein-related peptidase 14; LEKTI, lymphoepithelial Kazal-type–related inhibitor; PDB, Protein Data Bank; TFA, trifluoroacetic acid; THF, tetrahydrofuran; XTT, 2,3-Bis-(2-Methoxy-4-Nitro-5-sulfophenyl)-2H-Tetrazolium-5-Carboxanilide.

Author contributions

The manuscript was written through contributions of all authors. All authors have given approval to the final version of the manuscript.

Notes

The authors declare no competing financial interest.

Abstract:

The human tissue kallikrein-7 (KLK7) is a chymotryptic serine protease member of tissue kallikrein family. KLK7 is involved in skin homeostasis and inflammation. Excess of KLK7 activity is also associated with tumor metastasis processes, especially in ovarian carcinomas, prostatic and pancreatic cancers. Development of Kallikrein 7 inhibitors is thus of great interest in oncology but also for treating skin diseases. Most of the developed synthetic inhibitors present several drawbacks such as poor selectivity and unsuitable physico-chemical properties for *in vivo* use. Recently, we described a practical sequence for the synthesis of imidazopyridine-fused [1,3]-diazepines. Here, we report the identification of pyrido-imidazodiazepinone core as a new potential scaffold to develop selective and competitive inhibitors of kallikrein–related peptidase 7. Structure-activity relationships (SAR), inhibition mechanisms and selectivity as well as cytotoxicity against selected cancer cell lines were investigated.

Keywords: imidazo[1,2-*a*]pyridine, polyfused heterocycles, diazepinones, serine protease, human tissue kallikrein 7, non-covalent inhibitors

1. Introduction

Tumor invasion and dissemination are complex and multi-step processes involving several key cellular events. Among the many events leading to metastasis, loss of intercellular adhesion is one of the earliest phenomenon, which could lead to cells dissemination [1]. One of the most well characterized mechanisms by which tumor cells can lose adhesion is by up-regulating the expression of extracellular proteases, which are able to cleave one or more of these cellular adhesion proteins. Among these various families of proteases, the human tissue kallikrein serine proteases (KLKs) are known to be over-expressed in various cancers [2, 3].

In this context, kallikrein 7 (KLK7) a chymotryptic enzyme, [4, 5] was reported to be implicated in several tumor metastasis processes, especially in ovarian carcinomas, pancreatic cancers, by the hydrolysis of several cadherin subtypes [6, 7]. KLK7 facilitates metastasis *via* degradation of extracellular matrix components such as fibronectin, desmosomal proteins particularly desmogleins 1 and 2, thus reducing cell-cell adhesion. In prostatic cancers, KLK7 induces epithelial to mesenchymal transition-like changes in prostate carcinoma cells, implying a role in prostate cancer invasion and progression [8]. Furthermore, KLK7 like other kallikreins such as KLK5, KLK8, KLK14 and matriptase plays an important role in normal skin desquamation [9-11]. Such enzymes can hydrolyze extracellular proteins that are part of intercellular adhesion structures such as corneodesmosomes in the stratum corneum [12]. As a consequence, mutation in the *Spink5* gene of LEKTI, the physiological inhibitor of skin kallikreins, is responsible of the Netherton syndrome, a lethal recessive autosomal skin disorder [13]. Recently, in an organotypic human skin culture used as a model system of Netherton Syndrome, it has been shown that genetic inhibition of KLK5 and KLK7 ameliorates epidermal architecture demonstrating the relevance of these two enzymes as targets for treating this disease [14]. On the other hand, KLK7 transgenic mice exhibit a phenotype comparable to psoriasis with cutaneous hyperproliferation and immune cell infiltration [15]. Obese subjects often suffer from psoriatic lesions associated with high levels of adipokines such as chemerine. Beck-Sickinger and coll. have recently shown that KLK7 mediated pro-chemerine processing contributing thus to the development of these psoriatic lesions [16].

Consequently, the development of KLK7 inhibitors to control unopposed proteolytic cascades could represent a potential therapeutic approach to avoid or decrease

metastasis associated with over-expression of KLK7 as well as for treating some skin disorders. Among the reported inhibitors of KLK7 [17], a few consist in peptide derivatives such as chloromethylketones [5], LEKTI-derived peptides [18] and sunflower trypsin inhibitor (SFTI-1) peptide derivatives [19]. More recently some heterocyclic compounds such as natural isocoumarins (as 8,8'-paepalantine) [20] isomannide derivatives [21, 22] or a mercaptobenzimidazolyl-quinazoline derivative [23] have also shown significant activities against KLK7 (Figure 1). All of them are reversible KLK7 inhibitors with moderate activity ($10<IC_{50}<200$ µM). Additionally, some acyl-1,2,4-triazoles were reported to be more potent inhibitors ($0.04<IC_{50}<3.5$ µM), with the ability to form transient covalent complexes (acyl-enzymes) with both KLK7 and KLK5 [24]. Since, most of the identified inhibitors suffer from low selectivity, moderate activity and unsuitable physico-chemical properties for *in vivo* use, the identification of new chemical scaffold for potent and reversible inhibition of KLK7 is thus needed.

A survey of the literature shows that some compounds bearing various heterocyclic pharmacophores can be found as KLK7 inhibitors. However, very few structure-activity relationships were carried out in these series and no co-crystallization of small molecules in the active site of KLK7 has been reported yet. So, crucial determinants for KLK7 specific targeting and inhibition still need to be addressed. All these points prompted us to screen some heterocyclic derivatives from our internal library to study their potential inhibiting activity against KLK7. We report herein the identification of the pyrido-imidazodiazepinone structure as a new potential scaffold to develop selective and competitive KLK7 inhibitors. Structure-activity relationship (SAR), inhibition mechanisms and selectivity, as well as biological evaluations against selected cancer cells were investigated.

2.1. Screening of the diazepinone library and rationale for the synthesis of analogs

Due to the heterogeneity of the heterocyclic scaffolds used to obtain KLK7 inhibition, 65 heterocyclic derivatives from our internal library were chosen for an initial screening (data not shown), including imidazo[1,2-*a*]pyridine (IP) and 1,3-thiazole derivatives, due to our particular interest in these heterocyclic scaffolds [25-31].

Compounds were all tested at the single dose of 50 µM. Among them, a pyrido-imidazodiazepin-5-one showed an inhibition capability higher than 30% (compound

1a, Table 1) (IC_{50} = 57 ± 1.0 µM). The reversibility of the inhibition was evaluated by dilution of the reaction mixture after 15 and 60 min incubation of **1a** with KLK7 at pH8 and 37°C. The enzymatic activity was immediately re stored in agreement with no formation of a covalent bond between the protease and the inhibitor. Lineweaver-Burk double reciprocal plot was used to determine the mechanism of action of compound **1a**. Plots are consistent with a competitive inhibitor behavior with an inhibition constant K_i of 50.6 ± 0.8 µM (see Figure S1, SI). It is worth noting that no noticeable inhibition was observed at 50 µM on other screened serine proteases (KLK5, KLK8 and KLK14), meaning that compound **1a** had a selective action on KLK7.

A SAR study was then initiated, starting from compound **1a**. A set of 30 new pyrido-imidazodiazepinones as well as 9 acyl-IP derivatives, which can be seen as "opened pyrido-imidazodiazepinones", were synthesized and their potency was evaluated against KLK7 and other serine proteases to check selectivity.

2.2. Rationale for the synthesis of optimized diazepinone analogs

Modifications at positions 2, 3, 4 and 5 of the diazepinone core were envisioned (Figure 2). Synthesis of "opened-diazepinones" that possessed a higher flexibility was also investigated.

Pyrido-imidazodiazepinones **1a-ad** were synthesized starting from 2-amino-imidazo-[1,2-*a*]pyridine **5** by selective *C*-3 acylation of the IP nucleus (Scheme 1), using 7 different *N*-Boc amino-acids (Boc-Phe-OH, Boc-D-Phe-OH, Boc-Ala-OH, Boc-Ser(Bn)-OH, Boc-1-Nal-OH, Boc-Tyr(Bn)-OH, Boc-*N*-Me-Phe-OH) according to our previously reported methodology [25, 32]. *C*-3 acylated compounds **4a-g** were isolated in 27% to 88% yield after chromatography on alumina gel. Only traces of the corresponding *N*-acylated derivatives were detected by LC-MS analysis in the crude. After Boc removal in acidic media (by using concentrated hydrochloric acid or a mixture of trifluoroacetic acid/dichloromethane (50/50 v/v)), the resulting 2-amino-3-acyl-imidazo-[1,2-*a*]pyridines **3a-g** were isolated in basic medium, without further purification. Diamines **3a-g** were then successively reacted with a set of aldehydes in chloroform at reflux for one night. Intermediate aminals were then oxidized without isolation, using a mixture of lead tetraacetate and iodine, to lead to pyrido-imidazodiazepinones **1a-1w** that were purified by chromatography on alumina gel.

The pyrido-imidazodiazepine-2,5-dione **1aa** was synthesized by intracarbonylation of diamine **2a**, using 1,1'-carbonyldiimidazole in acetonitrile at 60°C and was isolated in 78% yield [32]. "Opened derivatives" **2a-i** were synthesized by a coupling reaction between the diamine **3a** and a set of commercially available carboxylic acids. Compounds **2a-i** were isolated after purification on an alumina gel column, in 20 to 89% yield. As the diamine **3a** possesses two free amines, the position of the *N*-acylation was investigated. The structure of the resulting coupling product was ascertained by $^{1}H–^{13}C$ HMBC analysis of compound **2a** (R^1 = Ph), which showed a correlation between the CH_α of the phenylalanine residue (5.85 ppm) and the carbonyl signal of the amide (168.7 ppm), which unambiguously proved the *N*-acylation position (see Figure S2, SI). This result confirmed that the aromatic amine in position 2 of the IP nucleus was poorly reactive, as previously observed [32].

Benzyl protected derivatives **1u** and **1v** were treated by a solution of 33% bromhydric acid in acetic acid to offer the corresponding hydroxy derivatives **1ab** and **1ac** in 93 and 99% yields respectively (Scheme 2). The 5-hydroxy derivative **1ad** was obtained as a mixture of diastereoisomers after reduction of compound **1o**, using sodium borohydride in methanol (Scheme 2). Finally, phenol derivatives **1x-z** were obtained by demethylation of the methoxy derivatives **1l-n** in 45-81% yields, using a 1M boron tribromide dichloromethane solution (Scheme 1).

2.3 Structure-activity relationships

As our initial hit (compound **1a**) possesses a chiral center, the significance of the stereochemistry was first investigated. Compared to compound **1a**, which showed a moderate activity (IC_{50} = 57 ± 1 µM), its (*R*)-enantiomer (compound **1e**) led to a decrease of the inhibitory potency (IC_{50} = 95.9 ± 1.7 µM), suggesting that the (*S)* configuration is important to maintain inhibition in these series (Table 1). Modulation of position 2 of the diazepinone ring (R^1) was then studied. Replacement of the aryl group by an aliphatic substituent (compound **1j**) or by a carbonyl group (urea derivative **1aa**) completely abolished the inhibition. Introduction of a phenyl (compound **1f**) or a 3-pyridinyl group (compound **1i**) also led to a loss of KLK7 inhibition. Introduction of an electro-withdrawing group on the *para* position of the phenyl group was also unfavorable (compounds **1g** and **1h**). The inhibiting capacity

was preserved when a *para*-methyl- or a *para*-methoxyphenyl group was present (compounds **1c** or **1d**), although the activity was lower than that of compound **1a** (IC_{50} ~70 µM).

The inhibitory potency observed with compound **1a**, **1c** and **1d** prompted us to further investigate compounds bearing methyl- or methoxyphenyl substituents at R^1. In the methyl series, the *meta* derivative (compound **1b**) was inactive, whereas the 2,4-dimethyl derivative (compound **1k**) showed a weaker activity compared to the two corresponding monomethyl derivatives (**1a** and **1c**). In the methoxy series, the *ortho*-methoxy and the *meta*-methoxyphenyl derivatives (**1l** and **1m**) were inactive. Some inhibition was recovered in the case of 2,5-dimethoxy- and 3,4,5-trimethoxyphenyl derivatives (compounds **1n** and **1p**). The best result was obtained with the 3,4-dimethoxyphenyl derivative **1o**, which showed the higher potency (IC_{50} = 33.5 µM). Whereas some methoxy derivatives exhibited different inhibition potencies, their corresponding phenol derivatives (compounds **1x** to **1z**) were totally inactive. These results suggest that one or several methoxy groups can be involved in hydrogen bonding within the KLK7 active site.

Study of the position 4 of the diazepine ring was then carried out, keeping constant the 2-methylphenyl or the 3,4-dimethoxyphenyl groups at R^1 (Figure 2). Replacement of the benzyl group at R^3 by a methyl group (compounds **1r** and **1s**) or a hydroxymethyl group (compound **1ab**) led to a loss of activity, suggesting that an aromatic group at this position is important for the interaction with the target. Introduction of bulkier groups like 1-naphtylmethyl or 4-benzyloxybenzyle (compounds **1q** and **1v**) or short elongation of the chain (compounds **1t** and **1u**) also led to inactive compounds. A 4-hydroxybenzyl substituent in R^3 was also unfavorable for KLK7 inhibition (compound **1ac**). These results suggest that no modification is tolerated at R^3 and a benzyl group is crucial to obtain KLK7 inhibition.

Finally, methylation of the diazepine *N*-3 or reduction of the carbonyl in position 5 of the most active compound **1o** led to a loss of activity (compounds **1w** and **1ad** respectively). These results suggest that the NH and the carbonyl of the diazepine ring could be implicated in important interactions with the KLK7 binding site.

Finally, “opened diazepinone” series was investigated (compounds **2a-i**). Only two derivatives bearing a benzyl or a 2-methylphenyl substituent at R^1 (compounds **2e** and **2g**, Scheme 1 and Table 1) showed a weak KLK7 inhibition activity (IC_{50}>100 µM). Although the flexibility of compounds **2** was higher than that of the diazepinone

derivatives, which could eventually lead to a better molecular recognition, the increase of conformational entropy in such molecules was unfavorable to the activity. This result suggests that the presence of the diazepine ring is crucial for the inhibition potency.

Starting from compound **1a**, which showed moderate inhibition potency against KLK7 (IC_{50} = 57.0 µM), modifications of positions 2, 3, 4 and 5 of the diazepinone ring were investigated. The SAR study indicated that position 3, 4 and 5 could not be modified to preserve potency. Replacement of the 2-methylphenyl substituent by a 3,4-dimethoxyphenyl group led to a slight increase of the inhibition potency *i.e.* compound **1o** (IC_{50} = 33.5 µM) (Figure 3A), which was selected for further studies.

*2.4. Mechanism of inhibition by compound **1o***

As already observed with compound **1a**, when using compound **1o**, the inhibition was reversed by dilution, in agreement with no formation of a stable covalent adduct between KLK7 and compound **1o** (Figure 3B-C). Lineweaver-Burk double reciprocal plots showed that compound **1o** is a competitive inhibitor indicating that **1o** exclusively binds to the free enzyme (Figure 3C). The K_i value for KLK7 was determined to be 27 ± 1.8 µM corresponding to an acceptable good affinity. The selectivity of compound **1o** was then evaluated against three other human tissue kallikreins (KLK5, KLK8 and KLK14). No significant inhibition was observed at a 50 µM concentration, indicating that compound **1o** was selective for kallikrein 7.

2.5 Structural basis for the inhibition

Models of **1o**/KLK7 complexes were built to corroborate the mechanistic data and to propose some structural basis for the inhibition. The lowest energy model of docking of compound **1o** into KLK7 showed several intermolecular interactions that are represented in Figure 4. The docking results suggest that the IP nucleus of compound **1o** occupies the S_1' pocket of the protease active site, the diazepinone ring being located in the S_1 pocket while the benzyl group is directed toward pocket S_2. The catalytic residue Ser195 of KLK7 might also be implicated in two hydrogen bonds with the two nitrogens of the IP ring. Finally, a key hydrogen bond between Asn 189 and one of the two methoxy groups could explain the higher affinity obtained

with compound **1o**, compared to **1m** that bears only one *meta* methoxy group. This polar contact will be taken into account in the design of further optimized derivatives.

2.6 Cytotoxicity potency towards cancer cell lines

Since KLK7 is involved in tumor progression through its proteolytic activity, we investigated the anticancer potential of the most potent compounds. The cytotoxic effects of 23 derivatives including compound **1o** were evaluated on three human cancer cell lines, *i.e.* the HeLa tumor cell line, the human prostatic PC-3 cell line [33] and the human colorectal adenocarcinoma SW-620 [34]. In particular, a recent study pointed out that aberrant expression of KLK7 in colon cancer cells and tissues is involved in cell proliferation resulting in human colon tumorogenesis [35].

Compounds were first screened at a 100 µM concentration by measuring cellular death using the colorimetric XTT assay. Only derivatives exhibiting cytotoxic effects over 50 % of cell death were retained. Several derivatives were found cytotoxic on cancer cell lines, including compounds **1k**, **1n**, **1o** and **1p** (Table 2) and their EC_{50} determined.

Overall, the HeLa cell line was the most sensitive toward these molecules, followed by PC-3 and SW-620. Interestingly compound **1o** reported as the best KLK7 inhibitor displayed a noticeable cytotoxic effect on both HeLa and PC-3 cells lines. Moreover, one can also notice that **1o** is the only compound that displays an effect, although moderate, on PC-3 cells (EC_{50}= 64.8 µM), while compound **1k** is specific of SW-620 cell line. This selective behavior of **1o** on PC-3 is particularly of great interest since KLK7 is highly expressed in prostate tissue and is believed to participate to cancer progression by its role in the induction of the epithelial-mesenchymal transition on *in vitro* cellular models [8].

3. Conclusion

Starting from an initial screening of 65 in-house heterocyclic derivatives, a pyrido-imidazodiazepinone **1a** was identified to be a moderate inhibitor of KLK7 (IC_{50} = 57 µM and K_i = 50 µM). Enzymatic studies showed that this derivative is a reversible and competitive KLK7 inhibitor. Compound **1a** was shown to have selective action toward

KLK7, when compared to others tested serine proteases, suggesting its potential as a good starting point to design potent selective, competitive and reversible KLK7 inhibitors. A SAR program was then initiated to identify the structural requirement for KLK7 inhibition. Modulation of positions 2, 3, 4 and 5 of the diazepinone ring and "opened diazepine" derivatives were investigated. First, the diazepinone ring has shown to be crucial for KLK7 inhibition. In addition, a (*S*)-benzyl substituent in position 4 of the diazepine, a carbonyl group in position 5, a NH in position 3 gave the best results. The phenyl ring at position 2 tolerates some modulations, *i.e.* substitution by one or two methyl or methoxy groups led to the most potent compounds. This study led to the discovery of compound **1o**, which is approximately twice more active than our initial hit **1a** (K_i = 27 µM compared to 50 µM for compound **1a)**. Moreover some analogs, including compound **1o**, were shown to exhibit a cytotoxic effect, although moderate, against selected colon and prostate cancer cell lines. A detailed study of the cellular events involving KLK7 with optimized compounds could be of great interest to address the correlation between KLK7 inhibition and potential anticancer activity.

4. Experimental

4.1 General

Commercially available reagents and solvents were used without further purification. Reactions were monitored by HPLC using an analytical Chromolith Speed Rod RP-C18 185 Pm column (50x4.6 mm, 5 mm) using a flow rate of 3.0 mL/min, and a gradient of 100/0 to 0/100 eluents A/B over 5 min, in which eluents A=H_2O/0.1% TFA and B=CH_3CN/0.1% TFA. Detection was at 214 nm using a Photodiode Array Detector. Retention times are reported as follows: Tr (min). ^{1}H and ^{13}C NMR spectra were recorded at room temperature in deuterated solvents. Chemical shifts (δ) are given in parts per million relative to the solvent [^{1}H: δ ($CDCl_3$) = 7.26 ppm, (DMSO d_6) = 2.50 ppm; (CD_3OD) = 3.31 ppm; ^{13}C: δ ($CDCl_3$) = 77.2 ppm, (DMSO d_6) = 39.5 ppm; (CD_3OD) = 49.0 ppm]. The following abbreviations are used to designate the signal multiplicities: s (singlet), d (doublet), t (triplet), q (quartet), m (multiplet), bs (broad singlet). Analytical thin-layer chromatography (TLC) was performed using aluminium-backed silica gel plates coated with a 0.2 mm thickness of silica gel or with aluminium oxide 60 F254, neutral. LC-MS spectra (ESI) were recorded on a HPLC using an analytical Chromolith Speed Rod RP-C18 185

Pm column (50x4.6 mm, 5 mm); solvent A, H_2O/HCOOH 0.1%; solvent B, CH_3CN/HCOOH 0.1%; gradient, 0% solvent B to 100% solvent B in solvent A in 3 min; flow rate, 3.0 mL min-1. High-resolution mass spectrometric analyses were performed with a time-of-flight mass spectrometer fitted with an electrospray ionisation source. All measurements were performed in the positive ion mode. Melting points (mp) are uncorrected and were recorded on a capillary melting point apparatus.

Compounds **5**, **3a-c**, **4a-c, 1a-d**, **1f-j** and **1aa** were synthesized according to our previous reported procedures and the spectral characteristics were in agreement with the published data [25, 32].

4.2 *Synthesis of compounds **4d-g***

To a suspension of 0.5 g of trifluoro-*N*-imidazo[1,2-*a*]pyridin-2-ylacetamide (2.18 mmol) in 9 mL of an aqueous 5 N sodium hydroxide solution was added 0.5 mL of THF. The solution was stirred at 40°C for 2 h. The solution was extracted with dichloromethane (3 x 20 mL). The organic layer was dried over Na_2SO_4, filtered, and the solvent was removed *in vacuo*. The residue was dissolved in 20 mL of DCM and Boc-1-Nal-OH (2.4 mmol, 1.1 equiv.) [or Boc-Tyr(Bn)-OH or Boc-Ser(Bn)-OH or Boc-*N*-Me-Phe-OH], HOBt (325 mg, 2.4 mmol, 1.1 equiv.), EDCI (460 mg, 2.4 mmol, 1.1 equiv.) and triethylamine (334 µL, 2.4 mmol, 1.1 equiv.) were added at 0°C. The solution was stirred at rt for 4 h. The solution was then washed with saturated $NaHCO_3$ aqueous solution (2 x 50 mL). The organic layer was dried over Na_2SO_4, filtered, and the solvent was concentrated *in vacuo*. The residue was purified by chromatography (Al_2O_3, DCM/EtOH 99/1 v/v) to offer compounds **4d-g**.

*4.2.1 (2S)-2-Boc-amino-1-(2-aminoimidazo[1,2-*a*]pyridin-3-yl)-3-(1-naphtyl)propan-1-one (**4d**)*

Yellow solid (m = 0.297 g, 63.5%); mp: 208.0-210.2°C; $[\alpha]_D^{20}$ = +3.6° (*c* 0.5, $CHCl_3$); ^{1}H NMR ($CDCl_3$, 300 MHz): δ ppm 1.33 (s, 9H), 3.50-3.70 (m, 2H), 5.46 (t, 1H, *J*= 8.4 Hz), 5.57 (d, 1H, *J* = 9.3 Hz), 5.86 (bs, 2H), 6.85 (bs, 1H), 7.29-7.49 (m, 6H), 7.66 (d, 1H, *J* = 7.8 Hz), 7.78 (d, 1H, *J* = 7.8 Hz), 8.12 (d, 1H, *J* = 8.7 Hz), 9.60 (bs, 1H) ; ^{13}C NMR ($CDCl_3$, 75 MHz): δ ppm 28.1 (3C), 35.6, 54.7, 80.3, 113.0, 113.9, 115.8, 123.3, 125.1, 125.5, 126.2, 127.3, 127.5, 128.7, 129.1, 130.7, 132.0, 132.7, 133.7, 147.2, 156.4, 158.1, 184.8; FT-IR (cm^{-1}) : 3329, 3189, 2971, 1679, 1588, 1497, 1449, 1366,

1342, 1253, 1162, 1055, 762 ; HPLC, Tr= 1.81 min; MS (ESI^+): m/z 431.3 $[M+H]^+$; HRMS calcd for $C_{25}H_{27}N_4O_3$ 431.2083, found 431.2085.

*4.2.2 (2S)-2-Boc-amino-1-(2-aminoimidazo[1,2-*a*]pyridin-3-yl)-3-benzyloxy-propan-1-one (**4e**)*

Yellow solid (m = 0.488 g, 54.5%); mp: 123-124℃; $[\alpha]_D^{20}$ = +3.66° (*c* 1.5, $CHCl_3$); ^1H NMR ($CDCl_3$, 300 MHz): δ ppm 1.46 (s, 9H), 3.77 (t, 1H, *J* = 9.0 Hz), 3.89 (dd, 1H, *J* = 6.0, 9.0 Hz), 4.54 (s, 2H), 5.30 (dd, 1H, *J* = 6.0, 12.0 Hz), 5.79 (d, 1H, *J* = 9.0 Hz), 5.89 (bs, 2H), 6.90 (t, 1H, *J* = 9.0 Hz), 7.21 - 7.33 (m, 5H), 7.37-7.47 (m, 2H), 9.62 (d, 1H, *J* = 6.0 Hz); ^{13}C NMR ($CDCl_3$, 75 MHz): δ ppm 28.4 (3C), 54.1, 71.7, 73.6, 80.2, 109.1, 113.1, 114.3, 127.7 (2C), 127.9, 128.4 (2C), 129.4, 130.7, 137.2, 147.8, 155.8, 159.1, 184.1; FT-IR (cm^{-1}) : 3356, 3204, 2970, 2849, 1678, 1631, 1578, 1456, 1297, 1163, 1057, 985, 763, 699 ; HPLC, Tr= 1.71 min; MS (ESI^+): m/z 411.3 $[M+H]^+$; HRMS calcd for $C_{22}H_{27}N_4O_4$ 411.2032, found 411.2035.

*4.2.3 (2S)-2-Boc-amino-1-(2-aminoimidazo[1,2-*a*]pyridin-3-yl)-3-(4-benzyloxy-phenyl)propan-1-one (**4f**)*

Light yellow solid (m = 0.561 g, 53%); mp: 108.1-120.0℃; $[\alpha]_D^{20}$ = +64.08° (*c* 0.76, $CHCl_3$); ^1H NMR ($CDCl_3$, 300 MHz): δ ppm 1.36 (s, 9H), 2.95 (dd, 1H, *J* = 15.0, 9.0 Hz), 3.11 (dd, 1H, *J* = 15.0, 9.0 Hz), 4.95 (s, 2H), 5.20 (bs, 1H), 5.50 (d, 1H, *J* = 6.0 Hz), 5.89 (bs, 1H), 6.83 (m, 3H), 7.12 (d, 2H, *J* = 9.0 Hz), 7.27-7.42 (m, 8H), 9.60 (bs, 1H) ; ^{13}C NMR ($CDCl_3$, 100 MHz): δ ppm 28.5 (3C), 38.0, 55.7, 70.2, 80.7, 108.5, 113.2, 114.3, 115.0 (2C), 127.6 (2C), 128.1, 128.7 (2C), 129.3, 129.4, 130.4 (2C), 130.8, 137.3, 147.7, 156.7, 157.8, 158.7, 185.1 ; FT-IR (cm^{-1}): 3330, 3207, 2976, 1681, 1581, 1510, 1496, 1450, 1366, 1343, 1242, 1161, 1074, 1045, 1013, 857, 762, 735, 695 ; HPLC, Tr= 3.38 min; MS (ESI^+): m/z 487.3 $[M+H]^+$; HRMS calcd for $C_{28}H_{31}N_4O_4$ 487.2346, found 487.2345.

*4.2.4 (2S)-2-Boc-*N*-methylamino-1-(2-aminoimidazo[1,2-*a*]pyridin-3-yl)-3-(4-phenyl)propan-1-one (**4g**)*

Yellow solid (m = 0.578 g, 67%), mp: 58.5 – 61.4℃; $[\alpha]_D^{20}$ = -164.9° (*c* 1.05, $CHCl_3$) ; ^1H NMR ($CDCl_3$, 400 MHz): δ ppm 1.31 (s, 9H), 2.83 (s, 3H), 3.12 (m, 2H), 5.63 (t, 1H, *J* = 8.0 Hz), 6.27 (s, 2H), 6.82 (t, 1H, *J* = 8.0 Hz), 7.14 (t, 1H, *J* = 8.0 Hz), 7.22-

7.29 (m, 5H), 7.37 (t, 1H, *J* = 8.0 Hz), 9.75 (bs, 1H) ; ^{13}C NMR ($CDCl_3$, 100 MHz): δ ppm 28.2 (3C), 29.7, 34.5, 59.2, 81.0, 108.5, 112.9, 113.9, 126.5, 128.4 (2C), 129.4, 129.8 (2C), 130.8, 137.5, 147.8, 157.7, 158.1, 182.3 ; FT-IR (cm^{-1}) : 3331, 3216, 2974, 2928, 1666, 1627, 1591, 1524, 1496, 1444, 1387, 1366, 1341, 1264, 1140, 1060, 1012, 951, 849, 760, 697 ; HPLC, Tr= 3.36 min ; MS (ESI^+): m/z 395.0 $[M+H]^+$; HRMS calcd for $C_{22}H_{27}N_4O_3$ 395.2083, found 395.2081.

4.3 *General procedure for the synthesis of diazepinones*

A solution of compound **4a-f** (0.33 mmol) in 12N aqueous hydrochloric acid (3 mL) was stirred a room temperature for 1 h. The solution was treated with 28% aqueous ammonia solution until pH 12 and then extracted with chloroform (3 x 20 mL). The organic layer was dried over Na_2SO_4, filtered, and the solvent was concentrated *in vacuo* to lead compounds **3a-f**, which were used in the next step without further purification. To a solution of **3a-f** in chloroform (2 mL) was added 1 equiv. of the appropriate aldehyde. The solution was stirred at 60°C for 6 h. After cooling, the mixture was pooled to a solution of iodine (91 mg, 0.36 mmol, 1.1 equiv) in chloroform (4 mL). Finally, a solution of lead tetraacetate (161 mg, 0.36 mmol, 1.1 equiv) in chloroform (6 mL) was added. The solution was stirred at room temperature for 1−6 h (monitoring by TLC). The solution was washed with 10% m/v sodium thiosulfate aqueous solution (3 × 30 mL) and then with saturated $NaHCO_3$ aqueous solution (2 × 30 mL). The organic layer was dried over Na_2SO_4, filtered, and the solvent was evaporated *in vacuo*. The residue was purified by chromatography on alumina, eluted by DCM/EtOH 99/1 v/v.

4.3.1 *(4*R*)-4-benzyl-2-(2-methylphenyl)-3,4-dihydro-5H-pyrido[1',2':1,2]imidazo[4,5-*d*][1,3]diazepin-5-one (**1e**)*

Yellow solid (m = 0.117 g, 37.5%); mp: 135.5-136.5°C; $[\alpha]_D^{20}$ = +9.1° (*c* 1, $CHCl_3$); other data were in agreement with those published for its *S* enantiomer.[25]

4.3.2 *(4S)-4-benzyl-2-(2,4-dimethylphenyl)-3,4-dihydro-5H-pyrido[1',2':1,2]imidazo [4,5-*d*][1,3]diazepin-5-one (**1k**)*

Yellow solid (m = 0.080 g, 38%); mp: 107.0-108.0°C; $[\alpha]_D^{20}$ = -20.2° (*c* 1, $CHCl_3$) ; ^{1}H NMR ($CDCl_3$, 300 MHz): δ ppm 2.12 (s, 3H), 2.21 (s, 3H), 3.25 (dd, 1H, *J* = 9.0, 12.0 Hz), 3.51 (dd, 1H, *J* = 6.0, 12.0 Hz), 4.20 (bs, 1H), 5.93 (bs, 1H), 6.89 (m, 3H), 7.19

(m, 8H), 9.40 (d, 1H, *J* = 6.0 Hz); ^{13}C NMR ($CDCl_3$, 75 MHz): δ ppm 20.4, 21.4, 36.9, 60.5, 111.9, 113.9, 115.2, 126.5, 126.8 (2C), 128.4, 128.5 (2C), 129.9, 130.1, 131.6, 132.0, 138.5, 141.5, 145.4, 152.6, 152.7, 156.8, 159.2, 181.6 ; FT-IR (cm^{-1}) : 3027, 2956, 2923, 1732, 1645, 1633, 1556, 1523, 1480, 1421, 1335, 1299, 1247, 1122, 1094, 1073, 1044, 949, 898, 820, 761 ; HPLC, Tr= 1.60 min ; MS (ESI^+): m/z 395.1 $[M+H]^+$; HRMS calcd for $C_{25}H_{23}N_4O$ 395.1872, found 395.1858.

4.3.3 *(4S)-4-benzyl-2-(2-methoxyphenyl)-3,4-dihydro-5H-pyrido[1',2':1,2]imidazo[4,5-*d*][1,3]diazepin-5-one (**1l**)*

Yellow solid (m = 0.255 g, 72%); mp: 104.0-105.0℃; $[\alpha]_D^{20}$ = -24.86° (*c* 1.5, $CHCl_3$) ; ^{1}HNMR ($CDCl_3$, 300 MHz): δ ppm 3.09 (m, 1H), 3.32 (m, 1H), 3.60 (s, 3H), 4.24 (dd, 1H, *J*= 9.0, 6.0 Hz), 6.80 (d, 1H, *J* = 9.0 Hz), 6.99 (m, 2H), 7.20-7.24 (m, 6H), 7.35-7.46 (m, 3H), 8.22 (bs, 1H), 9.50 (d, 1H, *J* = 6.0 Hz); ^{13}C NMR ($CDCl_3$, 75 MHz): δ ppm 36.5, 56.0, 66.4, 111.6, 112.6, 113.8, 116.0, 121.5, 122.3, 126.7 (2C), 128.6, 128.7 (2C), 129.8, 129.9, 130.6, 133.1, 133.3, 138.1, 146.5, 156.3, 158.1, 181.9 ; FT-IR (cm^{-1}) : 660, 680, 694, 722, 741, 842, 904, 921, 978, 1024, 1042, 1073, 1106, 1126, 1163, 1182, 1240, 1269, 1297, 1335, 1453, 1481, 1524, 1562, 1601, 1622, 1645, 2971 ; HPLC, Tr= 1.34 min ; MS (ESI^+): m/z 397.1 $[M+H]^+$; HRMS calcd for $C_{24}H_{21}N_4O_2$ 397.1665, found 397.1655.

4.3.4 *(4S)-4-benzyl-2-(3-methoxyphenyl)-3,4-dihydro-5H-pyrido[1',2':1,2]imidazo[4,5-*d*][1,3]diazepin-5-one (**1m**)*

Brown dough (m = 0.130 g, 94%); mp: 66.0-67.0℃; $[\alpha]_D^{20}$ = +3.2° (*c* 0.375, DMSO); ^{1}H NMR (DMSO-d_6, 400 MHz): δ ppm 2.96 (dd, 1H, *J* = 12.0, 8.0 Hz), 3.26 (dd, 1H, *J*= 12.0, 4.0 Hz), 3.75 (s, 3H), 4.56 (dd, 1H, *J* = 12.0, 4.0 Hz), 6.97-7.03 (m, 1H), 7.13-7.50 (m, 10H), 7.90-7.97 (m, 2H), 9.54 (d, 1H, *J* = 8.0 Hz) ; ^{13}C NMR (DMSO-d_6, 100 MHz): δ ppm 34.7, 55.4, 63.7, 111.7, 114.8, 115.1, 116.4, 120.2, 122.7, 127.0 (2C), 128.5, 128.6 (2C), 129.4, 129.8, 133.4, 136.1, 143.4, 150.1, 158.0, 158.3, 159.0, 180.3 ; FT-IR (cm^{-1}) : 2963, 1648, 1596, 1580, 1519, 1488, 1466, 1454, 1417, 1332, 1292, 1259, 1177, 1129, 1029, 762 ; HPLC, Tr= 1.42 min ; MS (ESI^+): m/z 397.1 $[M+H]^+$; HRMS calcd for $C_{24}H_{21}N_4O_2$ 397.1665, found 397.1654.

4.3.5 *(4S)-4-benzyl-2-(2,5-dimethoxyphenyl)-3,4-dihydro-5H-pyrido[1',2':1,2]imidazo [4,5-*d*][1,3]diazepin-5-one (**1n**)*

Yellow solid (m = 0.089 g, 39%); mp: 155.0-156.0℃; $[\alpha]_D^{20}$ = -12.0° (c 1, $CHCl_3$) ; ^{1}H NMR ($CDCl_3$, 300 MHz): δ ppm 3.13 (m, 1H), 3.31 (m, 1H), 3.59 (s, 3H), 3.79 (s, 3H), 4.25 (m, 1H), 6.76 (d, 1H, *J* = 9.0 Hz), 6.92-7.03 (m, 2H), 7.16-7.24 (m, 6H), 7.47 (t, 2H, *J* = 6.0 Hz), 7.80 (bs, 1H), 9.54 (d, 1H, *J* = 6.0 Hz); ^{13}C NMR ($CDCl_3$, 75 MHz): δ ppm 36.5, 54.2 (from ^{1}H-^{13}C HSQC correlation), 56.2, 56.7, 112.6, 113.4, 113.9, 116.0, 120.3, 126.5, 126.7, 128.6, 128.7, 129.8, 129.9, 130.7, 134.2, 138.0, 143.2, 146.4, 152.5, 154.1, 182.0; FT-IR (cm^{-1}) : 3019, 2928, 2832, 1647, 1635, 1565, 1526, 1480, 1460, 1448, 1412, 1335, 1318, 1268, 1240, 1220, 1178, 1099, 1074, 1042, 1024, 961, 941, 902, 870, 813, 755, 740, 697, 676,; HPLC, Tr= 1.66 min ; MS (ESI^+): m/z 427.1 $[M+H]^+$; HRMS calcd for $C_{25}H_{23}N_4O_3$ 427.1770, found 427.1778.

4.3.6 *(4S)-4-benzyl-2-(3,4-dimethoxyphenyl)-3,4-dihydro-5H-pyrido[1',2':1,2]imidazo [4,5-d][1,3]diazepin-5-one (**1o**)*

Yellow solid (m = 0.115 g, 77%); mp: 136.0-137.0℃; $[\alpha]_D^{20}$ = +36.8° (*c* 1, DMSO); ^{1}H NMR (DMSO-d_6, 400 MHz): δ ppm 2.90-3.17 (m, 3H), 3.70 (s, 3H), 3.81 (s, 3H), 4.15 (bs, 1H), 6.97 (d, 1H, *J* = 8.0 Hz), 7.14 (bs, 1H), 7.17 (td, 1H, *J* = 8.0, 4.0 Hz), 7.24-7.32 (m, 6H), 7.64-7.70 (m, 2H), 9.47 (d, 1H, *J* = 8.0 Hz); ^{13}C NMR (DMSO-d_6, 100 MHz): δ ppm 35.1, 54.9, 55.4, 55.6, 108.4, 110.8, 112.3, 113.6, 115.7, 122.6, 125.3, 126.5, 127.3 (2C), 127.8, 128.3 (2C), 129.5, 129.7, 130.5, 136.7, 146.1, 147.9, 151.8, 180.1; FT-IR (cm^{-1}) : 2925, 2853, 699, 739, 764, 814, 840, 937, 973, 1021, 1080, 1140, 1173, 1231, 1261, 1335, 1435, 1462, 1496, 1510, 1557, 1599, 1623 ; HPLC, Tr= 1.33 min ; MS (ESI^+): m/z 427.0 $[M+H]^+$; HRMS calcd for $C_{25}H_{23}N_4O_3$ 427.1770, found 427.1774.

4.3.7 *(4S)-4-benzyl-2-(3,4,5-trimethoxyphenyl)-3,4-dihydro-5H-pyrido[1',2':1,2] imidazo[4,5-d][1,3]diazepin-5-one (**1p**)*

Yellow solid (m = 0.192g, 59%); mp: 119.0-120.0℃; $[\alpha]_D^{20}$ = +22.98° (*c* 0.87, $CHCl_3$) ; ^{1}H NMR ($CDCl_3$, 300 MHz): δ ppm 3.35 (bs, 1H), 3.70 (s, 6H), 3.82 (s, 4H),4.31 (bs, 1H), 6.82 (bs, 2H), 7.03 (td, 1H, *J* = 14.5, 6.9 Hz), 7.33 (m, 8H), 9.58 (bs, 1H) ; ^{13}C NMR ($CDCl_3$, 100 MHz): δ ppm 29.9, 36.5, 56.4 (2C), 61.0, 105.1, 106.8 (2C), 112.1, 114.2, 115.9, 127.1, 128.8 (2C), 128.9, 129.9 (2C), 130.9, 141.7, 146.2, 153.1 (2C), 159.7, 166.5, 182.3 ; FT-IR (cm^{-1}) : 2937, 2836, 1719, 1625, 1559, 1462, 1409, 1333,

1232, 1122, 1000, 763, 700 ; HPLC,Tr= 1.50 min ; MS (ESI^+): m/z 457.1 $[M+H]^+$; HRMS calcd for $C_{25}H_{25}N_4O_4$ 457.1876, found 457.1874.

4.3.8 *(4S)-4-(1-naphthyl)methyl-2-(2-methylphenyl)-3,4-dihydro-5H-pyrido[1',2':1,2] imidazo[4,5-d][1,3]diazepin-5-one (**1q**)*

Yellow solid (m = 0.105 g, 45%); mp: 134.4-135.4℃; $[\alpha]_D^{20}$ = +29.4° (*c* 0.5, $CHCl_3$); ^1H NMR ($CDCl_3$, 300 MHz): δ ppm 2.20 (s, 3H), 3.71 (bs, 1H), 4.18 (bs, 2H), 6.9 (t, 1H, *J* = 9.0 Hz), 7.12-7.19 (m, 4H), 7.30-7.48 (m, 5H), 7.61 (bs, 1H), 7.76 (d, 1H, *J* = 9.0 Hz), 7.85 (dd, 2H, *J* = 9.0, 3.0 Hz), 8.05 (dd, 1H, *J* = 9.0, 3.0 Hz), 9.48 (d, 1H, *J* = 9.0 Hz); ^{13}C NMR ($CDCl_3$, 75 MHz): δ ppm 20.4, 33.9, 53.5 (from ^1H-^{13}C HSQC correlation), 113.7, 115.3, 120.2, 121.8, 124.0, 125.6, 126.0 (2C), 127.3, 128.4, 128.6, 128.9, 130.3, 130.7, 131.2, 132.3 (2C), 134.1, 135.6, 138.4, 145.6, 156.1, 157.4, 159.5, 181.2 ; FT-IR (cm^{-1}) : 2927, 1691, 1632, 1556, 1523, 1480, 1421, 1335, 1301, 1247, 1162, 1124, 760 ; HPLC, Tr= 1.69 min ; MS (ESI^+): m/z 431.2 $[M+H]^+$; HRMS calcd for $C_{28}H_{23}N_4O$ 431.1872, found 431.1873.

4.3.9 *(4S)-4-methyl-2-(2-methylphenyl)-3,4-dihydro-5H-pyrido[1',2':1,2]-imidazo[4,5-d][1,3]diazepin-5-one (**1r**)*

White solid (m = 0.023 g, 8%); mp: 124.0℃-125.0℃; $[\alpha]_D^{20}$ = -41.04° (*c* 0.57, $CHCl_3$); ^1H NMR ($CDCl_3$, 400 MHz): δ ppm 1.68 (bs, 3H), 2.42 (s, 3H), 4.09-4.16 (m, 1H), 6.93 (t, 1H, *J* = 8.0 Hz), 7.17-7.35 (m, 6H), 7.61 (d, 1H, *J* = 8.0 Hz), 9.48 (d, 1H, *J* = 8.0 Hz); ^{13}C NMR ($CDCl_3$, 100 MHz): δ ppm 16.6, 20.3, 63.4, 111.7, 113.4, 114.8, 126.0, 128.2, 130.0 (2C), 130.5, 131.0, 131.1, 135.6, 137.9, 145.4, 154.6, 182.5; FT-IR (cm^{-1}): 2929, 1645, 1627, 1558, 1523, 1482, 1419, 1337, 1300, 1248, 757; HPLC, Tr= 1.14 min; MS (ESI^+): m/z 305.3 $[M+H]^+$; HRMS calcd for $C_{18}H_{17}N_4O$ 305.1402, found 305.1404.

4.3.10 *(4S)-4-methyl-2-(3,4-dimethoxyphenyl)-3,4-dihydro-5H-pyrido[1',2':1,2] imidazo[4,5-d][1,3]diazepin-5-one (**1s**)*

Brown solid (m = 0.006 g, 6%); mp: 102.0-103.0℃; $[\alpha]_D^{20}$ = -40.8° (*c* 0.25, $CHCl_3$); ^1H NMR ($CDCl_3$, 300 MHz): δ ppm 1.61 (bs, 3H), 3.90 (s, 3H), 3.94 (s, 3H), 4.66 (bs, 1H), 6.84 (d, 1H, *J* = 9.0 Hz), 6.97 (t, 1H, *J* = 9.0 Hz), 7.45-7.48 (m, 3H), 7.67 (bs, 1H), 8.07 (bs, 1H), 9.53 (d, 1H, *J* = 6.0 Hz); ^{13}C NMR ($CDCl_3$, 75 MHz): δ ppm 16.4,

56.1, 56.2, 56.3, 109.7, 110.6, 112.3, 113.7, 115.9, 116.1, 117.6, 121.5, 128.0, 128.6, 129.9, 130.2, 149.3, 152.5, 183.1; HPLC, Tr= 1.10 min; MS (ESI^+): m/z 351.2 $[M+H]^+$; HRMS calcd for $C_{19}H_{19}N_4O_3$ 351.1457, found 351.1458.

4.3.11 *(4S)-4-benzyloxymethyl-2-(2-methylphenyl)-3,4-dihydro-5H-pyrido[1',2':1,2] imidazo[4,5-*d*][1,3]diazepin-5-one (**1t**)*

Yellow solid (m = 0.036 g,31%); mp: 102.0-103.0℃; $[\alpha]_D^{20}$ = -8.25° (*c* 0.4, $CHCl_3$); ^1H NMR ($CDCl_3$, 300 MHz): δ ppm 2.41 (bs, 3H), 4.10 (bs, 1H), 4.25 (dd, 1H, *J* = 9.0, 6.0 Hz), 4.54 (m, 1H), 4.71 (bs, 2H), 6.93 (t, 1H, *J* = 6.0 Hz), 7.17 (dd, 3H, *J* = 9.0, 6.0 Hz), 7.29-7.39 (m, 8H), 7.63 (d, 1H, *J* = 6.0 Hz), 9.47 (d, 1H, *J* = 6.0 Hz); ^{13}C NMR ($CDCl_3$, 100 MHz): δ ppm 29.8, 69.9, 73.7, 73.8, 113.8, 115.3, 126.0, 126.1, 126.2, 127.8 (2C), 128.0, 128.5 (2C), 128.6, 130.4, 130.8, 130.9, 131.2, 131.3, 135.6, 138.3, 138.4, 145.7, 180.6; FT-IR (cm^{-1}) : 3055, 3023, 2923, 2853, 2246, 1634, 1558, 1523, 1421, 1336, 1250, 1097, 907, 762, 729, 696 ; HPLC, Tr= 1.55 min; MS (ESI^+): m/z 411.3 $[M+H]^+$; HRMS calcd for $C_{25}H_{23}N_4O_2$ 411.1821, found 411.1825.

4.3.12 *(4S)-4-benzyloxymethyl-2-(3,4-dimethoxyphenyl)-3,4-dihydro-5H-pyrido [1',2':1,2]imidazo[4,5-*d*][1,3]diazepin-5-one (**1u**)*

Yellow solid (m = 0.069 g, 47%); mp: 80.5-81.5℃; $[\alpha]_D^{20}$ = -27.0° (*c* 0.8, $CHCl_3$) ; ^1H NMR ($CDCl_3$, 300 MHz): δ ppm 3.82 (s, 3H), 3.89 (bs, 5H), 4.26 (bs, 1H), 4.60 (bs, 2H), 6.79 (d, 1H, *J* = 6.0 Hz), 6.98 (t, 1H, *J* = 6.0 Hz), 7.30-7.52 (m, 8H), 7.66 (bs, 2H), 9.53 (bs,1H); ^{13}C NMR ($CDCl_3$, 100 MHz): δ ppm 55.8 (2C), 60.6, 67.1, 73.5, 110.2, 111.7, 113.5, 116.5, 121.9, 122.9, 127.9 (2C), 128.4 (2C), 130.1, 137.0, 142.5, 147.1, 148.9, 150.8, 152.3, 158.5, 159.0, 160.7, 181.1; FT-IR (cm^{-1}) : 3216, 2931, 2853, 1622, 1559, 1508, 1462, 1427, 1334, 1233, 1132, 1094, 1020, 764, 738, 697; HPLC, Tr= 1.54 min; MS (ESI^+): m/z 457.3 $[M+H]^+$; HRMS calcd for $C_{26}H_{25}N_4O_4$ 457.1876, found 457.1873.

4.3.13 *(4S)-4-(4-benzyloxy)benzyl-2-(3,4-dimethoxyphenyl)-3,4-dihydro-5H-pyrido [1',2':1,2]imidazo[4,5-*d*][1,3]diazepin-5-one (**1v**)*

Orange solid (m = 0.134g, 65%); mp: 129.0-130.0℃; $[\alpha]_D^{20}$ = +3.93° (*c* 1.5, $CHCl_3$); ^1H NMR ($CDCl_3$, 300 MHz): δ ppm 3.71-3.78 (bs, 4H), 3.81-3.88 (bs, 4H), 4.18 (bs,

1H), 5.02 (s, 2H), 6.64 (d, 1H, *J* = 6.0 Hz), 6.90 (d, 2H, *J* = 9.0 Hz), 6.98 (t, 1H, *J* = 6.0 Hz), 7.19-7.45 (m, 12H), 9.53 (d, 1H, *J* = 6.0 Hz); ^{13}C NMR ($CDCl_3$, 100 MHz): δ ppm 30.2, 31.4, 35.8, 56.5, 70.6, 110.8, 112.8, 113.1, 113.2, 114.4, 115.4, 115.6 (2C), 116.5, 123.0, 127.4, 127.9 (2C), 128.5, 129.1 (2C), 131.0, 131.2 (2C), 132.5, 137.4, 146.7, 149.4, 153.1, 153.8, 158.4, 183.0; FT-IR (cm^{-1}) : 3031, 2932, 2837, 1730, 1624, 1557, 1510, 1461, 1425, 1335, 1260, 1231, 1140, 1020, 811, 764, 736, 695; HPLC, Tr= 3.08 min; MS (ESI^+): m/z 533.2 $[M+H]^+$; HRMS calcd for $C_{32}H_{29}N_4O_4$ 533.2194, found 533.2189.

*4.3.14 (S)-4-benzyl-2-(3,4-dimethoxyphenyl)-3-methyl-3H-pyrido[1',2':1,2]imidazo [4,5-*d*][1,3]diazepin-5(4H)-one* ***(1w)***

Yellow solid (m=0.120 g, 54%); mp: 217.0-218.0℃; $[\alpha]_D^{20}$ = +174.1° (*c* 0.39, $CHCl_3$) ; ^{1}H NMR ($CDCl_3$, 300 MHz): δ ppm 2.69 (bs, 1H), 2.73 (bs, 1H), 2.98 (s, 3H), 3.71 (s, 3H), 3.86 (s, 3H), 4.32 (bs, 1H), 6.67 (d, 1H, *J* = 8.4 Hz), 6.85 (s, 2H), 6.98 (td, 1H, *J* = 5.7, 6.9 Hz), 7.28 (bs, 5H), 7.50 (td, 1H, *J* = 7.1, 14.6 Hz), 7.69 (d, 1H, *J* = 8.9 Hz), 9.55 (d, 1H *J* = 6.9 Hz); ^{13}C NMR ($CDCl_3$, 100 MHz): δ ppm 29.9, 34.3, 45.6, 56.2, 72.4, 110.3, 112.8, 113.7, 113.9, 116.9, 125.4, 127.4, 128.4 (2C), 128.6, 129.0 (2C), 129.6, 130.4, 136.7, 147.4, 148.5, 151.95, 158.5, 160.7, 183.0; FT-IR (cm^{-1}) : 3055, 3000, 2928, 2837, 1624, 1543, 1515, 1478, 1455, 1436, 1359, 1340, 1262, 1126, 1019, 879, 817, 757, 706; HPLC, Tr= 2.45 min; MS (ESI^+): m/z 441.2 $[M+H]^+$; HRMS calcd for $C_{26}H_{25}N_4O_3$ 441.1931, found 429.1927.

4.4 *General procedure for synthesis of phenol derivatives* ***1x-z***

To a solution of compound ***1l-n*** (100 mg) in DCM (10 mL) at 0℃, was added a solution of boron tribromide 1M in DCM (6 equiv.). The resulting mixture was stirred at rt for 3h (monitoring by TLC). The reaction was quenched by adding distilled water (30mL). The solution was extracted with ethyl acetate; the organic layer was dried over Na_2SO_4, filtered and the solvent was removed under reduced pressure. The residue was dissolved in ethyl acetate and precipitated by addition of diethyl ether. The precipitate was then filtered over Buchner funnel and washed with diethyl ether to afford phenol derivatives ***1x-z.***

4.4.1 *(4S)-4-benzyl-2-(2-hydroxyphenyl)-3,4-dihydro-5H-pyrido[1',2':1,2]imidazo-[4,5-d][1,3]diazepin-5-one (**1x**)*

Brown solid (m = 0.117 g, 81%); mp: 187.0-188.0°C; $[\alpha]_D^{20}$ = +35.2° (*c* 0.25, DMSO); ^{1}H NMR (DMSO-d_6, 300 MHz): δ ppm 2.90 (m, 1H), 3.15 (m, 1H), 4.41 (m, 1H), 6.70 (m, 1H), 6.86 (m, 1H), 7.17 (m, 9H), 7.35 (m, 1H), 7.80 (bs, 2H), 9.47 (m, 1H); ^{13}C NMR (DMSO-d_6, 75 MHz): δ ppm 35.0, 64.0, 112.1, 114.8, 114.9, 116.1, 117.6, 118.2, 126.8, 128.0, 128.4 (2C), 129.4 (2C), 131.6, 134.7, 136.5, 145.8, 150.1, 152.8, 159.1, 160.9, 181.2; FT-IR (cm^{-1}) : 3034, 2924, 1724, 1636, 1611, 1583, 1515, 1488, 1454, 1424, 1340, 1310, 1257, 1152, 1117, 1080, 1031, 749; HPLC, Tr= 1.56 min; MS (ESI$^+$): m/z 383.0 $[M+H]^+$; HRMS calcd for $C_{23}H_{19}N_4O_2$ 383.1502, found 383.1511.

4.4.2 *(4S)-4-benzyl-2-(3-hydroxyphenyl)-3,4-dihydro-5H-pyrido[1',2':1,2]imidazo-[4,5-d][1,3]diazepin-5-one (**1y**)*

Yellow solid (m = 0.030 g, 45%); mp: 145.0-146.0°C; $[\alpha]_D^{20}$ = -5.0° (*c* 1.0, MeOH); ^{1}H NMR (CD_3OD, 300 MHz): δ ppm 3.03 (dd, 1H, *J* = 12.0, 9.0 Hz), 3.37 (dd, 1H, *J* = 12.0, 6.0 Hz), 4.68 (dd, 1H, *J* = 12.0, 6.0 Hz), 6.83 (d, 1H, *J* = 6.0 Hz); 6.98 (bs, 1H), 7.15 (dd, 2H, *J* = 9.0, 6.0 Hz), 7.29-7.38 (m, 7H), 7.43 (t, 1H, *J* = 6.0 Hz), 7.85-7.96 (m, 2H), 9.66 (d, 1H, *J* = 6.0 Hz); ^{13}C NMR (CD_3OD, 75 MHz): δ ppm 36.9, 66.2, 116.4, 117.7, 118.2, 122.5, 123.1, 128.8 (2C), 129.6 (2C), 129.9, 130.2, 130.3, 130.7, 131.4, 131.8, 132.1, 134.8, 136.7, 159.5, 163.7, 181.4; FT-IR (cm^{-1}): 2930, 1779, 1650, 1594, 1530, 1450, 1420, 1331, 1296, 1264, 1244, 1197, 1126, 1080, 1033, 795; HPLC, Tr= 1.32 min; MS (ESI$^+$): m/z 383.1 $[M+H]^+$; HRMS calcd for $C_{23}H_{19}N_4O_2$ 383.1508, found 383.1495.

4.4.3 *(4S)-4-benzyl-2-(2,5-dihydroxyphenyl)-3,4-dihydro-5H-pyrido[1',2':1,2]imidazo-[4,5-d][1,3]diazepin-5-one (**1z**)*

Yellow solid (m = 0.037g, 79%); mp: 260.5-261.5°C; $[\alpha]_D^{20}$ = +81,48° (*c* 0.405, DMSO) ; ^{1}H NMR (DMSO-d_6, 300 MHz): δ ppm 2.82-3.01 (m, 3H), 3.61 (bs, 1H), 4.25 (m, 1H), 6.76 (m, 1H), 6.91 (bs, 1H), 7.14-7.25 (m, 7H), 7.76-7.78 (m, 2H), 8.64 (d, 1H, *J* = 3.4 Hz), 9.46 (d, 1H, *J* = 3.4 Hz) ; ^{13}C NMR (DMSO-d_6, 100 MHz): δ ppm 35.1, 63.3, 112.6, 113.6, 114.2, 114.9, 116.2, 118.2, 122.2, 126.7, 128.3, 128.4 (2C), 129.0, 129.3 (2C), 131.0, 136.6, 146.4, 148.7, 154.7, 158.9, 182.2; FT-IR (cm^{-1}):

3234, 2396, 1724, 1622, 1544, 1480, 1417, 1340, 1249, 1219, 1130, 823; HPLC, Tr= 1.358 min; MS (ESI^+): m/z 399.2 $[M+H]^+$; HRMS calcd for $C_{23}H_{19}N_4O_3$ 399.1457, found 399.1459.

4.5 *General procedure for synthesis of deprotected derivatives* ***1ab-ac***

A solution of compound ***1u-v*** (95 mg) in DCM was cooled at 0℃. A mixture of HBr 33% in acetic acid (5 mL) was added and the resulting solution was stirred for 3 h (monitoring by TLC) at room temperature. The solvent was then removed under reduced pressure to afford compound ***1ab-ac.***

4.5.1 *(4S)-4-hydroxymethyl-2-(3,4-dimethoxyphenyl)-3,4-dihydro-5H-pyrido[1',2':1,2] imi-dazo[4,5-*d*][1,3]diazepin-5-one (**1ab**)*

Brown gum (m = 0.030 g, 93%); $[\alpha]_D^{20}$ = +16.0° (*c* 0.175, DMSO); ^{1}H NMR (DMSO-d_6, 400 MHz): δ ppm 3.81-3.86 (m, 4H), 3.91 (s, 6H), 4.44 (m, 1H), 7.28 (d, 1H, *J* = 8.0 Hz), 7.42-7.49 (m, 1H), 7.56 (d, 1H, *J* = 4.0 Hz), 7.63 (dd, 1H, *J* = 12.0 Hz, *J* = 4.0 Hz), 7.92 (d, 2H, *J* = 4.0 Hz), 9.52 (d, 1H, *J* = 8.0 Hz); ^{13}C NMR (DMSO-d_6, 100 MHz): δ ppm 55.9, 56.2, 60.0, 65.3, 111.5, 112.1, 113.9, 115.8, 116.4, 120.1, 125.6, 128.6, 133.2, 144.6, 148.3, 148.8, 154.6, 160.9, 179.4; FT-IR (cm^{-1}): 3380, 3206, 3027, 2928, 1708, 1647, 1589, 1512, 1489, 1319, 1272, 1222, 1170, 1013, 810, 747; HPLC, Tr= 1.7 min; MS (ESI^+): m/z 367.2 $[M+H]^+$; HRMS calcd for $C_{19}H_{19}N_4O_4$ 367.1406, found 367.1405.

4.5.2 *(4S)-4-(4-hydroxyphenyl)-2-(3,4-dimethoxyphenyl)-3,4-dihydro-5H-pyrido [1',2':1,2]imidazo[4,5-*d*][1,3]diazepin-5-one (**1ac**)*

Yellow solid (m = 0.080 g, 99%); mp: 167.0-168.0℃; $[\alpha]_D^{20}$ = +36.4° (*c* 0.75, DMSO); ^{1}H NMR (DMSO-d_6, 300 MHz): δ ppm 2.72 (m, 1H), 2.97 (m, 1H), 3.72 (s, 3H), 3.83 (s, 3H), 4.25 (d, 1H, *J* = 8.1 Hz), 6.68 (d, 1H, *J* = 6.0 Hz), 7.04-7.34 (m, 9H), 7.74 (bs, 1H), 9.29 (s, 1H), 9.48 (d, 1H, *J* = 6.0 Hz); ^{13}C NMR (DMSO-d_6, 100 MHz): δ ppm 34.2, 55.4, 55.8, 64.0, 111.0, 112.0, 112.7, 114.5, 115.2 (2C), 115.7, 123.6, 123.9, 126.7, 128.0, 130.4 (2C), 131.3, 135.2, 145.7, 148.0, 152.6, 156.2, 158.0, 182.1; FT-IR (cm^{-1}): 3230, 3087, 3031, 2916, 1722, 1613, 1591, 1557, 1510, 1462, 1337, 1236, 1175, 1141, 1111, 1021, 843, 811, 762, 694; HPLC, Tr= 2.44 min; MS (ESI^+): m/z 443.2 $[M+H]^+$; HRMS calcd for $C_{25}H_{23}N_4O_4$ 443.1722, found 443.1719.

*4.8 Synthesis of (4S)-4-benzyl-2-(3,4-dimethoxyphenyl)-4,5-dihydro-3H-pyrido [1',2':1,2]imidazo[4,5-*d*][1,3]diazepin-5-ol (**1ad**)*

A solution of compound ***1o*** (200 mg, 0.047 mmol) in MeOH (2mL) was cooled at 0℃. Then $NaBH_4$ (3 equiv., 53.5 mg, 1.4 mmol) was added and the mixture was stirred at 0℃ for 3 h (monitoring by TLC). After reaction com pletion, 1 mL of saturated $NaHCO_3$ aqueous solution was added to quench the reaction. The solvent was then removed and the resulting residue was dissolved in ethyl acetate. The solution was washed with saturated $NaHCO_3$ aqueous solution. The organic layer was dried over Na_2SO_4, filtered and the solvent was removed under reduced pressure to afford compound ***1ad*** as a light yellow solid (m = 30 mg, 15%). Mp: 174.0℃-175.0℃; $[\alpha]_D^{20}$ = -45.31° (*c* 0.49, DMSO); ^{1}H NMR (DMSO-d_6, 400 MHz): δppm 1.23 (s, 1H), 3.72 (s, 4H), 3.81 (s, 5H), 5.40 (s, 1H), 5.87 (bs, 1H), 6.99 (bs, 2H), 7.00 (bs, 1H), 7.11-7.35 (m, 5H), 7.49 (bs, 3H), 8.36 (bs, 1H); ^{13}C NMR (DMSO-d_6, 100 MHz): δ ppm 36.1, 55.5, 55.6, 60.0, 66.5, 110.9, 112.1, 112.3, 112.9, 115.5, 118.9, 122.8, 124.4, 125.0, 126.5, 128.5 (2C), 129.4 (2C), 138.9, 141.2, 144.9, 148.0, 152.0, 158.0; FT-IR(cm^{-1}): 3379, 2921, 2869, 2853, 1702, 1597, 1570, 1501, 1455, 1414, 1350, 1267, 1100, 1027, 948, 746, 707; HPLC, Tr= 2.27 min; MS (ESI^+): m/z 429.2 $[M+H]^+$; HRMS calcd for $C_{25}H_{25}N_4O_3$ 429.1924, found 429.1927.

4.6 *General procedure for synthesis of opened derivatives **2a-i***

To a solution of diamine derivative ***3a*** (100 mg) in DCM (10 mL) at 0℃, were added HOBt (1.1equiv.), EDCI (1.1 equiv.) and Et_3N (1.1 equiv.) and the resulting mixture was stirred at 0℃ for 30 min. The solution was the n stirred at rt for 6 h (monitoring by TLC). The solution was washed with saturated $NaHCO_3$ aqueous solution (3 x 30 mL). The organic layers were combined, dried over Na_2SO_4, filtered and the solvent was removed under reduced pressure. The residue was dissolved in dichloromethane and filtered through alumina gel using sintered glass Buchner funnel. The solvent was removed *in vacuo* to afford pure opened derivatives ***2a-i.***

4.6.1 *(S)-N-(1-(2-amino-imidazo[1,2-a]pyridin-3-yl)-1-oxo-3-phenylpropan-2-yl)benzamide (**2a**)*

White solid (m = 0.038 g, 68%); mp: 214.0-215.0℃; $[\alpha]_D^{20}$ = +96.59° (*c* 0.44, $CHCl_3$); ^{1}H NMR ($CDCl_3$, 300 MHz): δ ppm 3.24 (dd, 1H, *J* = 9.0, 6.0 Hz), 3.35 (dd, 1H, *J* = 9.0, 6.0 Hz), 5.78 (dd, 1H, *J* = 12.0, 3.0 Hz), 6.22 (bs, 2H), 6.65 (td, 1H, *J* = 6.0, 3.0 Hz), 7.13 (t, 1H, *J* = 6.0 Hz), 7.20 (t, 2H, *J* = 6.0 Hz), 7.26-7.30 (m, 4H), 7.33 (t, 2H, *J* = 6.0 Hz), 7.39-7.48 (m, 2H), 7.68 (d, 2H, *J* = 6.0 Hz), 9.60 (d, 1H, *J* = 6.0 Hz); ^{13}C NMR ($CDCl_3$, 75 MHz): δ ppm 38.6, 54.8, 108.5, 113.2, 114.3, 127.0, 127.2 (2C), 128.7 (4C), 129.3 (2C), 129.8, 131.1, 132.1, 133.6, 136.7, 148.0, 159.3, 168.3, 184.2; FT-IR (cm^{-1}): 3311, 3184, 1633, 1574, 1526, 1495, 1455, 1339, 1263, 1054, 760, 695; HPLC, Tr= 1.62 min; MS (ESI^+): m/z 385.2 $[M+H]^+$; HRMS calcd for $C_{23}H_{21}N_4O_2$ 385.1665, found 385.1665.

4.6.2 *(S)-N-(1-(2-amino-imidazo[1,2-a]pyridin-3-yl)-1-oxo-3-phenylpropan-2-yl)picolinamide (**2b**)*

Yellow solid (m = 0.045 g, 53%); mp: 74.0-75.0℃; $[\alpha]_D^{20}$ =+62.8° (*c* 0.53, $CHCl_3$) ; ^{1}H NMR ($CDCl_3$, 300 MHz) : δ ppm 3.23 (dd, 1H, *J* = 13.6, 7.4 Hz), 3.40 (dd, 1H, *J* = 13.7, 7.0 Hz), 5.78 (dd, 1H, *J* = 16.9, 7.3 Hz), 6.86 (td, 1H, *J* = 6.8, 1.4 Hz), 7.11-7.44 (m, 10H), 7.8 (td, 1H, *J* = 7.7, 1.8 Hz), 8.10 (d, 1H, *J* = 7.9 Hz), 8.57 (d, 1H, *J* = 4.0 Hz), 8.78 (d, 1H, *J* = 9.5 Hz), 9.64 (bs, 1H); ^{13}C NMR ($CDCl_3$, 75 MHz) : δ ppm 38.6, 54.5, 108.7, 113.2, 114.4, 122.5, 126.7, 126.8, 127.4, 128.6 (2C), 129.3 (2C), 130.9, 136.9, 137.5, 147.9, 148.6, 149.1, 159.1, 165.2, 183.7; FT-IR (cm^{-1}) : 3312, 3187, 3026, 1659, 1577, 1523, 1495, 1448, 1339, 1265, 1223, 1146, 1063, 753, 698; HPLC, Tr= 1.59 min; MS (ESI^+): m/z 386.2 $[M+H]^+$; HRMS calcd for $C_{22}H_{20}N_5O_2$ 386.1617, found 386.1618 .

4.6.3 *(S)-N-(1-(2-amino-imidazo[1,2-a]pyridin-3-yl)-1-oxo-3-phenylpropan-2-yl)isonicotinamide (**2c**)*

Yellow solid (m = 0.086 g, 80%); mp: 205.0-206.0℃; $[\alpha]_D^{20}$ = +69.5° (*c* 0.4, $CHCl_3$) ; ^{1}H NMR ($CDCl_3$, 300 MHz) : δ ppm 3.30 (dd, 1H, *J* = 13.8, 7.4 Hz), 3.4 (dd, 1H, *J* = 13.8, 6.7 Hz), 5.76 (dd, 1H, *J* = 15.5, 6.9 Hz), 5.98 (s, 2H), 6.9 (td, 1H, *J* = 6.9, 1.3 Hz), 7.14-7.23 (m, 4H), 7.30 (d, 1H, *J* = 8.7 Hz), 7.44 (td, 1H, *J* = 7.0, 1.1 Hz), 7.53 (d, 4H, *J* = 6.0 Hz), 8.67 (dd, 2H, *J* = 4.6, 1.4 Hz), 9.55 (bs, 1H) ; ^{13}C NMR ($CDCl_3$, 75 MHz): δ ppm 38.6, 55.1, 108.5, 113.5, 114.5, 121.0 (2C), 127.2, 128.5, 128.7 (2C), 129.3 (2C), 129.8, 131.4, 136.3, 140.8, 148.1, 150.7 (2C), 159.2, 166.4 ; FT-IR (cm^{-1})

: 3311, 3188, 1650, 1579, 1495, 1455, 1339, 1310, 1265, 1063, 846, 752, 696, 667 ; HPLC, Tr= 1.19 min ; MS (ESI^+): m/z 386.2 $[M+H]^+$; HRMS calcd for $C_{22}H_{20}N_5O_2$ 386.1617, found 386.1619.

4.6.4 *(S)-N-(1-(2-amino-imidazo[1,2-a]pyridin-3-yl)-1-oxo-3-phenylpropan-2-yl)-1H-pyrrole-2-carboxamide (**2d**)*

Yellow solid (m = 0.117 g, 88%); mp: 197.5-198.5°C; $[\alpha]_D^{20}$ =+15.8° (*c* 0.54, DMSO); ^1H NMR (DMSO-d_6, 300 MHz) : δ ppm 3.15 (m, 2H), 5.46 (dd, 1H, *J* = 13.0, 7.0 Hz), 6.1 (m, 1H), 6.87 (m, 1H), 6.95 (t, 1H, *J* = 8.1 Hz), 7.02 (m, 1H), 7.1-7.25 (m, 7H), 7.33 (t, 1H, *J* = 7.2 Hz), 7.48 (t, 1H, *J* = 7.4 Hz), 8.8 (d, 1H, *J* = 8.7 Hz), 9.55 (d, 1H, *J* = 6.6 Hz), 11.48 (s, 1H); ^{13}C NMR (DMSO-d_6, 75 MHz) : δ ppm 37.0, 54.3, 107.3, 108.8, 111.6, 112.6, 113.6, 122.1, 124.8, 126.2, 128.0 (2C), 128.3, 129.0 (2C), 130.7, 138.0, 147.2, 158.8, 161.2, 184.0; FT-IR (cm^{-1}): 3305, 3194, 1577, 1556, 1495, 1442, 1338, 1264, 1193, 1129, 1041, 844, 733, 696; HPLC, Tr= 1.54 min; MS (ESI^+): m/z 374.2 $[M+H]^+$; HRMS calcd for $C_{21}H_{20}N_5O_2$ 374.1617, found 374.1616.

4.6.5 *(S)-N-(1-(2-amino-imidazo[1,2-a]pyridin-3-yl)-1-oxo-3-phenylpropan-2-yl)-2-methylbenzamide (**2e**)*

White solid (m = 0.111 g, 76%); mp: 87.0-88.0°C; $[\alpha]_D^{20}$ =+31.1° (*c* 1.0, $CHCl_3$) ; ^1H NMR ($CDCl_3$, 300 MHz): δ ppm 1.86 (bs, 1H), 2.21 (s, 3H), 3.26 (dd, 1H, *J* = 13.9, 8.3 Hz), 3.33 (dd, 1H, *J* = 13.9, 6.3 Hz), 5.80 (dd, 1H, *J* = 13.9, 8.3 Hz), 6.31 (s, 2H), 6.84 (td, 1H, *J* = 13.8, 6.9 Hz), 7.22 (m, 10H), 7.38 (td, 1H, *J* = 15.8, 6.9 Hz), 9.55 (bs, 1H) ; ^{13}C NMR ($CDCl_3$, 75 MHz): δ ppm 19.7, 38.4, 54.8, 113.2, 114.3, 125.7, 126.9, 127.0, 127.3, 128.6 (2C), 128.7, 129.4 (2C), 130.2, 131.0, 131.1, 135.3, 136.3, 136.8, 148.1, 159.3, 170.9, 184.0 ; FT-IR (cm^{-1}) : 3331, 3179, 2828, 1731, 1633, 1578, 1526, 1496, 1452, 1338, 1318, 1203, 1158, 1056, 735, 698 ; HPLC, Tr= 1.70 min ; MS (ESI^+): m/z 399.1 $[M+H]^+$; HRMS calcd for $C_{24}H_{23}N_4O_2$ 399.1821, found 399.1820.

4.6.6 *(S)-N-(1-(2-amino-imidazo[1,2-a]pyridin-3-yl)-1-oxo-3-phenylpropan-2-yl)-3,4-dimethoxybenzamide (**2f**)*

White solid (m = 0.141 g, 89%), mp: 85.0-86.0°C; $[\alpha]_D^{20}$ =+47.2° (*c* 1.0, $CHCl_3$) ; ^1H NMR ($CDCl_3$, 300 MHz) : δ ppm 1.99 (bs, 1H), 3.25 (dd, 1H, *J* = 12.0, 6.0 Hz), 3.34

(dd, 1H, *J* = 15.0, 6.0 Hz), 3.83 (s, 3H) 3.86 (s, 3H), 5.77 (dd, 1H, *J* = 15.0, 6.0 Hz), 6.27 (bs, 2H), 6.72 (d, 1H, *J* = 9.0 Hz), 6.82 (td, 1H, *J* = 6.0, 3.0 Hz), 7.11-7.24 (m, 4H), 7.29-7.42 (m, 5H) 9.59 (bs, 1H) ; ^{13}C NMR ($CDCl_3$, 75 MHz) : δ ppm 38.6, 54.8, 56.1 (2C), 110.4, 110.7, 113.2, 114.4, 120.0, 126.0, 126.9, 128.6 (2C), 128.9, 129.3 (2C), 130.3, 131.1, 136.7, 148.0, 149.1, 152.3, 159.3, 167.9, 184.5 ; FT-IR (cm^{-1}): 3331 , 2925, 2852, 1724, 1577, 1542, 1494, 1440, 1339, 1262, 1229, 1055, 1019, 757, 698 ; HPLC, Tr= 1.35 min ; MS (ESI^+): m/z 445.1 $[M+H]^+$; HRMS calcd for $C_{25}H_{25}N_4O_4$ 445.1876, found 445.1877.

4.6.7 *(S)-N-(1-(2-amino-imidazo[1,2-a]pyridin-3-yl)-1-oxo-3-phenylpropan-2-yl)-2-phenylacetamide (**2g**)*

Yellow solid (m = 0.120 g, 84%); mp: 161.0-162.0℃; $[\alpha]_D^{20}$ =+23.8° (*c* 0.5, DMSO) ; ^{1}H NMR (DMSO d_6, 300 MHz) : δ ppm 3.06 (dd, 1H, *J* = 13.6, 8.0 Hz), 3.15 (dd, 1H, *J* = 13.6, 6.0 Hz), 3.35 (bs, 1H), 3.48 (d, 1H, *J* = 14.0 Hz), 3.55 (d, 1H, *J* = 14.0 Hz), 5.33 (dd, 1H, *J* = 13.0, 8.0 Hz), 6.96 (s, 2H), 7.02 (t, 1H, *J* = 6.8 Hz), 7.21 (m, 10H), 7.36 (d, 1H, *J* = 8.7 Hz), 7.54 (t, 1H, *J* = 8.0 Hz), 9.15 (d, 1H, *J* = 8.0 Hz) ; ^{13}C NMR (DMSO d_6, 75 MHz) : δ ppm 37.1, 41.5, 54.4, 107.1, 112.7, 113.6, 126.2, 126.3, 128.0 (2C), 128.1 (2C), 129.0 (2C), 129.1 (2C), 130.8, 135.8, 136.9, 137.6, 147.2, 158.8, 171.4, 183.7; FT-IR (cm^{-1}): 694, 716, 759, 1065, 1264, 1317, 1337, 1454, 1494, 1574, 1522, 1646, 1630, 2922, 3003, 3195, 3326 ; HPLC, Tr=1.6 min ; MS(ESI^+) : m/z 399.1 $[M+H]^+$; HRMS calcd for $C_{24}H_{23}N_4O_2$ 399.1821, found 399.1818

4.6.8 *(S)-N-(1-(2-amino-imidazo[1,2-a]pyridin-3-yl)-1-oxo-3-phenylpropan-2-yl)cinnamamide (**2h**)*

Yellow solid (m = 0.017 g, 20%); mp: 85.0-86.0℃; $[\alpha]_D^{20}$ =+16.5° (*c* 0.6, $CHCl_3$); ^{1}H NMR ($CDCl_3$, 300 MHz): δ ppm 3.08 (dd, 1H, *J* = 13.8, 7.5 Hz), 3.21 (dd, 1H, *J* = 13.9, 6.6 Hz), 5.64 (dd, 1H, *J* = 15.9, 7.4 Hz), 6.15 (s, 2H), 6.28 (d, 1H, *J* = 15.6 Hz), 6.76 (t, 1H, *J* = 6.8 Hz), 6.98-7.30 (m, 13H), 7.44 (d, 1H, *J* = 15.6 Hz), 9.50 (bs, 1H) ; ^{13}C NMR ($CDCl_3$, 75 MHz): δ ppm 38.6, 54.6, 108.6, 113.3, 114.4, 119.7, 127.0, 128.0 (2C), 128.3, 128.6 (2C), 128.9 (2C), 129.3 (2C), 130.1, 131.1, 134.6, 136.7, 142.4, 148.2, 159.6, 166.8, 184.6; FT-IR (cm^{-1}): 3285, 3185, 2974, 1720, 1574, 1494,

1455, 1337, 1265, 1221, 979, 753, 731, 683; HPLC, Tr=1.5 min; MS (ESI^+): m/z 411.1 $[M+H]^+$; HRMS calcd for $C_{25}H_{23}N_4O_2$ 411.1821, found 411.1821

4.6.9 *(S)-N-(1-(2-amino-imidazo[1,2-a]pyridin-3-yl)-1-oxo-3-phenylpropan-2-yl)-3-phenylpropanamide (**2i**)*

White solid (m = 0.085 g, 59%); mp: 69.0℃-70.0℃; $[\alpha]_D^{20}$ = +69.0° (*c* 1.0, $CHCl_3$) ; ^1H NMR ($CDCl_3$, 300 MHz): δ ppm 2.43 (t, 2H, *J* = 9.0 Hz), 2.83 (t, 2H, *J* = 9.0 Hz), 3.04 (dd, 1H, *J* = 12.0, 6.0 Hz), 3.18 (dd, 1H, *J* = 15.0, 6.0 Hz), 5.58 (dd, 1H, *J* = 15.0, 6.0 Hz), 6.29 (bs, 2H), 6.81 (td, 1H, *J* = 9.0, 3.0 Hz), 6.94-7.18 (m, 11H), 7.28 (bs, 1H), 7.37 (td, 1H, *J* = 9.0, 3.0 Hz), 9.58 (bs, 1H); ^{13}C NMR ($CDCl_3$, 75 MHz): δ ppm 31.6, 38.0, 38.3, 54.2, 108.4, 113.2, 114.3, 126.3, 126.9, 128.3 (4C), 128.4, 128.6 (2C), 129.2 (2C), 131.1, 136.8, 140.5, 148.0, 159.4, 173.2, 184.3; FT-IR (cm^{-1}): 3325, 3178, 3028, 1734, 1644, 1571, 1495, 1452, 1339, 1264, 1065, 762; HPLC, Tr= 1.6 min; MS (ESI^+): m/z 413.3 $[M+H]^+$; HRMS calcd for $C_{25}H_{25}N_4O_2$ 413.1978, found 413.1981.

4.7. Enzyme and inhibition assays.

The enzyme activities of KLK5, KLK7, KLK8 and KLK14 (R&D Systems, France) were determined using 96-well plates monitored using a BMG Fluostar apparatus. The hydrolysis of the appropriate fluorogenic substrate was measured (λ_{exc} = 360 nm, λ_{em} = 460 nm) for 15 min at 37 ℃ in the presence of untreated enzyme (control) and treated enzyme incubated with a test compound. Substrates (Bachem, Weil am Rhein, Germany) were previously dissolved in DMSO, with the final solvent concentration kept constant at 2 % (v/v). The composition of the activity buffers was (pH 8.0): 50 mM Tris-HCl, Tween 20 0.01 % (v/v) and 150 mM NaCl for KLK5, 1M NaCl for KLK7 and KLK14. The final concentrations were 0.6 nM (KLK5), 100 µM (Boc-Val-Pro-Arg-AMC); 7.6 nM (KLK7), 40 µM (Suc-Leu-Leu-Val-Tyr-AMC); 1 nM (KLK8), 100 µM (Boc-Val-Pro-Arg-AMC); 0.2 nM (KLK14), 10 µM (Boc-Val-Pro-Arg-AMC). Compounds were tested in triplicate for different concentrations to detect their inhibitory potency. The enzyme and the inhibitors were incubated for 15 min before the determination of the enzyme activity. Initial rates determined in control experiments (V_0) were considered to be 100 % of the proteinase activity; initial rates

(V_i) that were below 100 % in the presence of a tested compound were considered to be inhibitions. The inhibitory activity of compounds was expressed as IC_{50} (inhibitor concentrations giving 50% inhibition). The values of IC_{50} were calculated by fitting the experimental data either to equation 1: % Inhibition = 100 x ($1-V_i/V_0$) = 100 $[I]_0/(IC_{50} + [I]_0)$, or equation 2, % Inhibition = 100 $[I]_0^{nH}/(IC_{50}^{nH} + [I]_0^{nH})$ with n_H = Hill number.

4.8. Mechanisms of inhibition

Reversibility was analysed by diluting the reaction mixtures (dilution factor of 40) after 15 and 60 min preincubation of the enzyme with inhibitor. Aliquots of reaction mixtures (2.5 µL) were added to 97.5 µL of buffer containing the fluorogenic substrate (experimental conditions identical to the routine protocol used for a given enzyme). The mechanism of inhibition was determined by varying substrate and inhibitor concentrations and using classical Lineweaver-Burk plots.

4.9. *Structure-based Molecular Docking*.

The docking study of compound **1o** was carried out using the docking engine Molegro virtual docker version 5.5.0. The enzyme structures used for the docking were obtained from 2QXH PDB file corresponding to KLK7 complexed with succinyl-Ala-Ala-Pro-Phe chloromethylketone inhibitor. Heteroatoms and ligands were removed from the crystal structures and hydrogen atoms were added. The scoring function Moldock Score and the Moldock SE search algorithm were used; the resolution of the grid for estimation of the computed binding affinity was 0.3 Å with a radius of 15 Å around the catalytic triad residues. Fifteen runs were launched and up to 50 (maximum) poses subsequently analyzed. Figures were prepared with Pymol (DeLano Scientific LLC, San Carlos, CA, USA).

4.10 Cell culture and cytotoxicity assay.

PC3 and SW-60 cells were kindly supplied by Dr Dalila Darmoul (INSERM U976, Université Paris Diderot, and Sorbonne Paris Cité). Cells were spread at a rate of 5000 cells per well of 96-well plates in 100 µL of medium/well consisting of DMEM medium complemented with fetal bovine serum (10%), penicillin (100 µg/mL) and streptomycin (100 µg/mL), at 37℃ and 5% of CO_2. 20 h after seeding the cells, 1µL of different concentrations of each inhibitor previously dissolved in DMSO was added to the wells. An equivalent volume of DMSO was used in controls for a final DMSO

concentration of 1% (v/v). For each condition, at least three wells were measured. 48 to 72 h after incubation, culture medium was removed and replaced by 100 µL of new medium/well (without phenol red) supplemented with XTT (0,3 mg/mL) and PMS (8,3 µM). After 3 h incubation the absorbance at 485 nm was read. The XTT assay is based on the mitochondrial deshydrogenase activity. The relative cell viability was expressed as a percentage to the viability of cells treated with DMSO only.

5. References

[1] G.P. Gupta, J. Massagué, Cancer Metastasis: Building a Framework, Cell, 127 (2006) 679-695.
[2] C.A. Borgono, E.P. Diamandis, The emerging roles of human tissue kallikreins in cancer, Nat. Rev. Cancer, 4 (2004) 876-890.
[3] C.A. Borgono, I.P. Michael, E.P. Diamandis, Human tissue kallikreins: physiologic roles and applications in cancer, Mol. Cancer Res., 2 (2004) 257-280.
[4] M. Debela, V. Magdolen, N. Schechter, M. Valachova, F. Lottspeich, C.S. Craik, Y. Choe, W. Bode, P. Goettig, Specificity profiling of seven human tissue kallikreins reveals individual subsite preferences, J. Biol. Chem., 281 (2006) 25678-25688.
[5] M. Debela, P. Hess, V. Magdolen, N.M. Schechter, T. Steiner, R. Huber, W. Bode, P. Goettig, Chymotryptic specificity determinants in the 1.0 A structure of the zinc-inhibited human tissue kallikrein 7, Proc. Natl Acad. Sci. U.S.A., 104 (2007) 16086-16091.
[6] V.C. Ramani, R.S. Haun, Expression of kallikrein 7 diminishes pancreatic cancer cell adhesion to vitronectin and enhances urokinase-type plasminogen activator receptor shedding, Pancreas, 37 (2008) 399-404.
[7] M. Devetzi, T. Trangas, A. Scorilas, D. Xynopoulos, M. Talieri, Parallel overexpression and clinical significance of kallikrein-related peptidases 7 and 14 (KLK7KLK14) in colon cancer, Thromb. Haemost., 109 (2013) 716-725.
[8] L. Mo, Zhang, J., Shi, J., Xuan, Q., Yang, X., Qin, M., Lee, C., Klocker, H., Li, QQ., Mo, Z., Human kallikrein 7 induces epithelial-mesenchymal transition-like changes in prostate carcinoma cells: a role in prostate cancer invasion and progression., Anticancer Res., 30 (2010) 3413-3420.
[9] C.A. Borgono, I.P. Michael, N. Komatsu, A. Jayakumar, R. Kapadia, G.L. Clayman, G. Sotiropoulou, E.P. Diamandis, A potential role for multiple tissue kallikrein serine proteases in epidermal desquamation, J. Biol. Chem., 282 (2007) 3640-3652.
[10] T. Egelrud, M. Brattsand, P. Kreutzmann, M. Walden, K. Vitzithum, U.C. Marx, W.G. Forssmann, H.J. Magert, hK5 and hK7, two serine proteinases abundant in human skin, are inhibited by LEKTI domain 6, Br J Dermatol, 153 (2005) 1200-1203.
[11] M. Brattsand, K. Stefansson, C. Lundh, Y. Haasum, T. Egelrud, A proteolytic cascade of kallikreins in the stratum corneum, J. Invest. Dermatol., 124 (2005) 198-203.
[12] C. Caubet, N. Jonca, M. Brattsand, M. Guerrin, D. Bernard, R. Schmidt, T. Egelrud, M. Simon, G. Serre, Degradation of corneodesmosome proteins by two serine proteases of the kallikrein family, SCTE/KLK5/hK5 and SCCE/KLK7/hK7, J. Invest. Dermatol., 122 (2004) 1235-1244.

[13] A. Hovnanian, Netherton syndrome: skin inflammation and allergy by loss of protease inhibition, Cell Tissue Res., 351 (2013) 289-300.
[14] S. Wang, S. Olt, N. Schoefmann, A. Stuetz, A. Winiski, B. Wolff-Winiski, SPINK5 knockdown in organotypic human skin culture as a model system for Netherton syndrome: effect of genetic inhibition of serine proteases kallikrein 5 and kallikrein 7, Exp. Dermatol., (2014).
[15] L. Hansson, A. Backman, A. Ny, M. Edlund, E. Ekholm, B. Ekstrand Hammarstrom, J. Tornell, P. Wallbrandt, H. Wennbo, T. Egelrud, Epidermal overexpression of stratum corneum chymotryptic enzyme in mice: a model for chronic itchy dermatitis, J. Invest. Dermatol., 118 (2002) 444-449.
[16] S. Schultz, A. Saalbach, J.T. Heiker, R. Meier, T. Zellmann, J.C. Simon, A.G. Beck-Sickinger, Proteolytic activation of prochemerin by kallikrein 7 breaks an ionic linkage and results in C-terminal rearrangement, Biochem. J., 452 (2013) 271-280.
[17] P. Goettig, V. Magdolen, H. Brandstetter, Natural and synthetic inhibitors of kallikrein-related peptidases (KLKs), Biochimie, 92 (2010) 1546-1567.
[18] C. Deraison, C. Bonnart, F. Lopez, C. Besson, R. Robinson, A. Jayakumar, F. Wagberg, M. Brattsand, J.P. Hachem, G. Leonardsson, A. Hovnanian, LEKTI fragments specifically inhibit KLK5, KLK7, and KLK14 and control desquamation through a pH-dependent interaction, Mol. Biol. Cell, 18 (2007) 3607-3619.
[19] S.J. de Veer, S.S. Ukolova, C.A. Munro, J.E. Swedberg, A.M. Buckle, J.M. Harris, Mechanism-based selection of a potent kallikrein-related peptidase 7 inhibitor from a versatile library based on the sunflower trypsin inhibitor SFTI-1, Biopolymers, (2013).
[20] T.S. Teixeira, R.F. Freitas, O. Abrahao, Jr., K.F. Devienne, L.R. de Souza, S.I. Blaber, M. Blaber, M.Y. Kondo, M.A. Juliano, L. Juliano, L. Puzer, Biological evaluation and docking studies of natural isocoumarins as inhibitors for human kallikrein 5 and 7, Bioorg. Med. Chem. Lett., 21 (2011) 6112-6115.
[21] R.F. Freitas, T.S. Teixeira, T.G. Barros, J.A. Santos, M.Y. Kondo, M.A. Juliano, L. Juliano, M. Blaber, O.A. Antunes, O. Abrahao, Jr., S. Pinheiro, E.M. Muri, L. Puzer, Isomannide derivatives as new class of inhibitors for human kallikrein 7, Bioorg. Med. Chem. Lett., 22 (2012) 6072-6075.
[22] J.P. Oliveira, R.F. Freitas, L.S. Melo, T.G. Barros, J.A. Santos, M.A. Juliano, S. Pinheiro, M. Blaber, L. Juliano, E.M. Muri, L. Puzer, Isomannide-based peptidomimetics as inhibitors for human tissue kallikreins 5 and 7, ACS Med. Chem. Lett., 5 (2014) 128-132.
[23] X. Tan, C. Bertonati, L. Qin, L. Furio, C. El Amri, A. Hovnanian, M. Reboud-Ravaux, B.O. Villoutreix, Identification by in silico and in vitro screenings of small organic molecules acting as reversible inhibitors of kallikreins, Eur. J. Med. Chem., 70 (2013) 661-668.
[24] X. Tan, L. Furio, M. Reboud-Ravaux, B.O. Villoutreix, A. Hovnanian, C. El Amri, 1,2,4-Triazole derivatives as transient inactivators of kallikreins involved in skin diseases, Bioorg. Med. Chem. Lett., 23 (2013) 4547-4551.
[25] N. Masurier, R. Aruta, V. Gaumet, S. Denoyelle, E. Moreau, V. Lisowski, J. Martinez, L.T. Maillard, Selective C-Acylation of 2-Aminoimidazo[1,2-a]pyridine: Application to the Synthesis of Imidazopyridine-Fused [1,3]Diazepinones, J. Org. Chem., 77 (2012) 3679-3685.
[26] N. Masurier, E. Debiton, A. Jacquemet, A. Bussiere, J.M. Chezal, A. Ollivier, D. Tetegan, M. Andaloussi, M.J. Galmier, J. Lacroix, D. Canitrot, J.C. Teulade, R.C. Gaudreault, O. Chavignon, E. Moreau, Imidazonaphthyridine systems (part 2): Functionalization of the phenyl ring linked to the pyridine pharmacophore and its

replacement by a pyridinone ring produces intriguing differences in cytocidal activity, Eur. J. Med. Chem., 52 (2012) 137-150.
[27] N. Masurier, E. Moreau, C. Lartigue, V. Gaumet, J.-M. Chezal, A. Heitz, J.-C. Teulade, O. Chavignon, New Opportunities with the Duff Reaction, J. Org. Chem., 73 (2008) 5989-5992.
[28] M. Andaloussi, E. Moreau, N. Masurier, J. Lacroix, R.C. Gaudreault, J.-M. Chezal, A. El Laghdach, D. Canitrot, E. Debiton, J.-C. Teulade, O. Chavignon, Novel imidazo[1,2-a]naphthyridinic systems (part 1): Synthesis, antiproliferative and DNA-intercalating activities, Eur. J. Med. Chem., 43 (2008) 2505-2517.
[29] G. Chaubet, L.T. Maillard, J. Martinez, N. Masurier, A tandem aza-Friedel-Crafts reaction/Hantzsch cyclization: a simple procedure to access polysubstituted 2-amino-1,3-thiazoles, Tetrahedron, 67 (2011) 4897-4904.
[30] L.T. Maillard, S. Bertout, O. Quinonero, G. Akalin, G. Turan-Zitouni, P. Fulcrand, F. Demirci, J. Martinez, N. Masurier, Synthesis and anti-Candida activity of novel 2-hydrazino-1,3-thiazole derivatives, Bioorg. Med. Chem. Lett., 23 (2013) 1803-1807.
[31] A. Gallud, O. Vaillant, L.T. Maillard, D.P. Arama, J. Dubois, M. Maynadier, V. Lisowski, M. Garcia, J. Martinez, N. Masurier, Imidazopyridine-fused [1,3]-diazepinones: Synthesis and antiproliferative activity, Eur. J. Med. Chem., 75 (2014) 382-390.
[32] D.P. Arama, V. Lisowski, E. Scarlata, P. Fulcrand, L.T. Maillard, J. Martinez, N. Masurier, An efficient synthesis of pyrido-imidazodiazepinediones, Tetrahedron Lett., 54 (2013) 1364-1367.
[33] M.E. Kaighn, K.S. Narayan, Y. Ohnuki, J.F. Lechner, L.W. Jones, Establishment and characterization of a human prostatic carcinoma cell line (PC-3). Invest. Urol., 17 (1979) 16-23.
[34] A. Leibovitz, J.C. Stinson, W.B. McCombs III, C.E. McCoy, K.C. Mazur, N.D. Mabry, Classification of human colorectal adenocarcinoma cell lines., Cancer Res., 36 (1976) 4562-4569.
[35] F. Walker, P. Nicole, A. Jallan, A. Soosaipillai , V. Mosbach, K. Oikonomopoulou, E.P. Diamandis , V. Magdolen, D. Darmoul, Kallikrein-related peptidase 7 (KLK7) is a proliferative factor that is aberrantly expressed in human colon cancer, Biol. Chem., 395 (2014) 1075-1086.

ACKNOWLEDGMENTS

This work was supported by Université of Montpellier, Institut National pour la Recherche Médicale (INSERM), Université Pierre et Marie Curie (UPMC), Centre National de la Recherche Scientifique (CNRS), and Région Languedoc-Roussillon (Chercheur d'avenir 2011 grant to V.L.). The authors are grateful to the French Ministry of Research and Education for F. S. and the Mali Government for D.A PhD fellowships. CE and NM thanks Prof Michèle Reboud-Ravaux and Dr Alain Chavanieu for fruitful discussions and are grateful to Christina Lymperopoulou and Isabelle Bequignon for technical assistance.

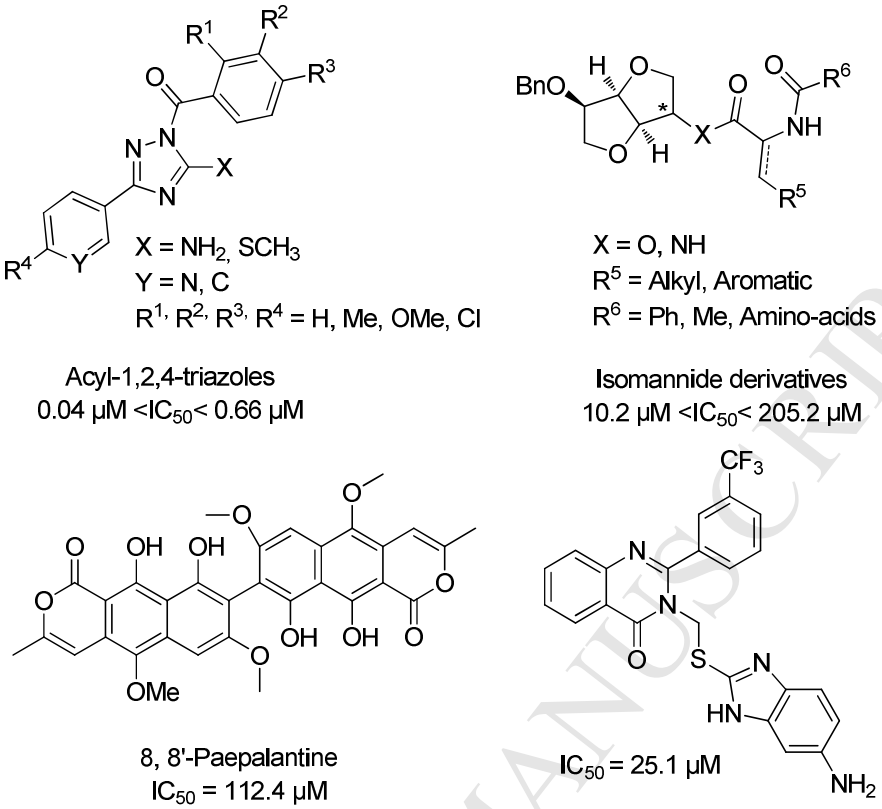

Figure 1. Heterocyclic compounds reported as KLK7 inhibitors

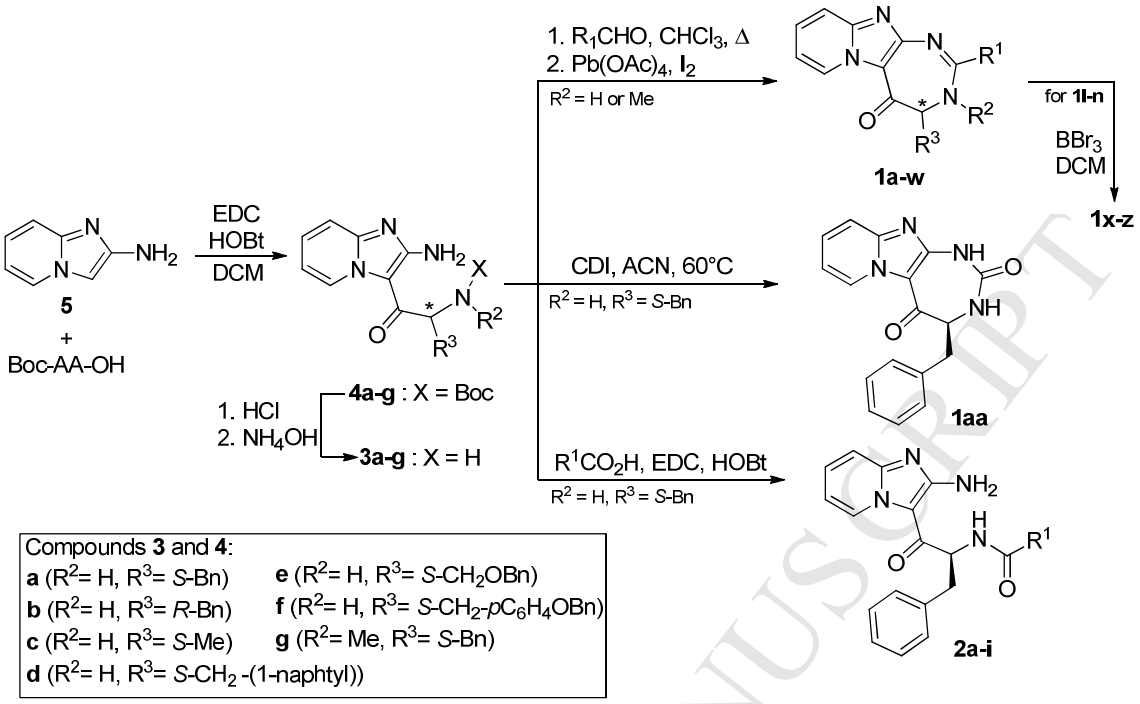

Reagents and conditions: Boc-AA-OH = Boc-Phe-OH, Boc-D-Phe-OH, Boc-Ala-OH, Boc-Ser(Bn)-OH, Boc-1-Nal-OH, Boc-Tyr(Bn)-OH or Boc-*N*-Me-Ala-OH

Scheme 1. Synthesis of compounds **1a-w**, **1aa** and **2a-i** (R^1, R^2 and R^3 substituents are referenced in Table 1).

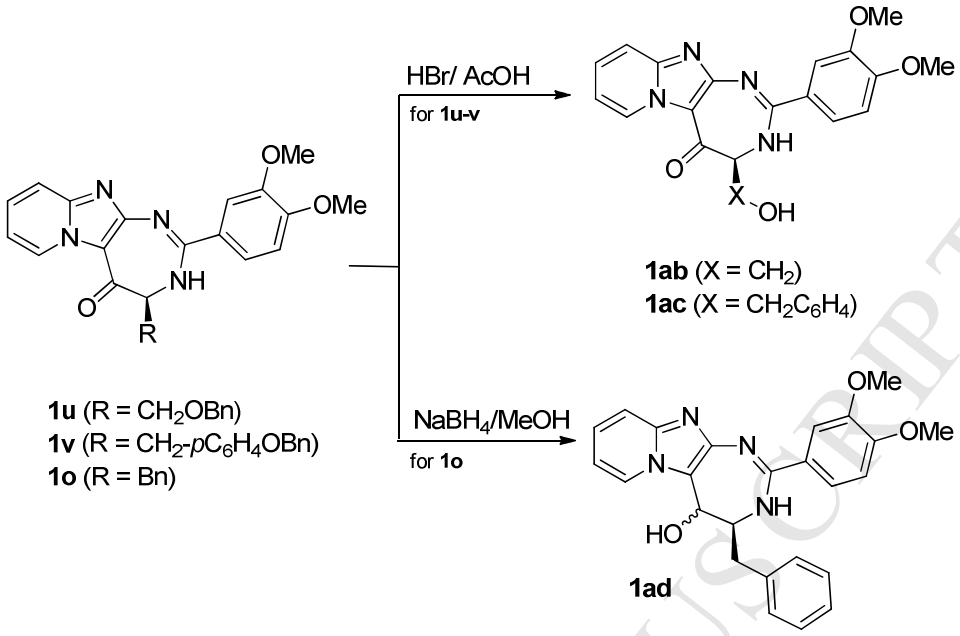

Scheme 2. Synthesis of compounds **1ab-1ad**.

Table 1. Structure and IC_{50} against KLK7 of compounds **1** and **2** after 15 min of incubation at pH 8.0 and 37°C. [1] ni = no inhibition (<30% inhibition at 50 µM).

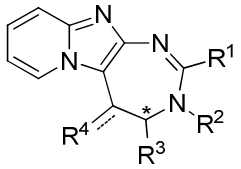

1a-1ad

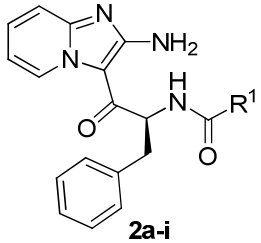

2a-i

Compounds					
	R^1	**R^2**	**R^3**	**R^4**	**IC_{50} (µM)**
1a	2-Me-C_6H_4	H	(*S*)-Bn	=O	57.0 ± 1.0
1b	3-Me-C_6H_4	H	(*S*)-Bn	=O	ni[1]
1c	4-Me-C_6H_4	H	(*S*)-Bn	=O	68.0 ± 3.1
1d	4-OMe-C_6H_4	H	(*S*)-Bn	=O	72.0 ± 1.9
1e	2-Me-C_6H_4	H	(*R*)-Bn	=O	95.9 ± 1.7
1f	C_6H_5	H	(*S*)-Bn	=O	ni
1g	4-BrC_6H_4	H	(*S*)-Bn	=O	ni
1h	4-$NO_2C_6H_4$	H	(*S*)-Bn	=O	ni
1i	3-pyridinyl	H	(*S*)-Bn	=O	ni
1j	$CH_2CH(CH_3)_2$	H	(*S*)-Bn	=O	ni
1k	2,4-diMe-C_6H_3	H	(*S*)-Bn	=O	83.9 ± 1.7
1l	2-OMe-C_6H_4	H	(*S*)-Bn	=O	ni
1m	3-OMe-C_6H_4	H	(*S*)-Bn	=O	ni
1n	2,5-diOMe-C_6H_3	H	(*S*)-Bn	=O	80.9 ± 2.5
1o	3,4-diOMe-C_6H_3	H	(*S*)-Bn	=O	33.5 ± 1.5
1p	3,4,5-triOMe-C_6H_2	H	(*S*)-Bn	=O	55.7 ± 2.3
1q	2-Me-C_6H_4	H	(*S*)-(1-naphtyl)CH_2	=O	ni
1r	2-Me-C_6H_4	H	(*S*)-Me	=O	ni
1s	3,4-diMeO-C_6H_3	H	(*S*)-Me	=O	ni
1t	2-Me-C_6H_4	H	(*S*)-BnOCH_2	=O	ni
1u	3,4-diMeO-C_6H_3	H	(*S*)-BnOCH_2	=O	ni
1v	3,4-diMeO-C_6H_3	H	(*S*)-4-Bn$OC_6H_4CH_2$	=O	ni
1w	3,4-diMeO-C_6H_3	Me	(*S*)-Bn	=O	ni
1x	2-HO-C_6H_4	H	(*S*)-Bn	=O	ni

1y	3-HO-C_6H_4	H	(*S*)-Bn	=O	124.8 ± 1.4
1z	2,5-diHO-C_6H_3	H	(*S*)-Bn	=O	ni
1aa	=O	H	(*S*)-Bn	=O	ni
1ab	3,4-diMeO-C_6H_3	H	(*S*)-$HOCH_2$	=O	ni
1ac	3,4-diMeO-C_6H_3	H	(*S*)-4-$HOC_6H_4CH_2$	=O	ni
1ad	3,4-diMeO-C_6H_3	H	(*S*)-Bn	OH	ni
2a	Ph	-	-	-	ni
2b	2-pyridinyl	-	-	-	ni
2c	4-pyridinyl	-	-	-	ni
2d	2-pyrrolyl	-	-	-	ni
2e	2-Me-C_6H_4	-	-	-	135.4 ± 9.2
2f	3,4-diOMe-C_6H_3	-	-	-	ni
2g	CH_2-Ph	-	-	-	149.2 ±19.2
2h	CH=CH-Ph	-	-	-	ni
2i	CH_2-CH_2-Ph	-	-	-	ni

Table 2. Evaluation of cytotoxic effect of compounds **1k**, **1n-p** on human cancer cell lines HeLa, PC-3 and SW-620. Cytotoxicity is expressed as EC_{50}, which refers to the concentration that induces 50% of cell death determined by XTT assay.

Compounds	Cell lines		
	HeLa	PC-3	SW-620
1k	nc[1]	nc	67.8 ±3.4
1n	40.0 ±1.5	nc	nc
1o	24.3 ±1.6	64.8 ±2.3	nc
1p	53.8 ±3.5	nc	nc

[1]nc: non cytotoxic

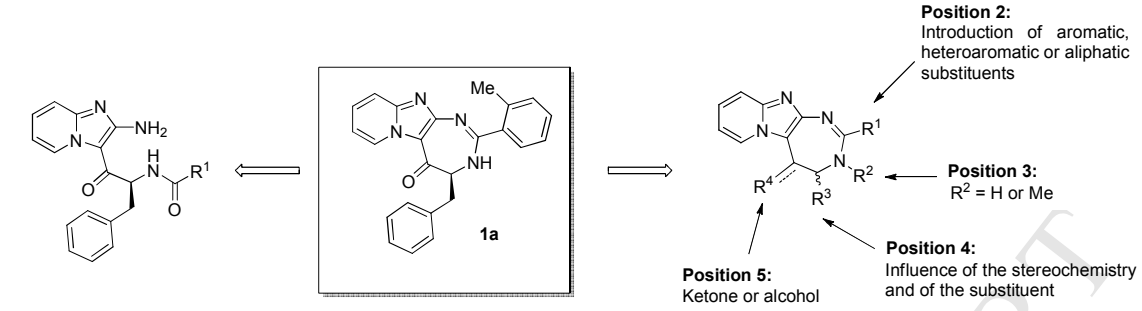

Figure 2: Study of the compound **1a** pharmacomodulation

A.

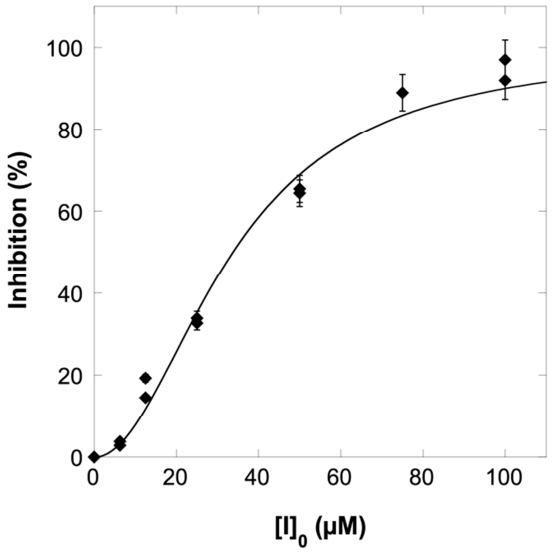

B.

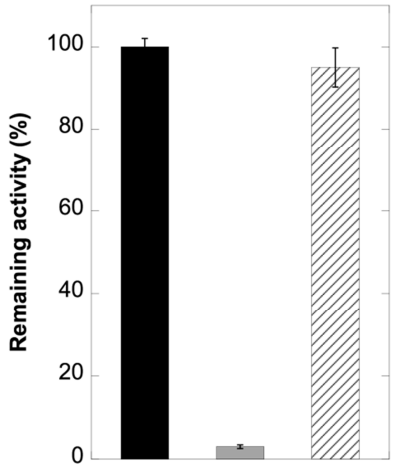

C.

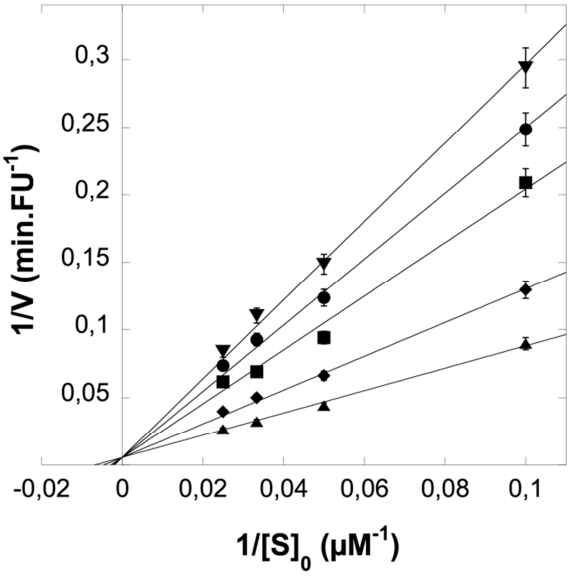

Figure 3. Inhibition of KLK7 by compound 1o. A- IC_{50} curve after 15 min incubation of KLK7 (7.6 nM) at pH 8.0 and 37 ℃ in 50 mM TRIS-HCl pH 8.0, Tween 20 0.01% (v/v) and 1M NaCl. The enzyme activity was monitored at 40 µM final concentration of substrat (Suc-Leu-Leu-Leu-Val-Tyr-AMC). B- Remaining activity of hK7 in absence of inhibitor (black), after 15 min incubation with 50 µM of compound **1o** (grey), after dilution (1/40) of the formed complex KLK7-**1o** (striped). C- Lineweaver-Burk plot at different concentrations of **1o**: 0 (▲); 6,25 µM (◆); 12,5 µM (■); 25 µM (●); 50 µM (▼).

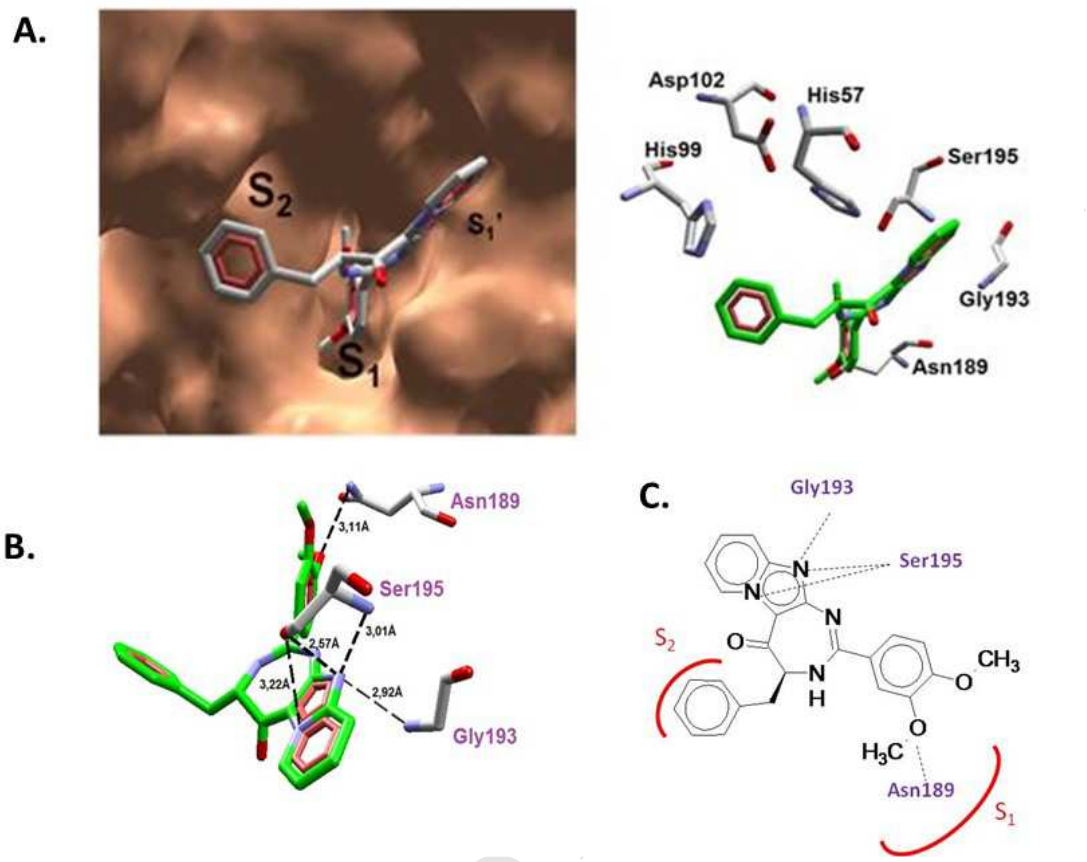

Figure 4. Putative binding mode of compound 1o within KLK7 active site.
A- Positioning of **1o** (CPK colors) in the $S_{1'}$, S_1 and S_2 pockets of KLK7. B-Residues (sticks, carbon in gray) nearby of **1o** (sticks, carbon in green). Hydrogen bonds (black dotted lines) between residues Asn189, Gly193, Ser195 and **1o**. C- Binding topology of compound **1o** within the KLK7 active site. The protease surfaces are colored in light brown and the ligands are shown in stick representation. Subsites S_1, $S_{1'}$ and S_2 are indicated. The chymotrypsinogen numbering is used; the residues Ser195, His57 and Asp102 form the catalytic triad.

Pyrido-imidazodiazepinone as a new chemical scaffold for designing KLK7 inhibitors

Selective non-covalent inhibitors of human kallikrein 7

Cytotoxicity evaluation against cancer cells lines overexpressing KLK7

Potential starting points for the development of anticancer drugs

SUPPORTING INFORMATION

PYRIDO-IMIDAZODIAZEPINONES AS A NEW CLASS OF REVERSIBLE INHIBITORS OF HUMAN KALLIKREIN 7

Dominique P. Arama,[a†] Feryel Soualmia,[b†] Vincent Lisowski,[a] Jean-François Longevial,[a] Elodie Bosc[b], Ludovic T. Maillard,[a] Jean Martinez,[a] Nicolas Masurier[a]*, Chahrazade El Amri[b]*.

[a] Institut des Biomolécules Max Mousseron, UMR 5247, CNRS, Université de Montpellier, UFR des Sciences Pharmaceutiques et Biologiques, 15 Avenue Charles Flahault, 34093 Montpellier Cedex 5, France

[b] Sorbonne Universités, UPMC Univ Paris 06, UMR 8256, B2A, Biological Adaptation and Ageing, Integrated Cellular Ageing and Inflammation, Molecular & Functional Enzymology, 7 Quai St Bernard, F-75005 Paris.

[†] These authors contributed equally to the work.

***Corresponding authors:** Nicolas Masurier. Tel: + (33) 4 11 75 96 42, Fax: + (33) 4 11 75 96 41, E-mail: nicolas.masurier@univ-montp1.fr; Chahrazade El Amri. Tel: + (33) 1 44 27 69 52, Fax: + (33) 44 27 51 40 , E-mail: chahrazade.el_amri@upmc.fr

Table of contents

A.

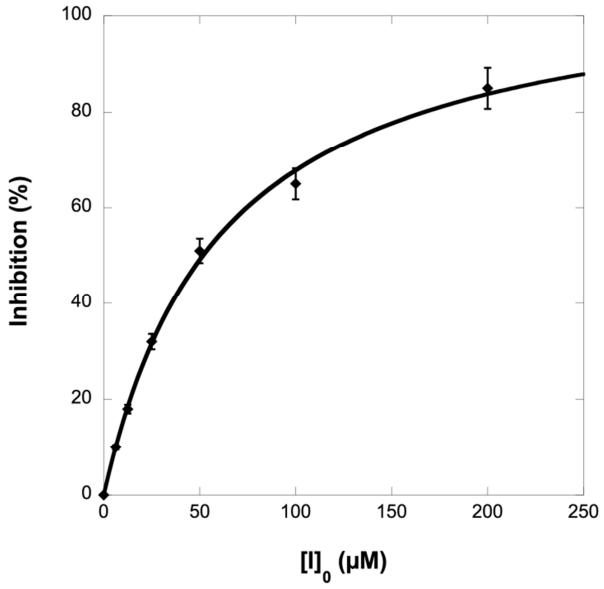

B.

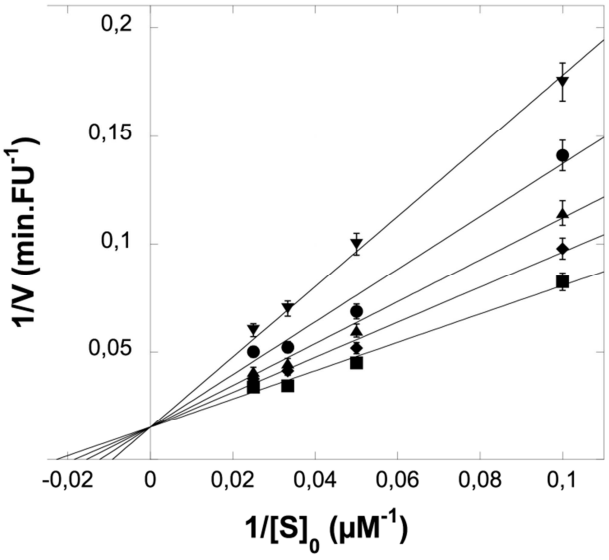

Figure S1. Inhibition of KLK7 by compound **1a**. **A.** IC_{50} determination after 15 min incubation at 37°C. Experimental points were fitted to equation 1.$[KLK7]_0$ = 7.6 nM; $[Succ\text{-}LLVY\text{-}AMC]_0$ = 40 µM. **B.** Determination of the mechanism of inhibition. Lineweaver and Burk plot with $[I]_0$ =▼, 50 µM; ●, 25 µM; ▲, 12.5 µM; ◆, 6.25 µM;■, 0 µM. F.U = arbitrary fluorescence unit.

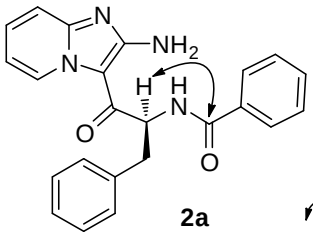

2a : ^{1}H-^{13}C HMBC correlation

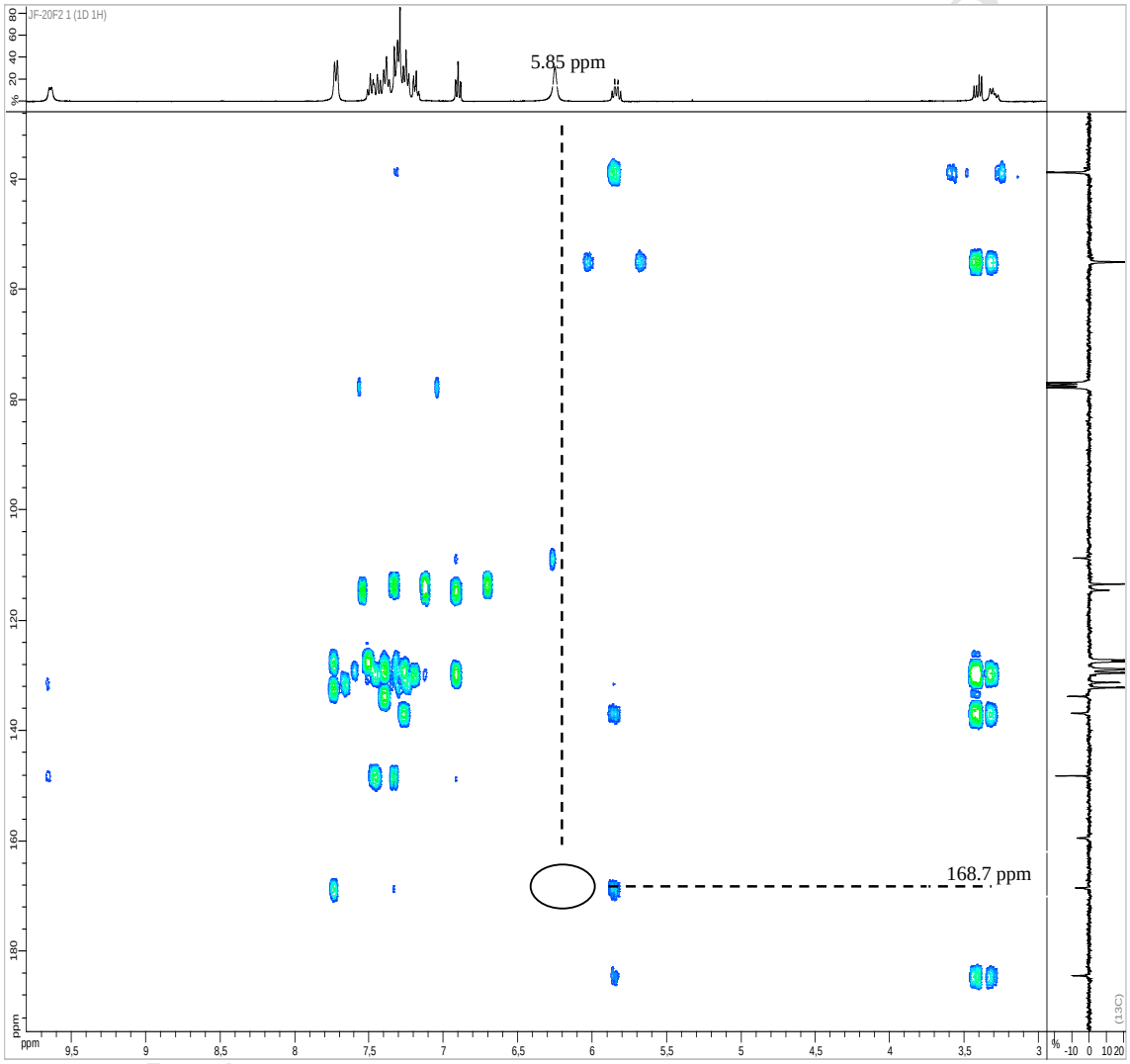

Figure S2. ^{1}H-^{13}C HMBC NMR spectrum of compound **2a** in $CDCl_3$.

Compound **4d** ($CDCl_3$, 300MHz)

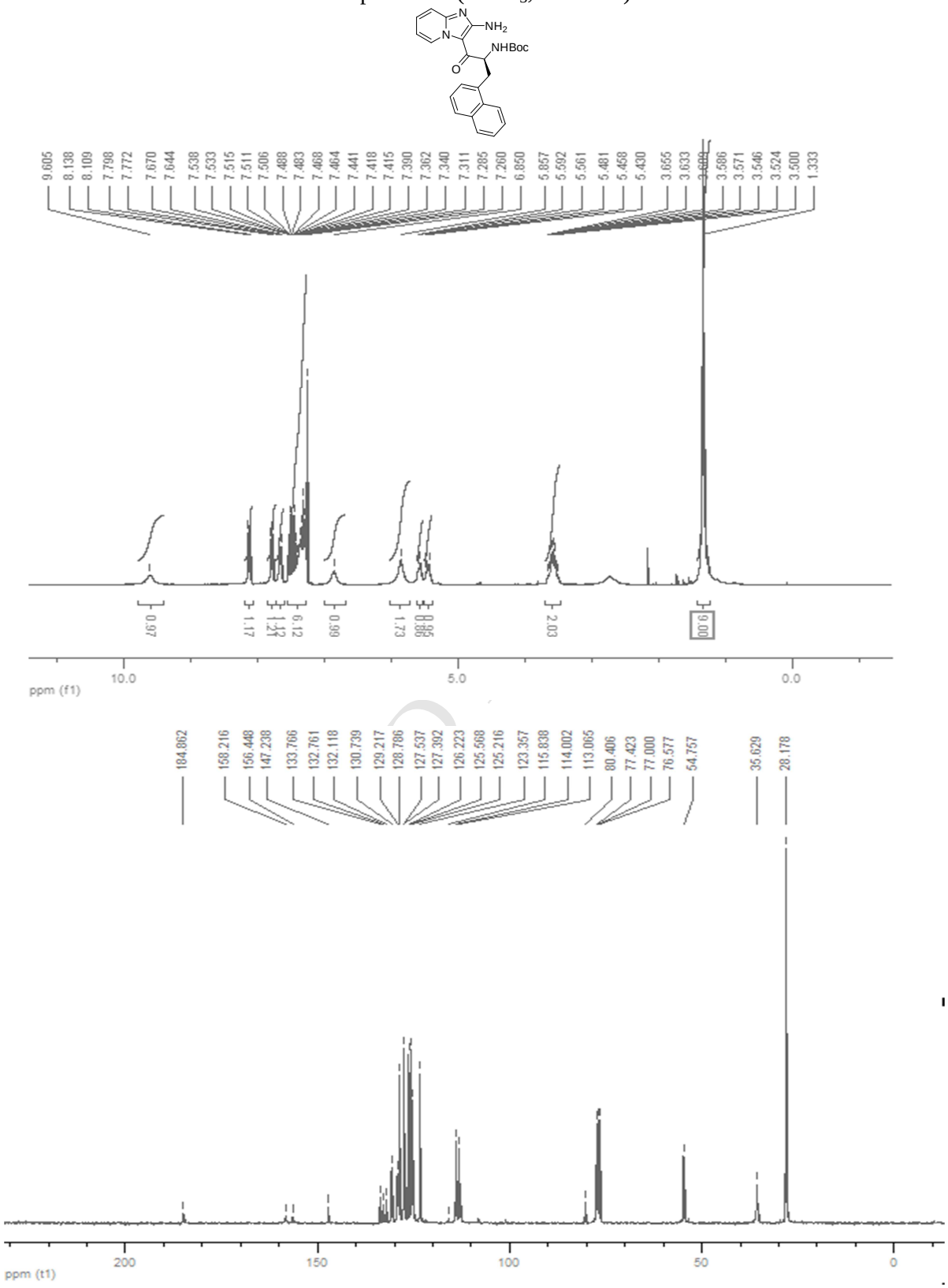

Compound **4e** ($CDCl_3$, 300MHz)

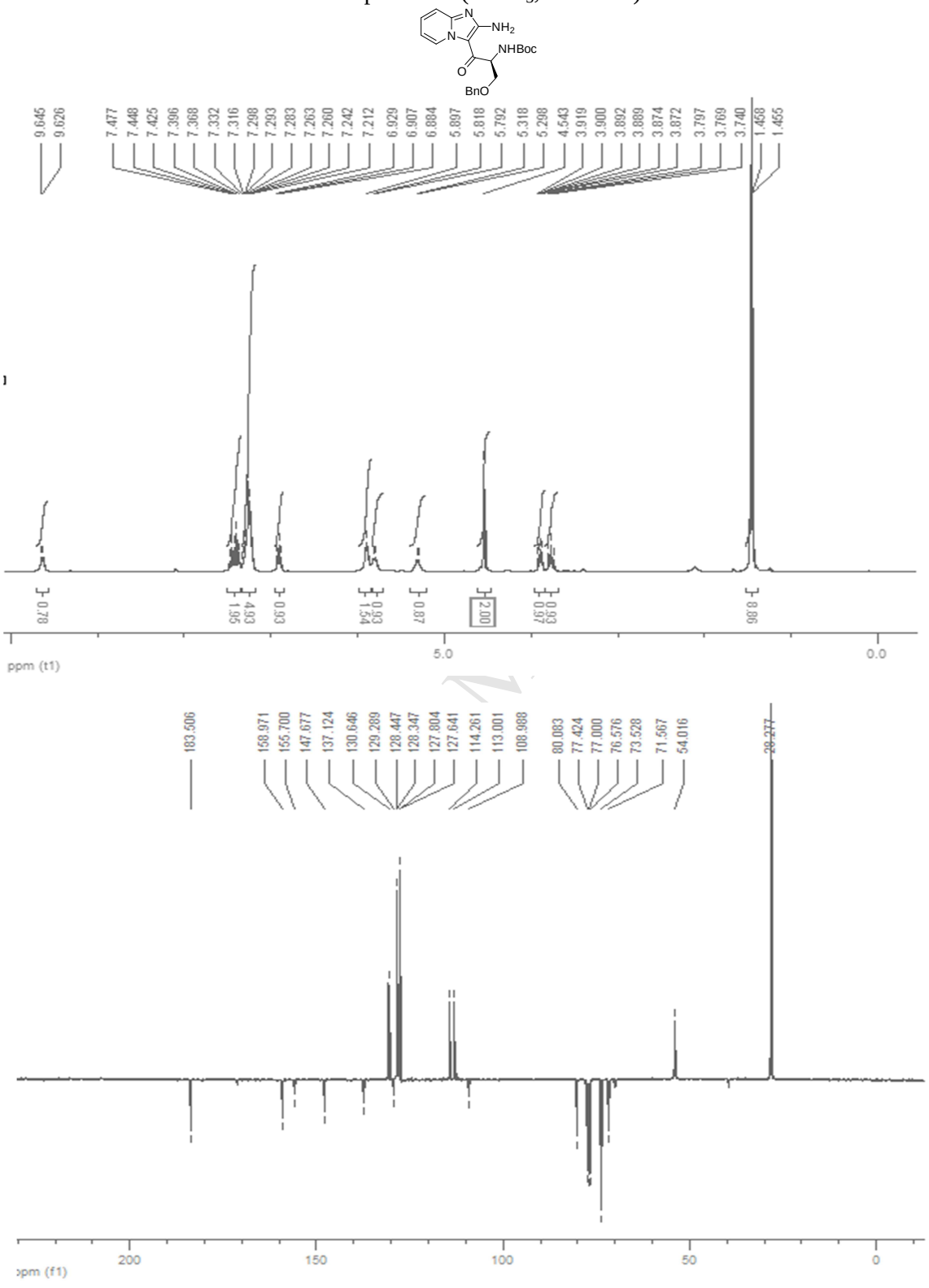

Compound **4f** ($CDCl_3$, 300MHz)

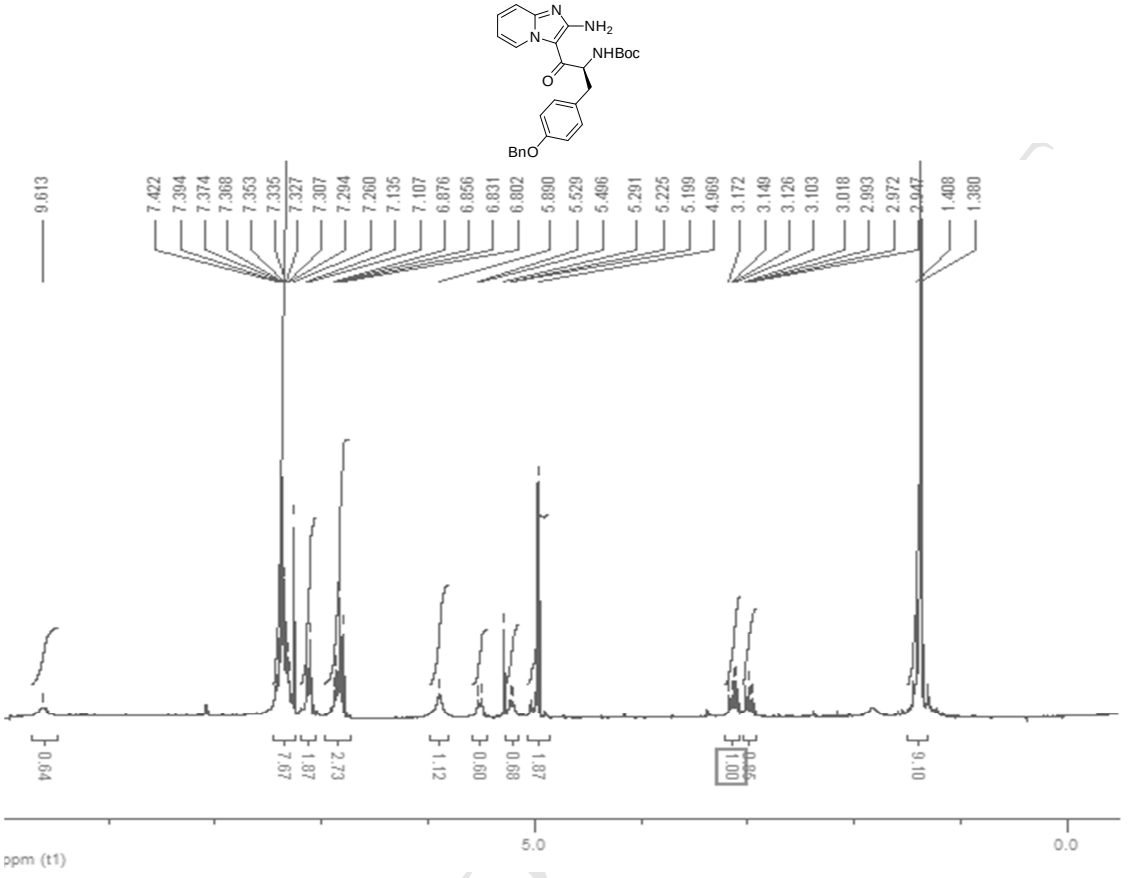

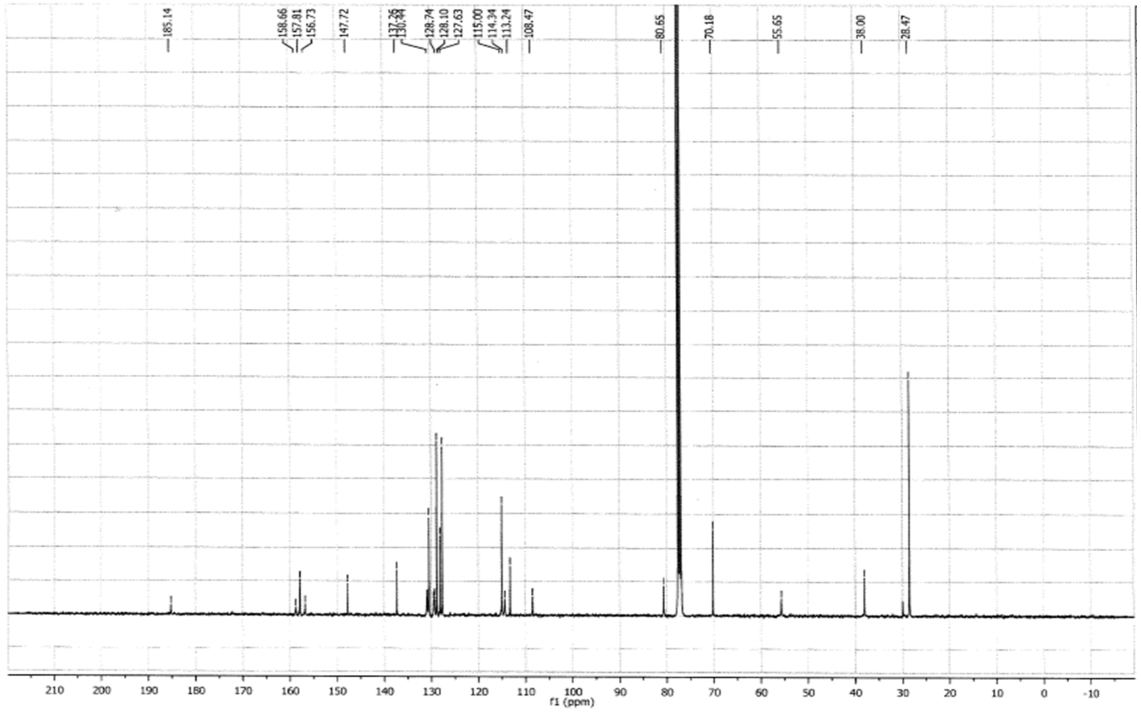

Compound **4g** ($CDCl_3$, 300MHz)

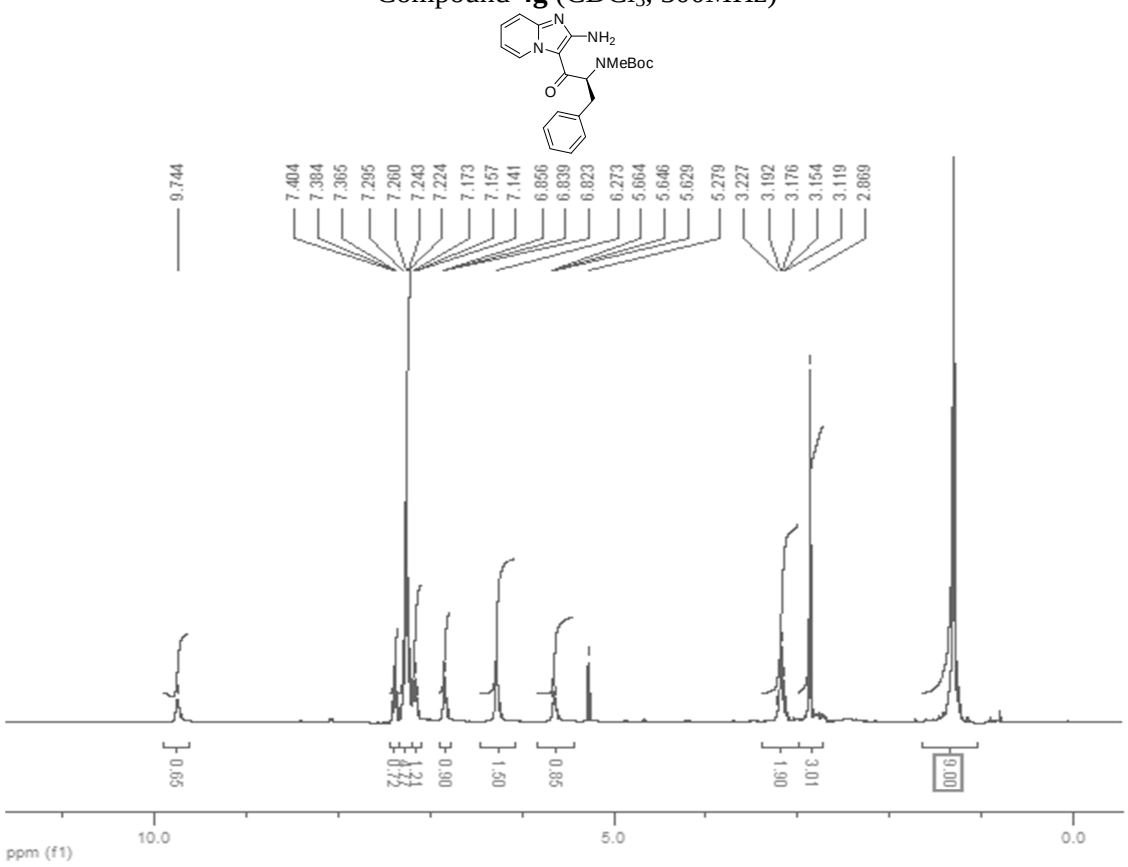

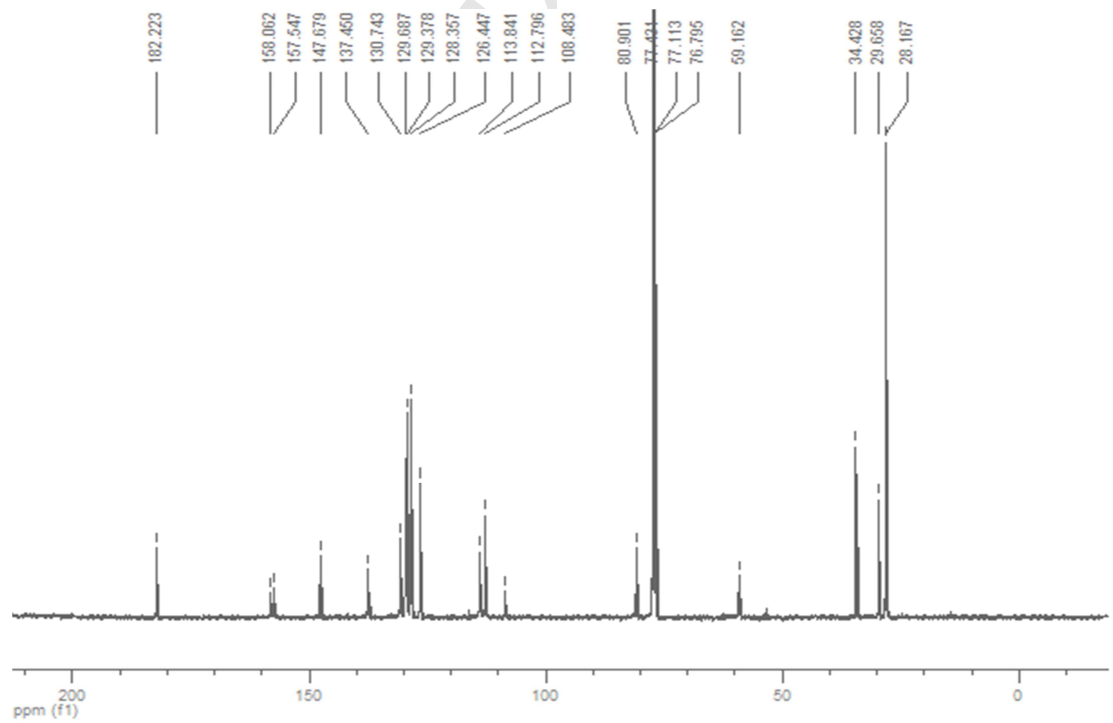

Compound **1k** ($CDCl_3$, 300MHz)

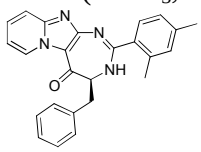

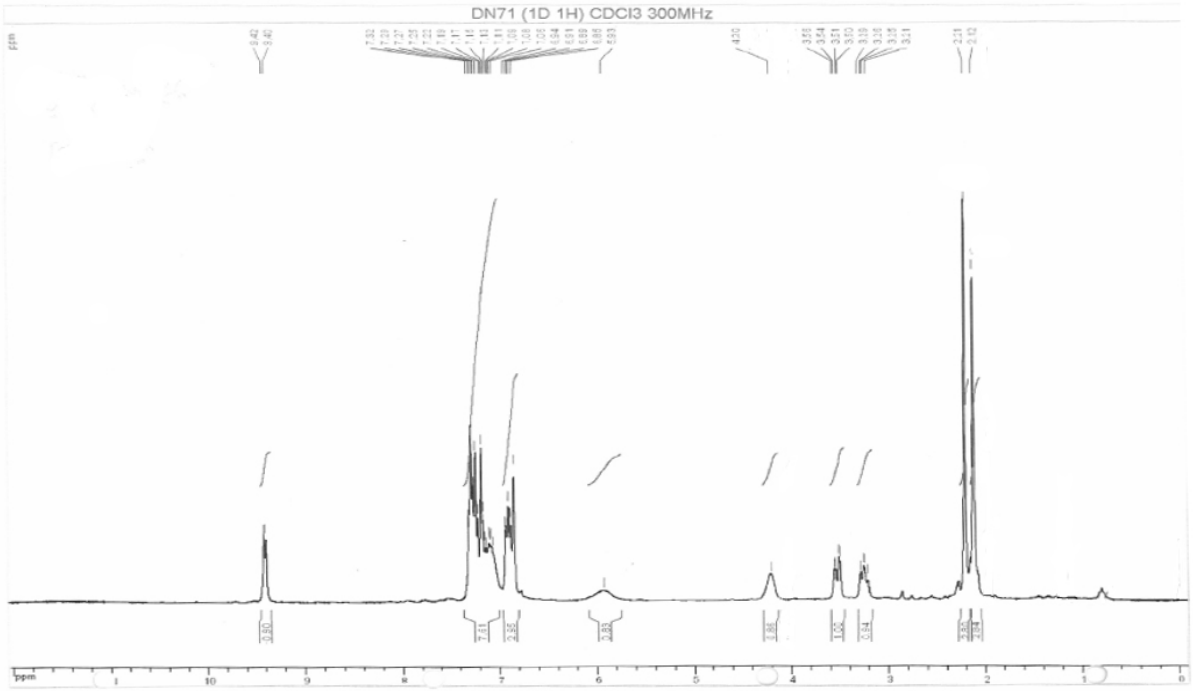

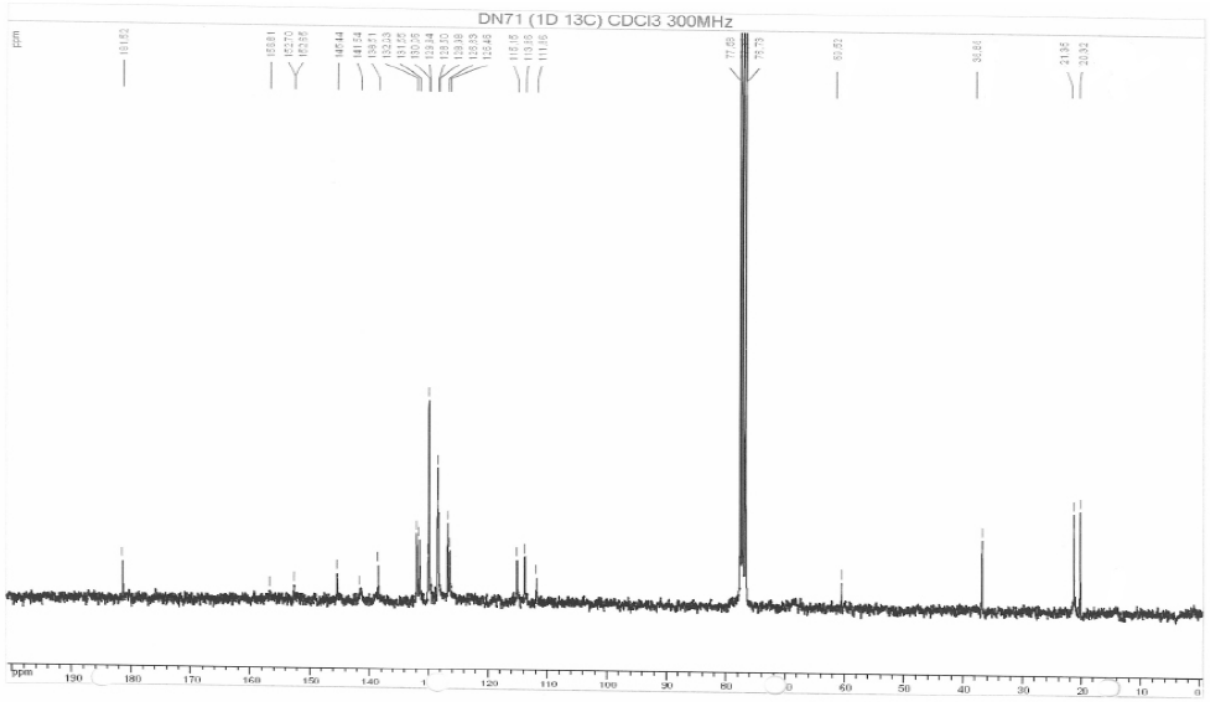

Compound **1l** ($CDCl_3$, 300MHz)

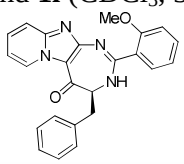

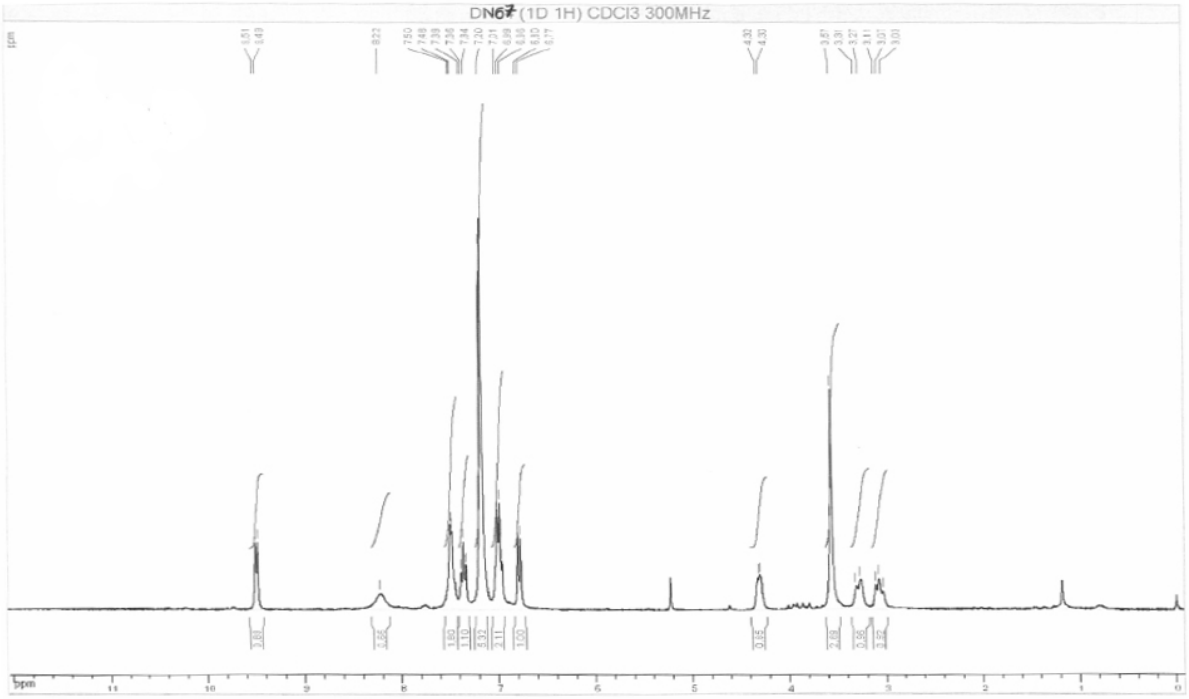

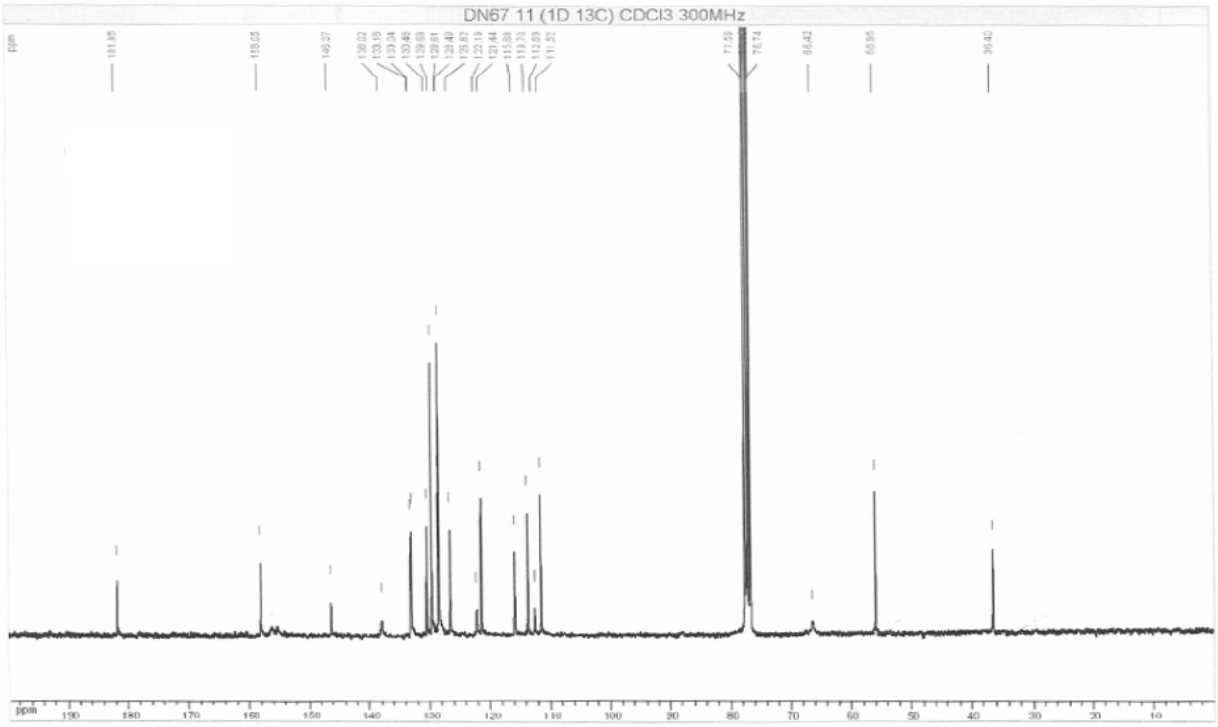

Compound **1m** (DMSO d_6, 400MHz)

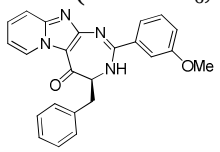

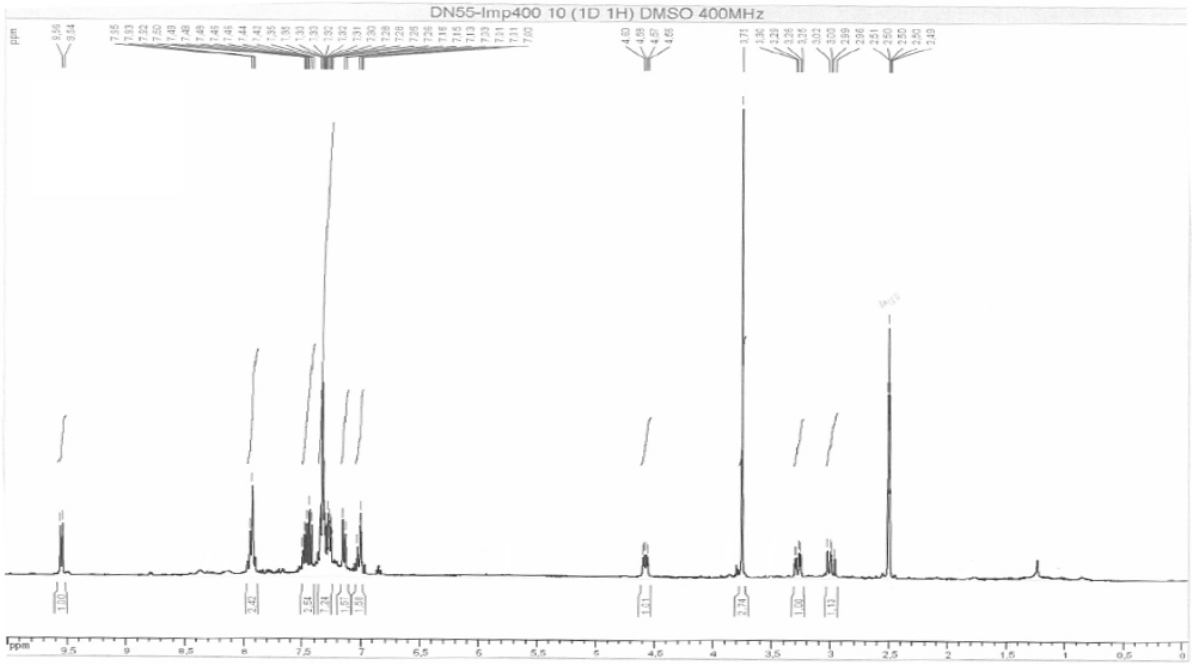

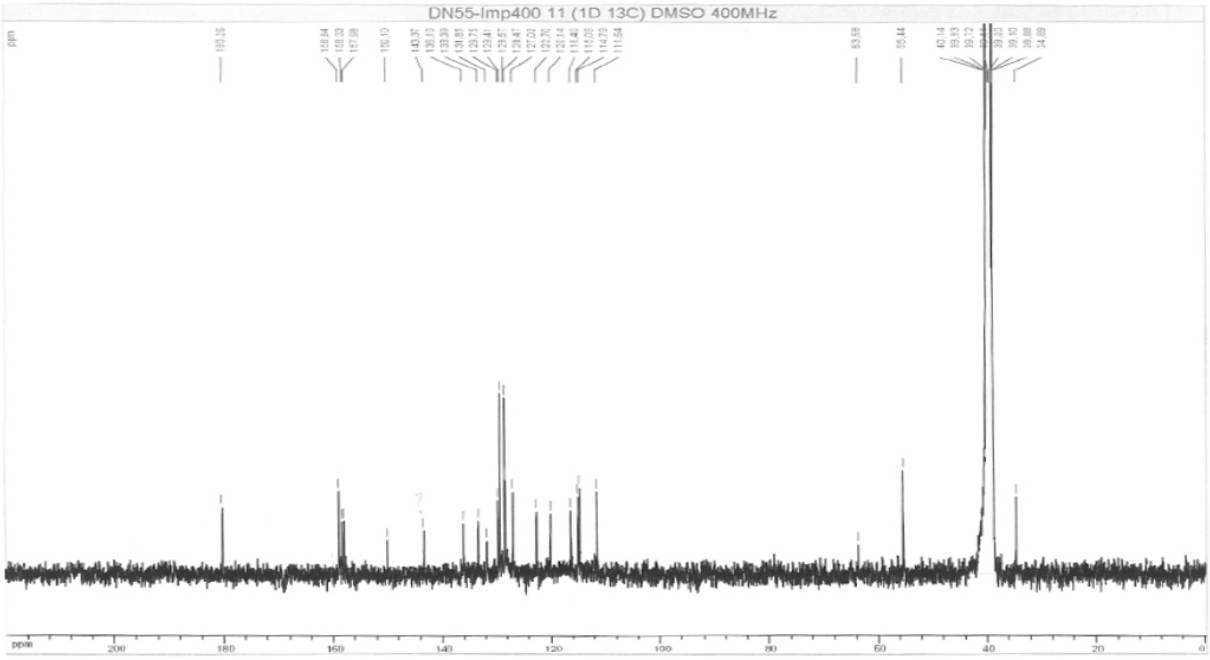

Compound **1n** ($CDCl_3$, 300MHz)

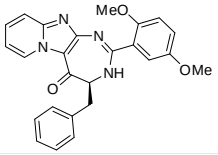

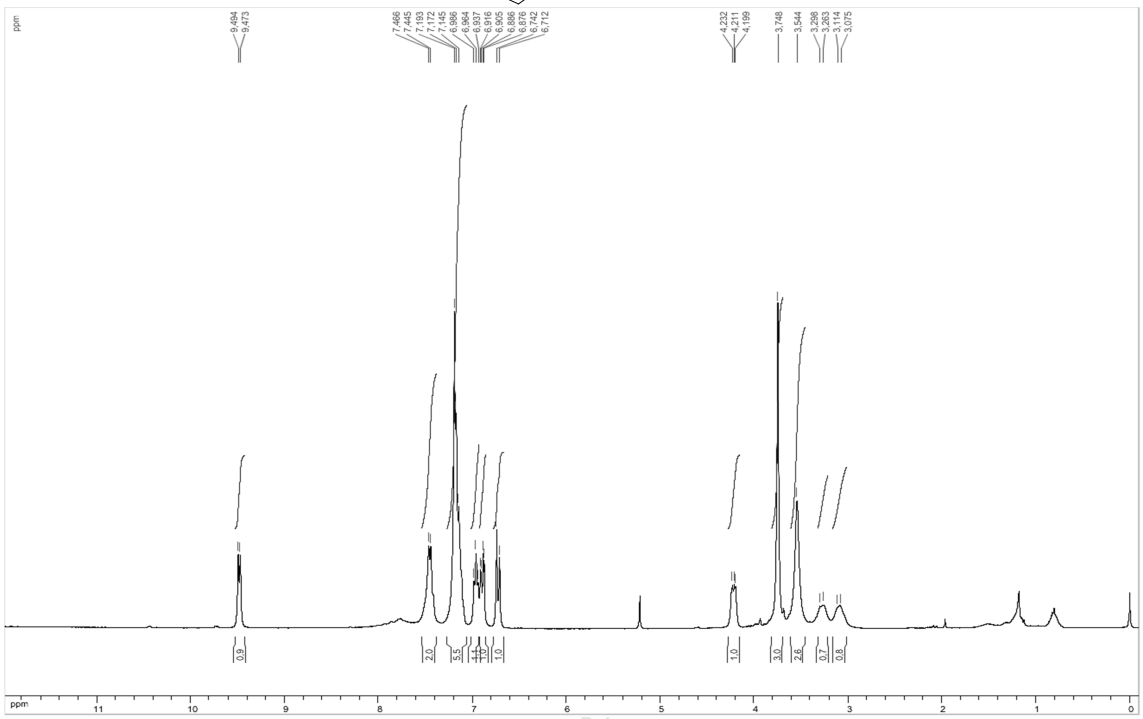

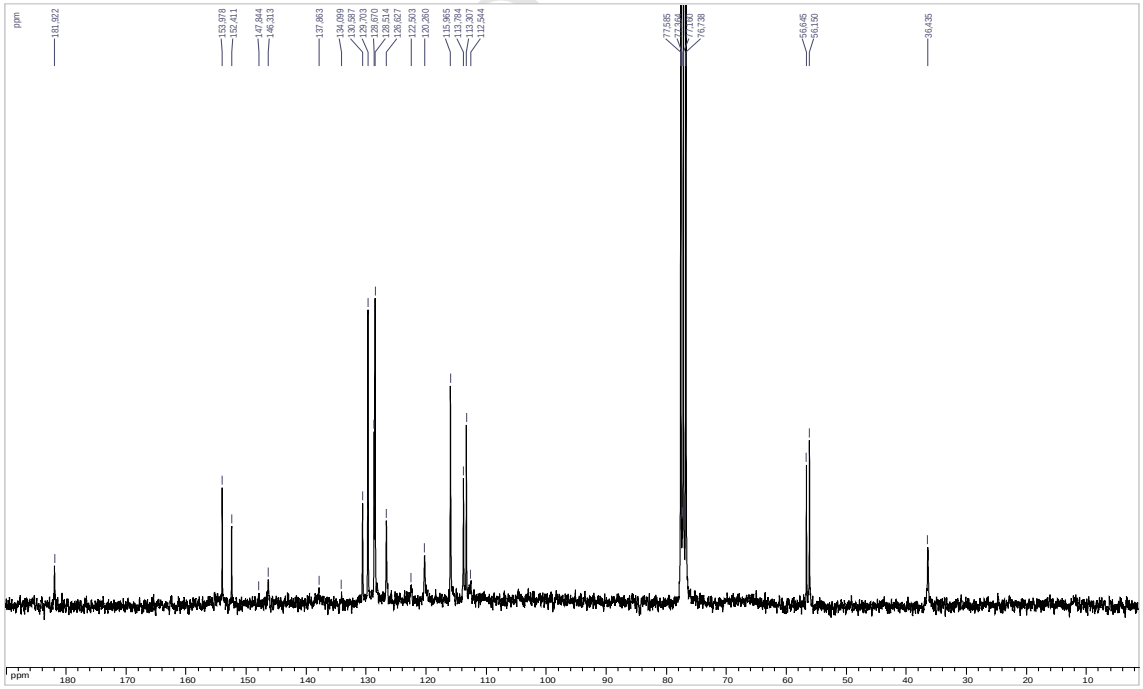

Compound **1o** (DMSO d_6, 400MHz)

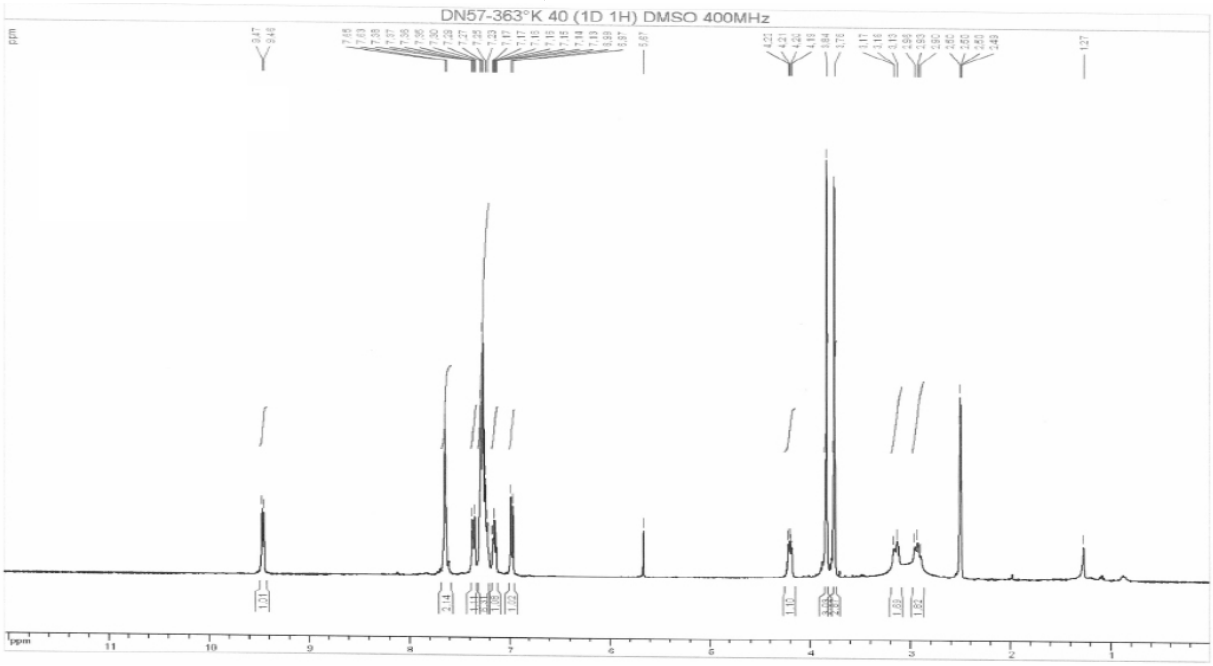

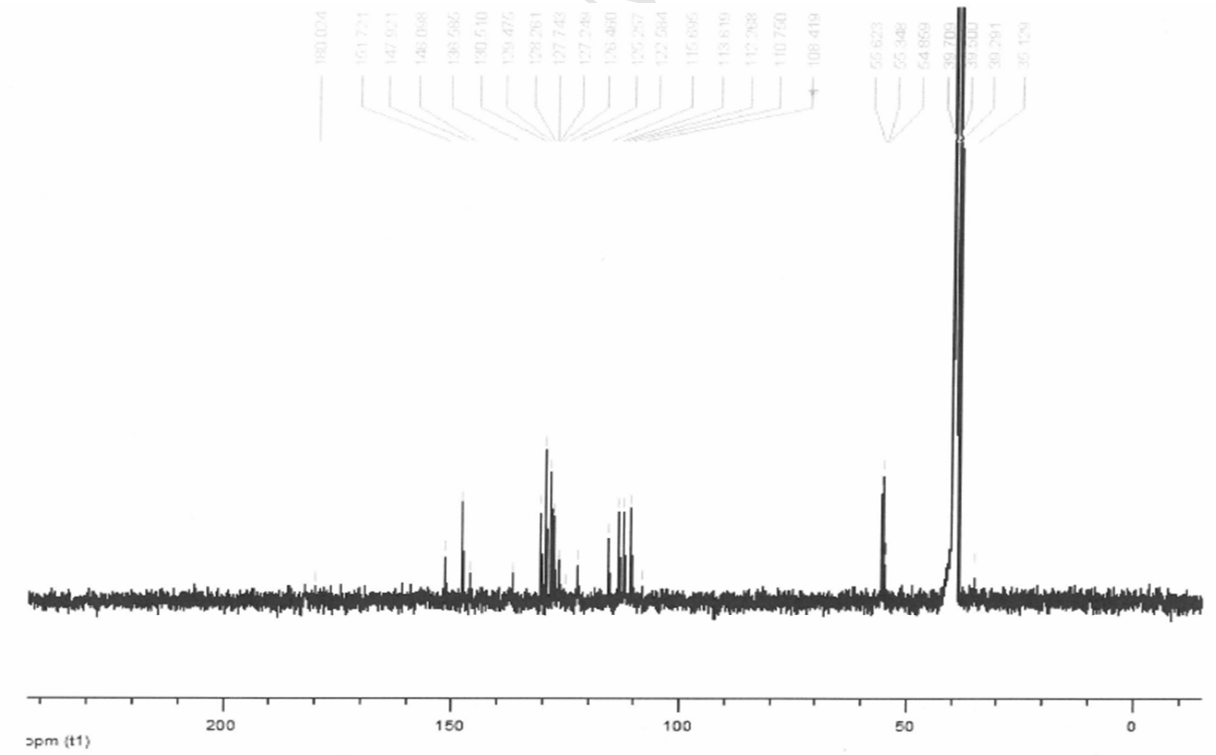

Compound **1p** ($CDCl_3$, 300MHz)

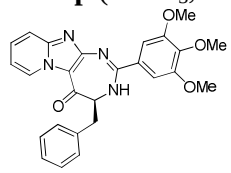

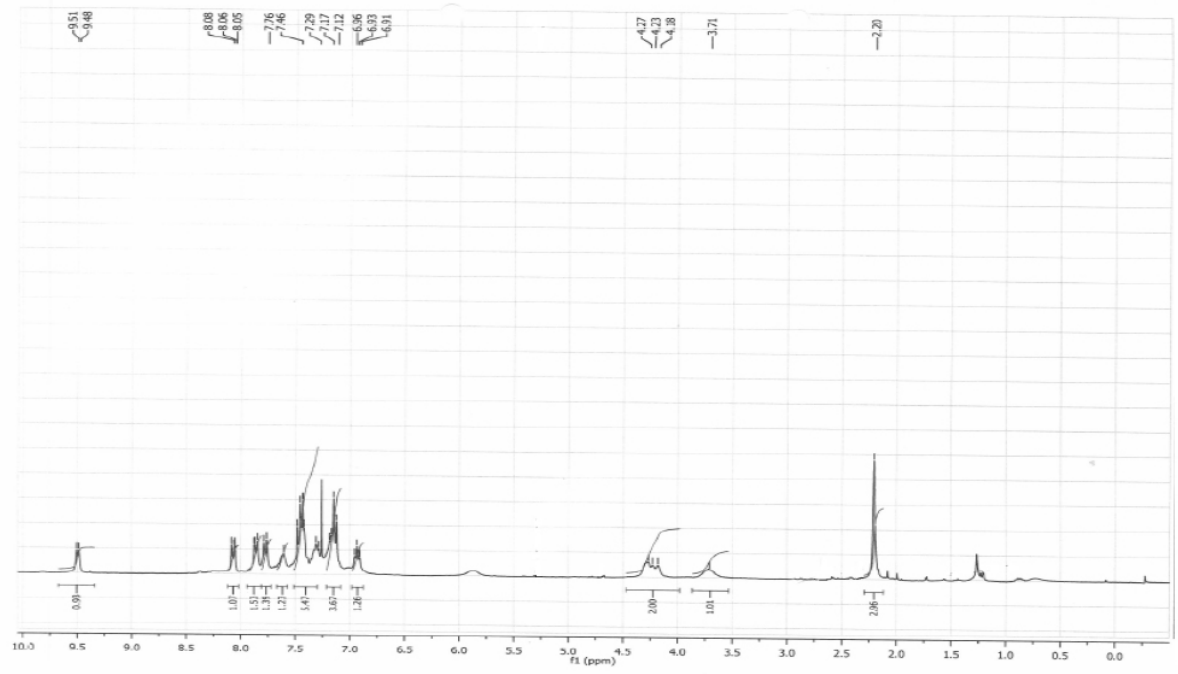

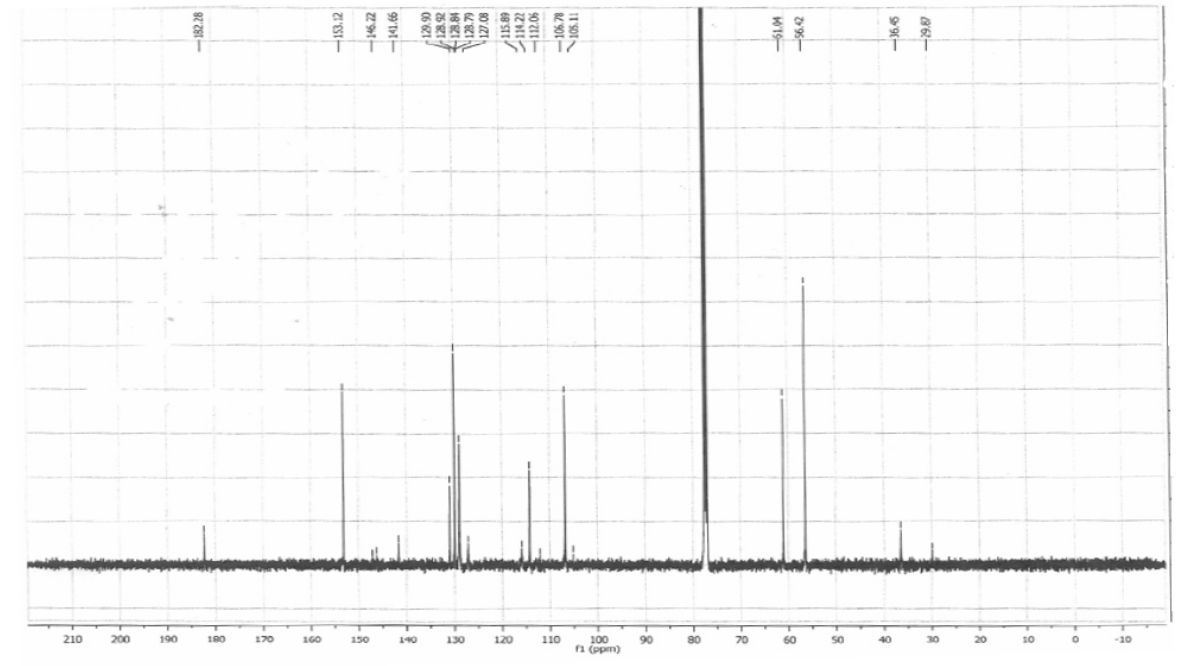

Compound **1q** ($CDCl_3$, 300MHz)

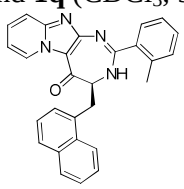

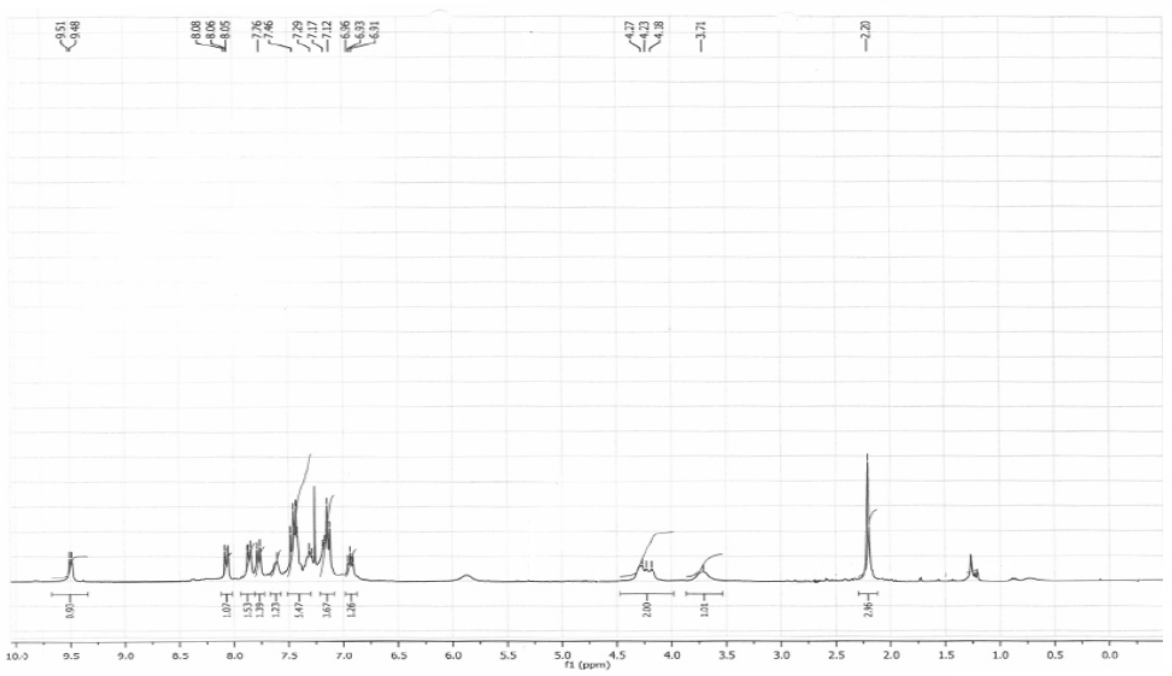

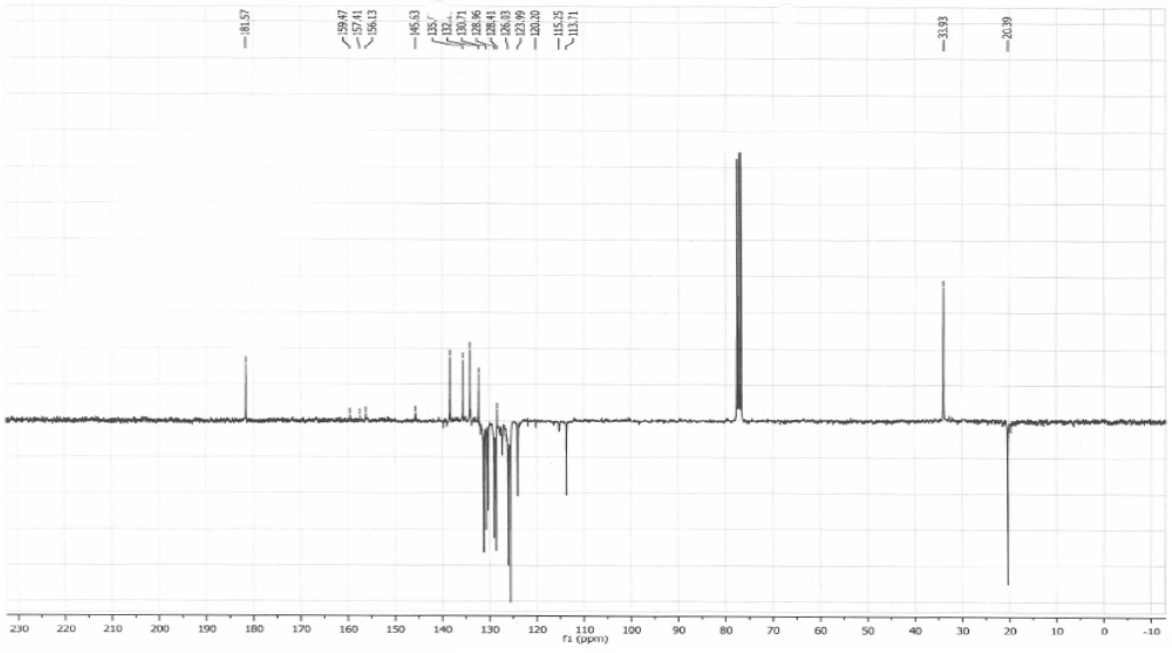

Compound **1r** ($CDCl_3$, 300MHz)

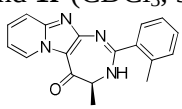

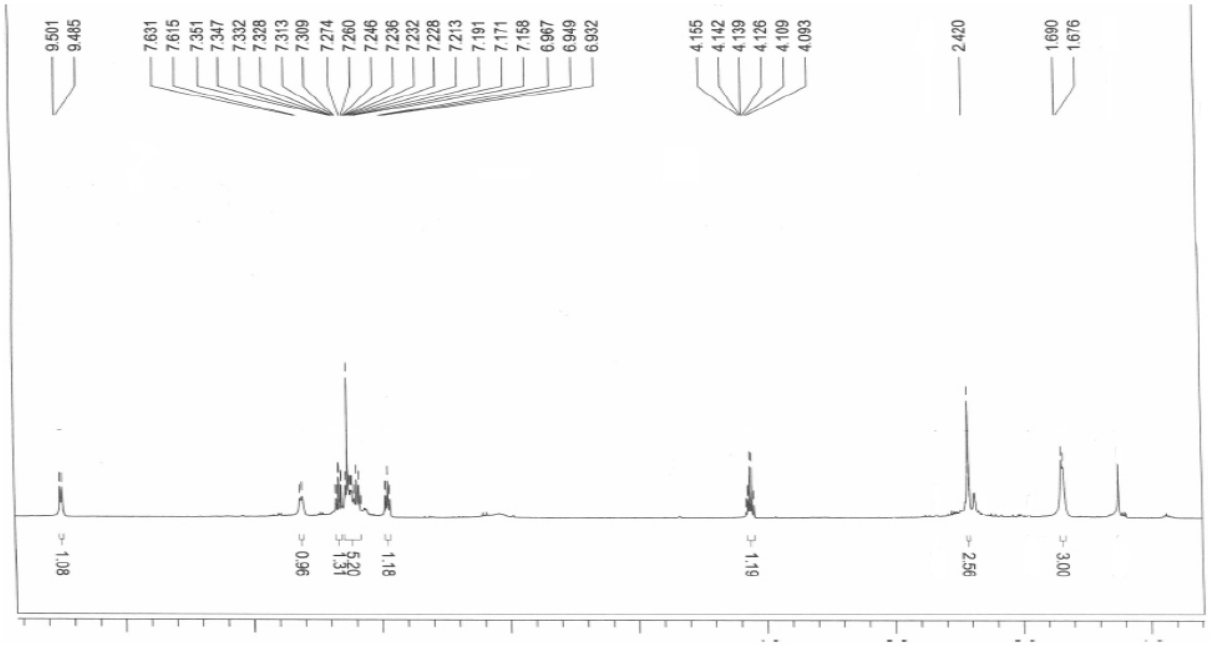

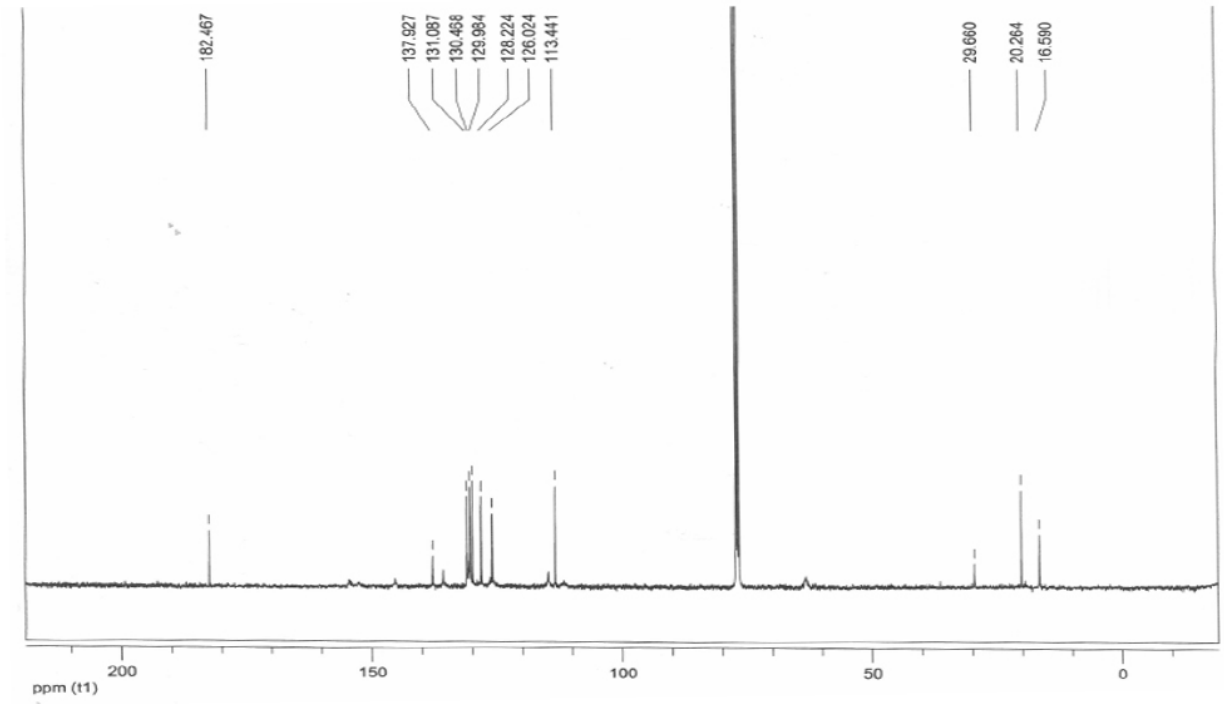

Compound **1s** ($CDCl_3$, 300MHz)

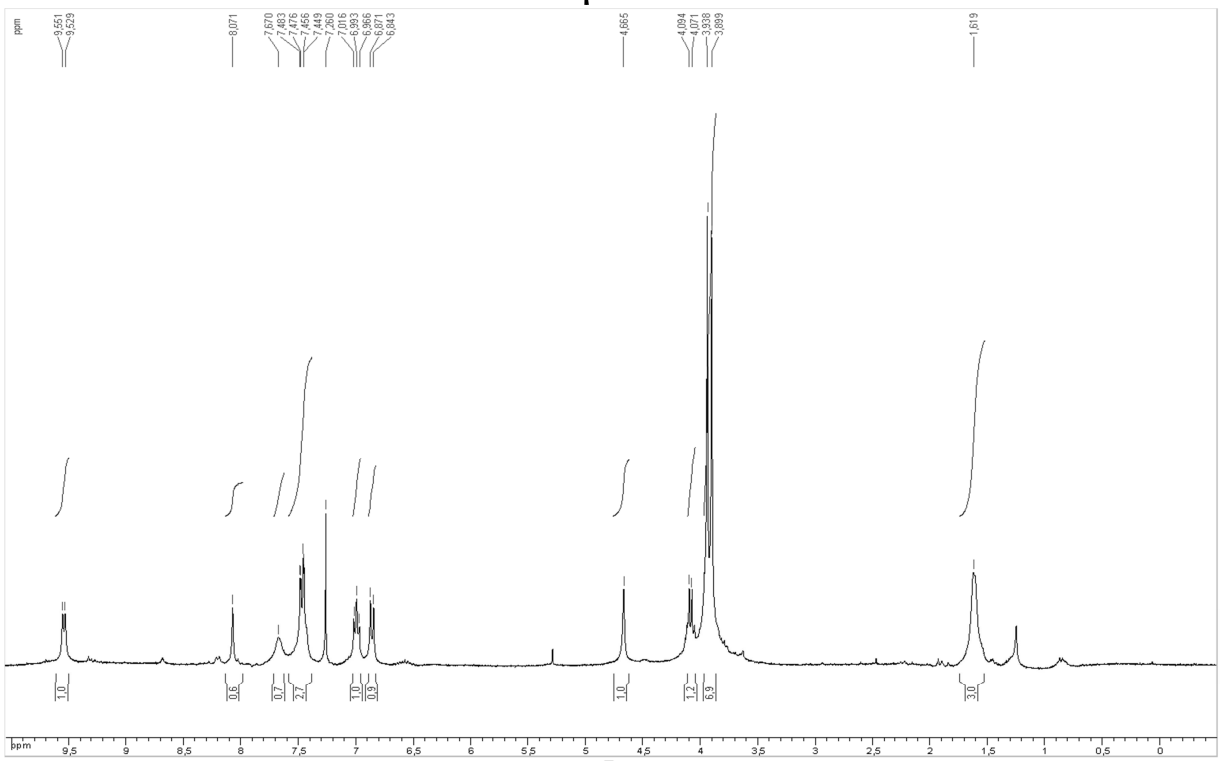

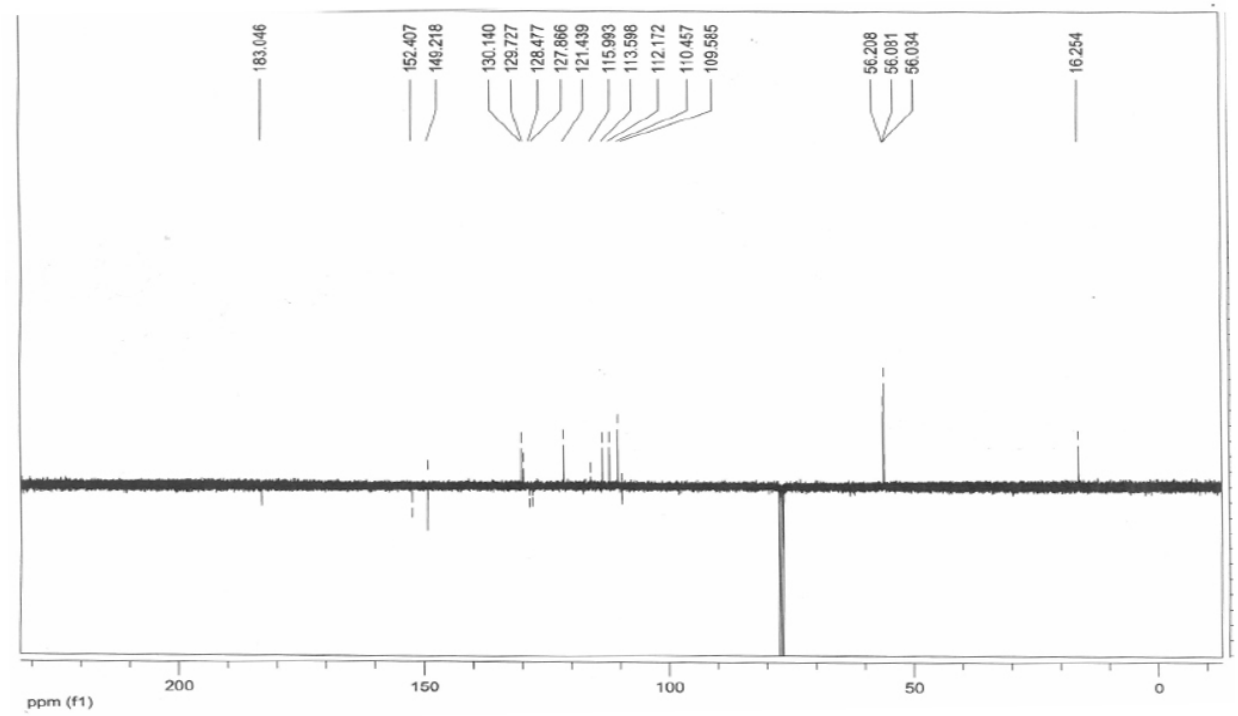

Compound **1t** ($CDCl_3$, 300MHz)

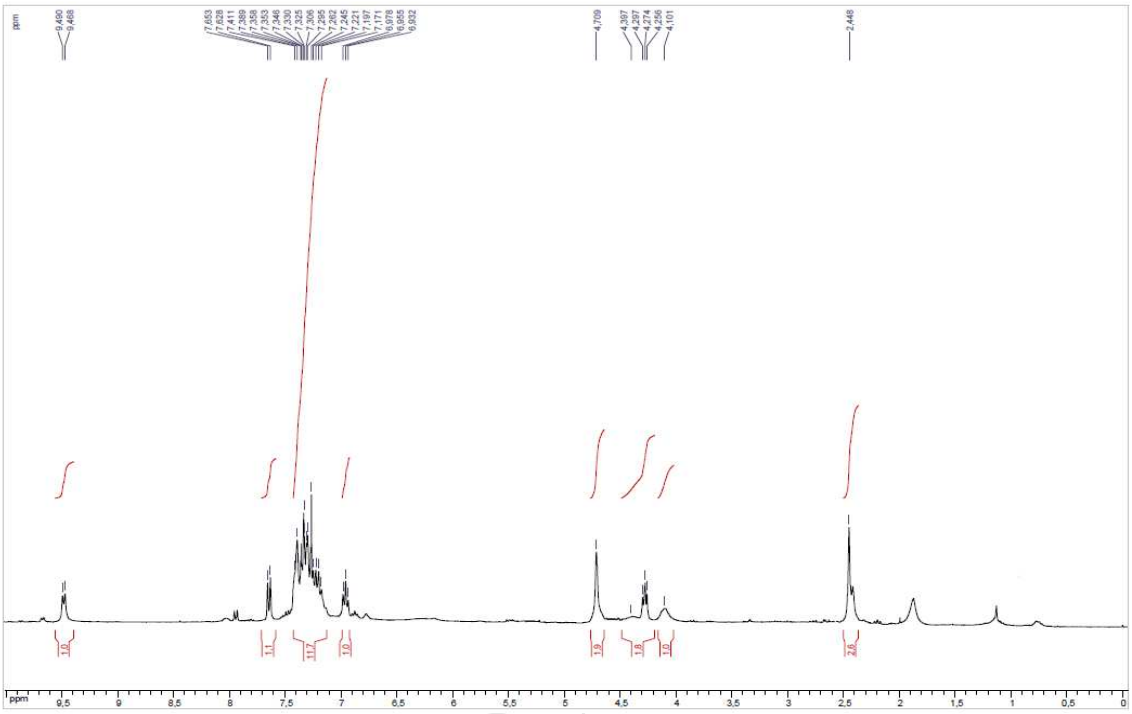

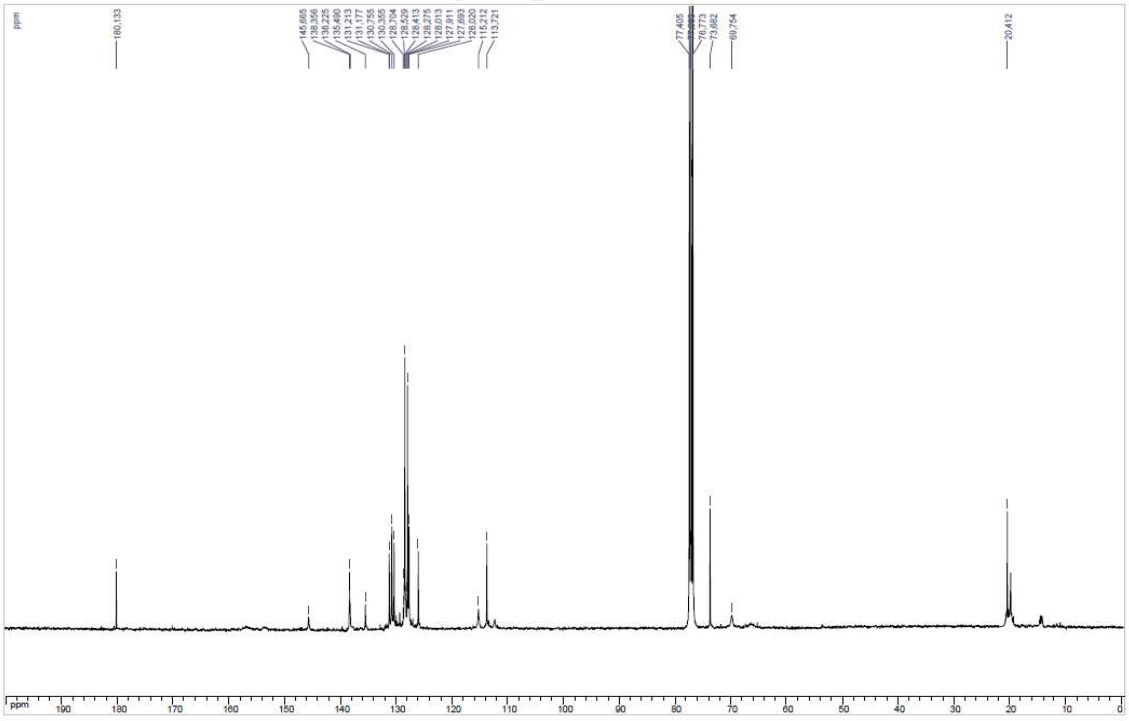

Compound **1u** ($CDCl_3$, 300MHz)

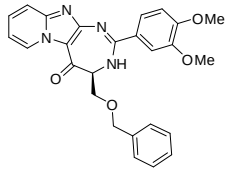

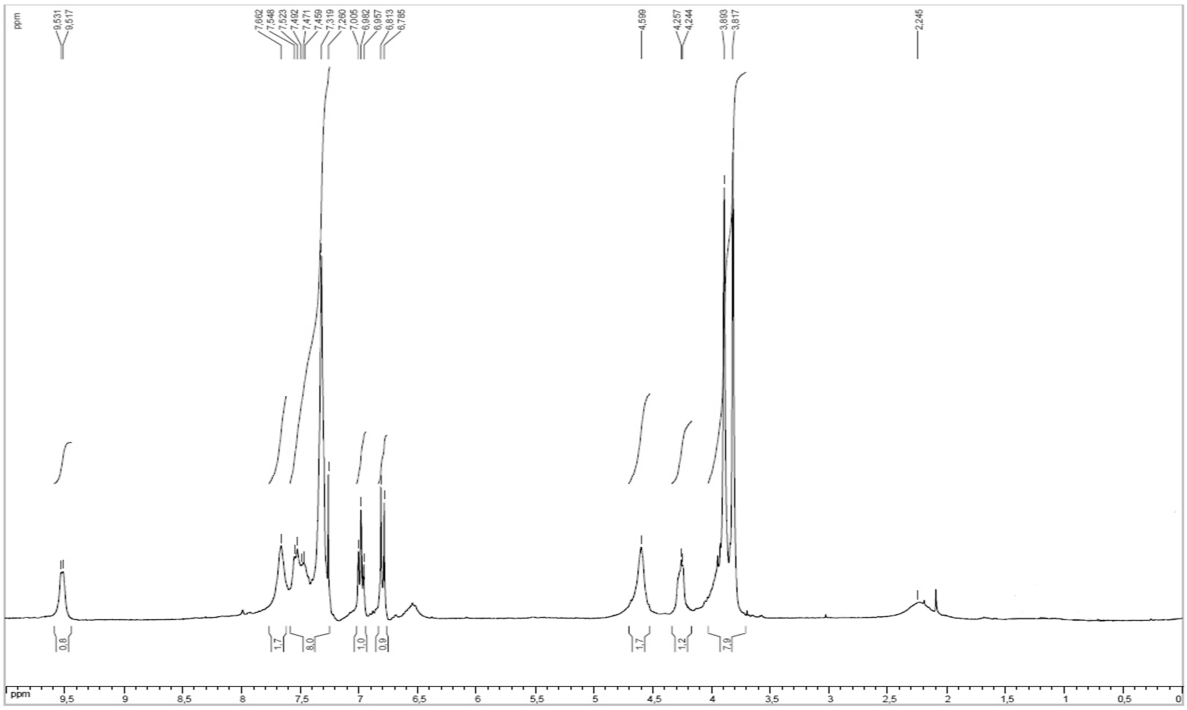

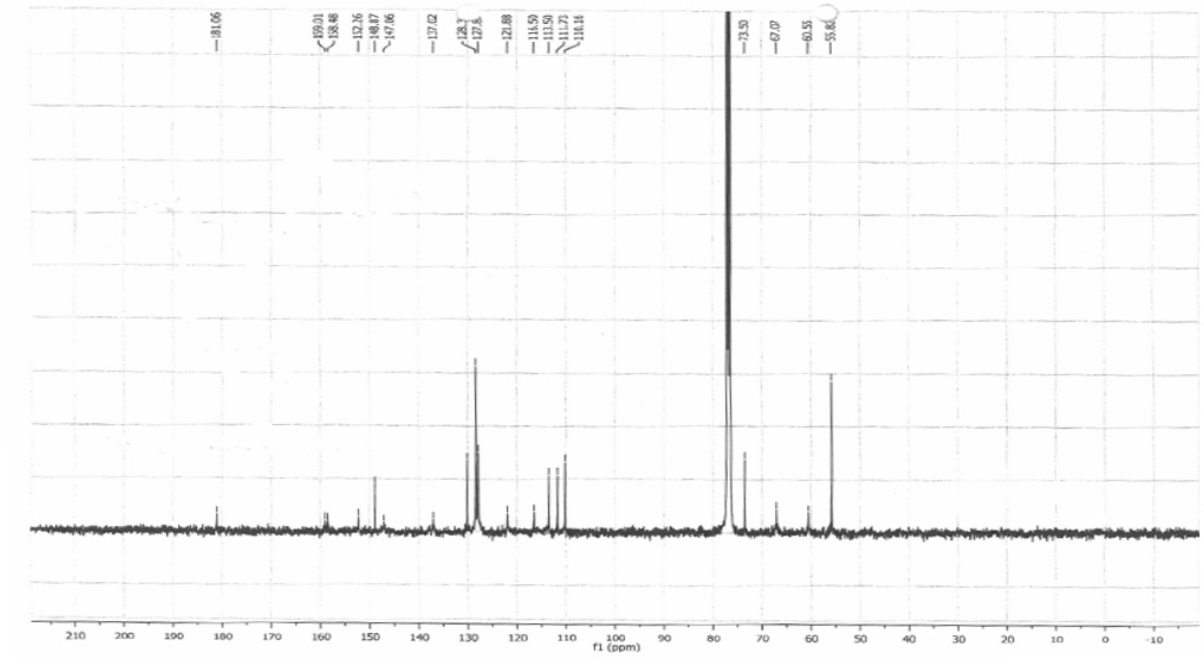

Compound **1v** (DMSO d_6, 300MHz)

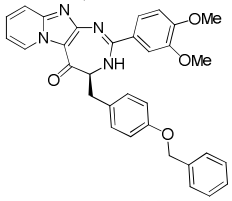

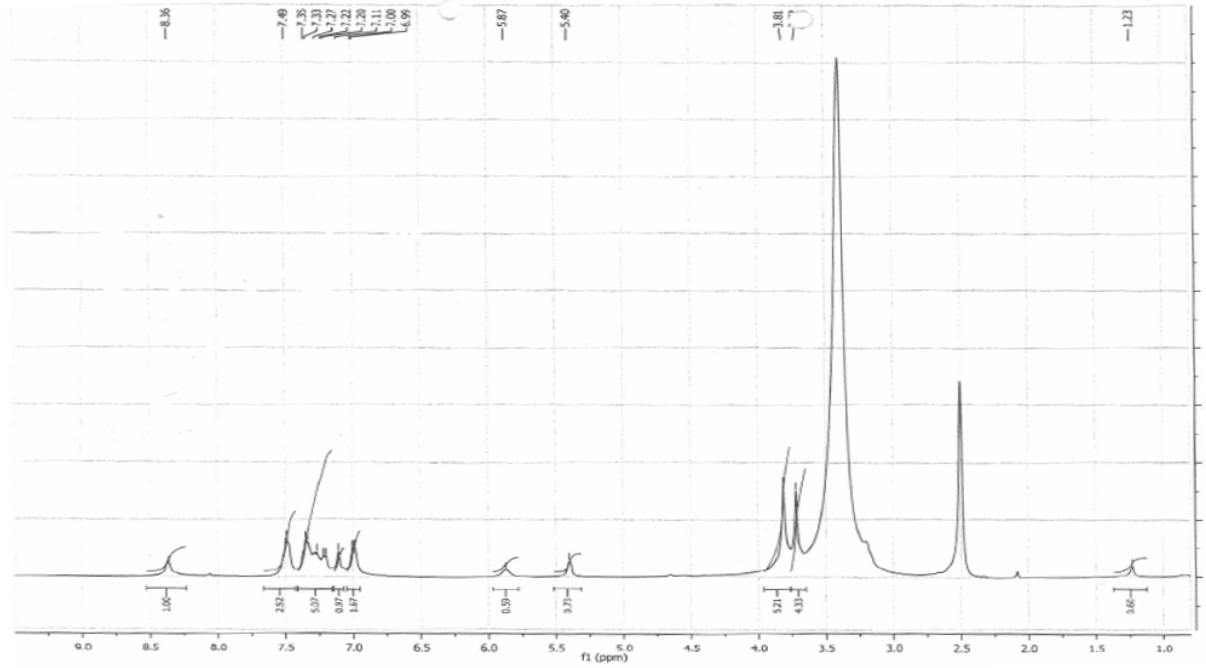

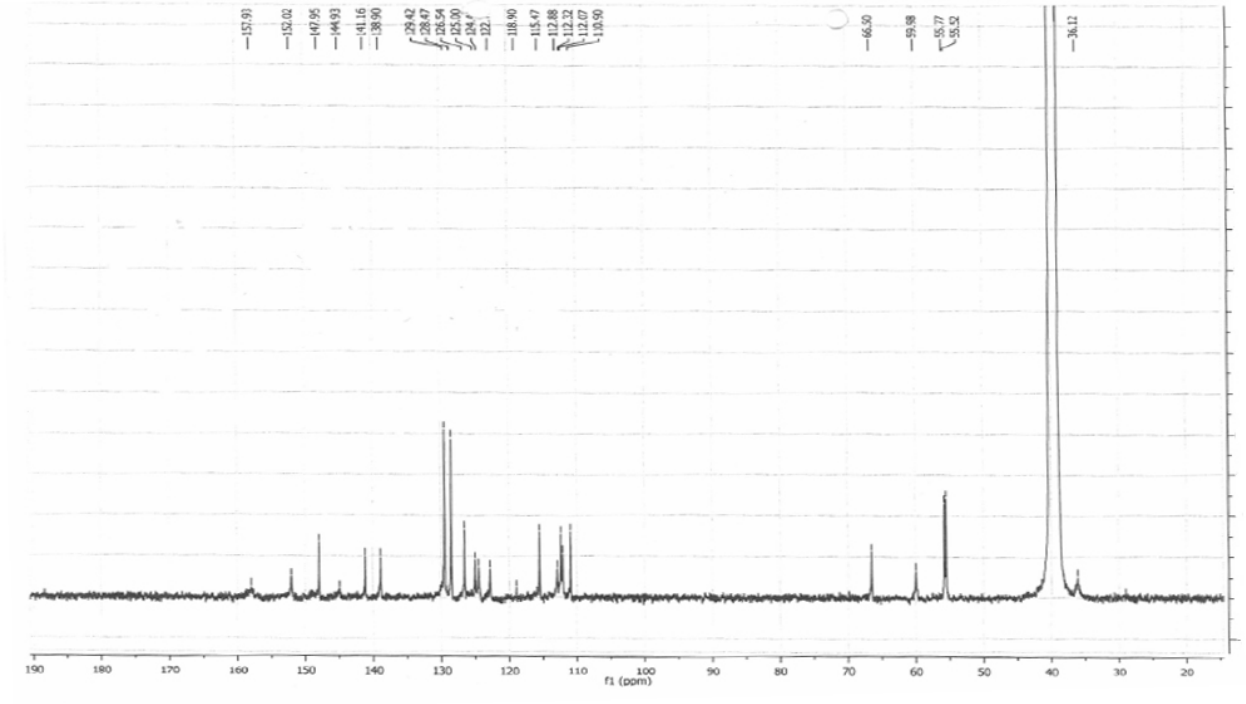

Compound **1w** ($CDCl_3$, 300MHz)

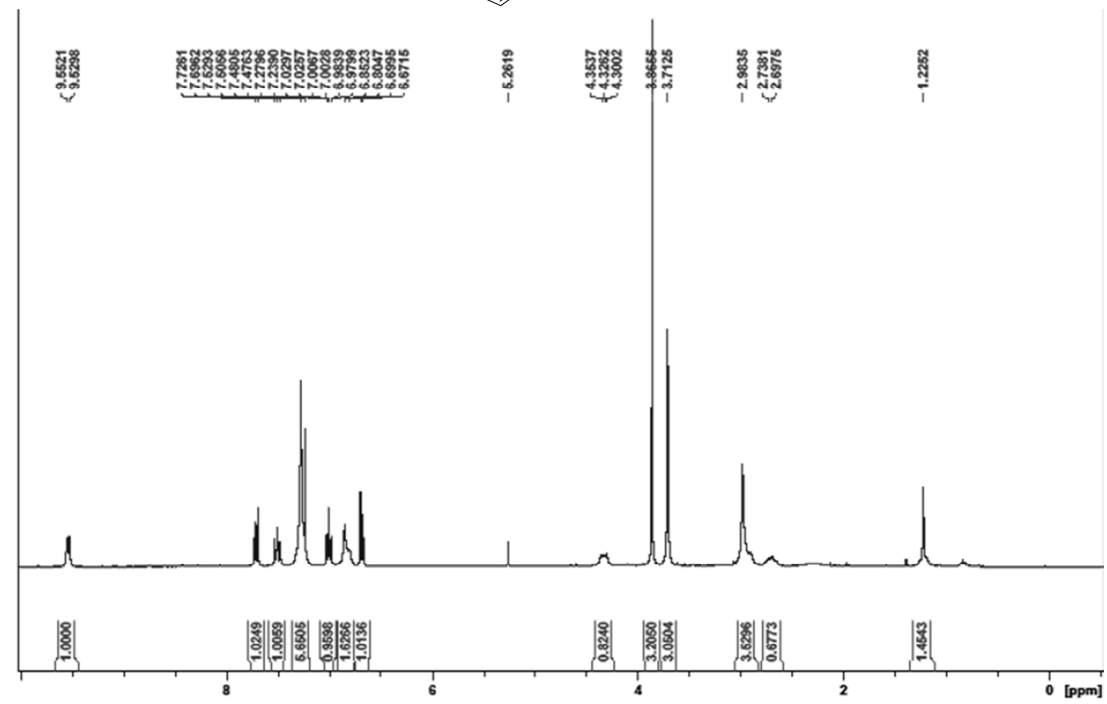

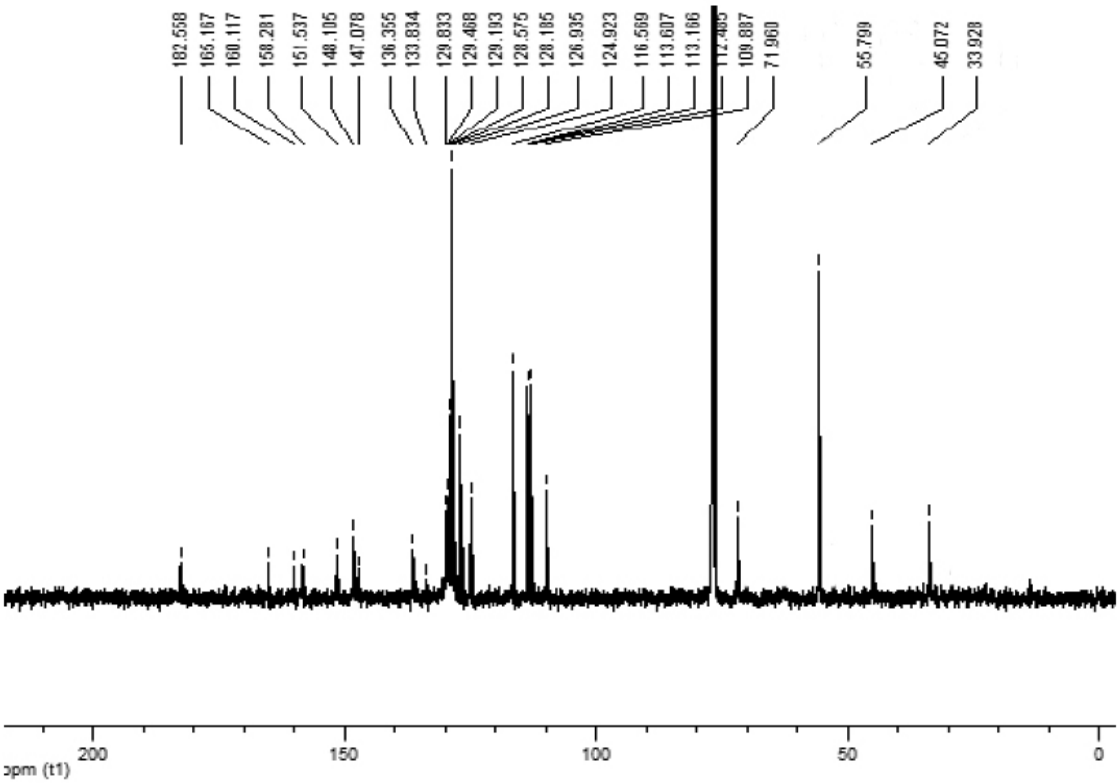

Compound **1x** (DMSO d_6, 300MHz)

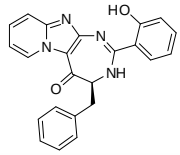

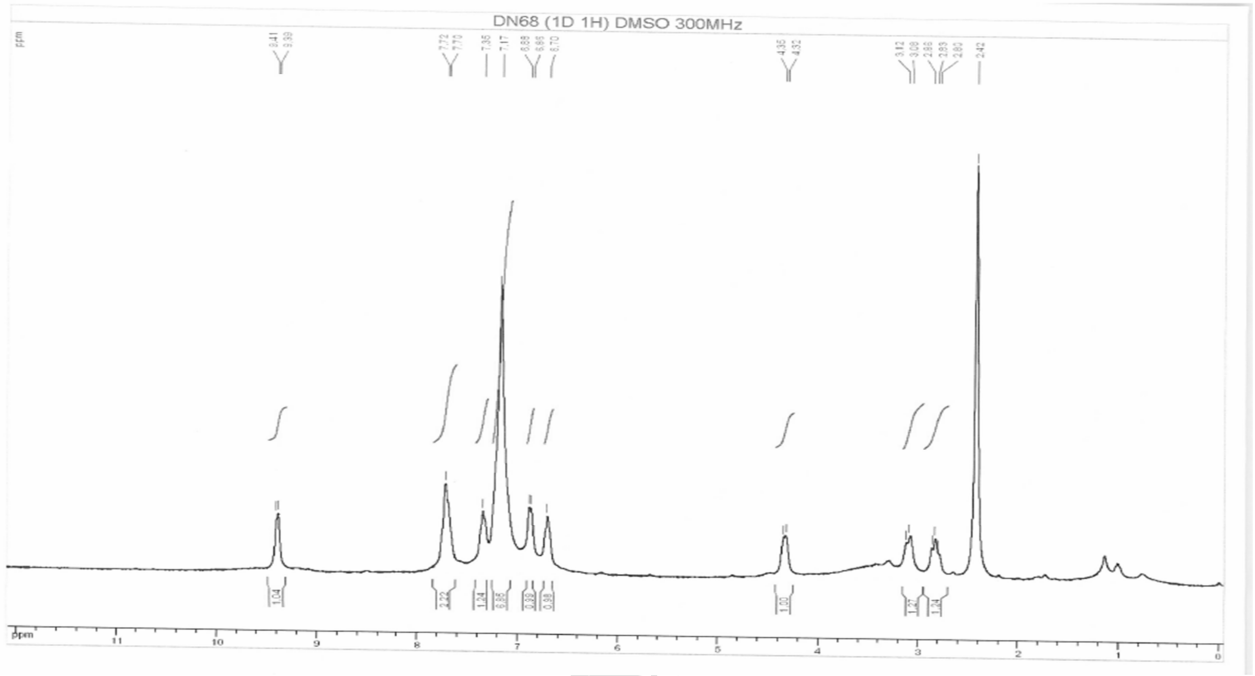

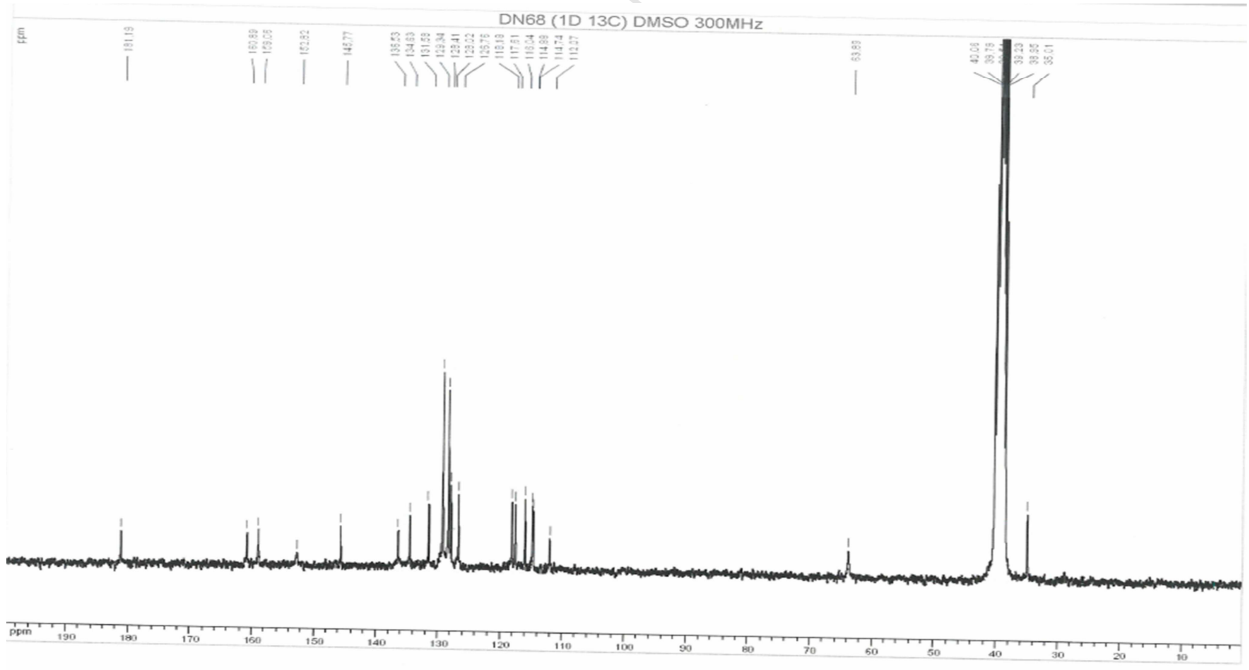

Compound **1y** (MeOD, 300MHz)

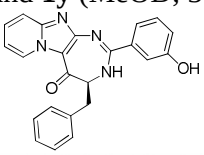

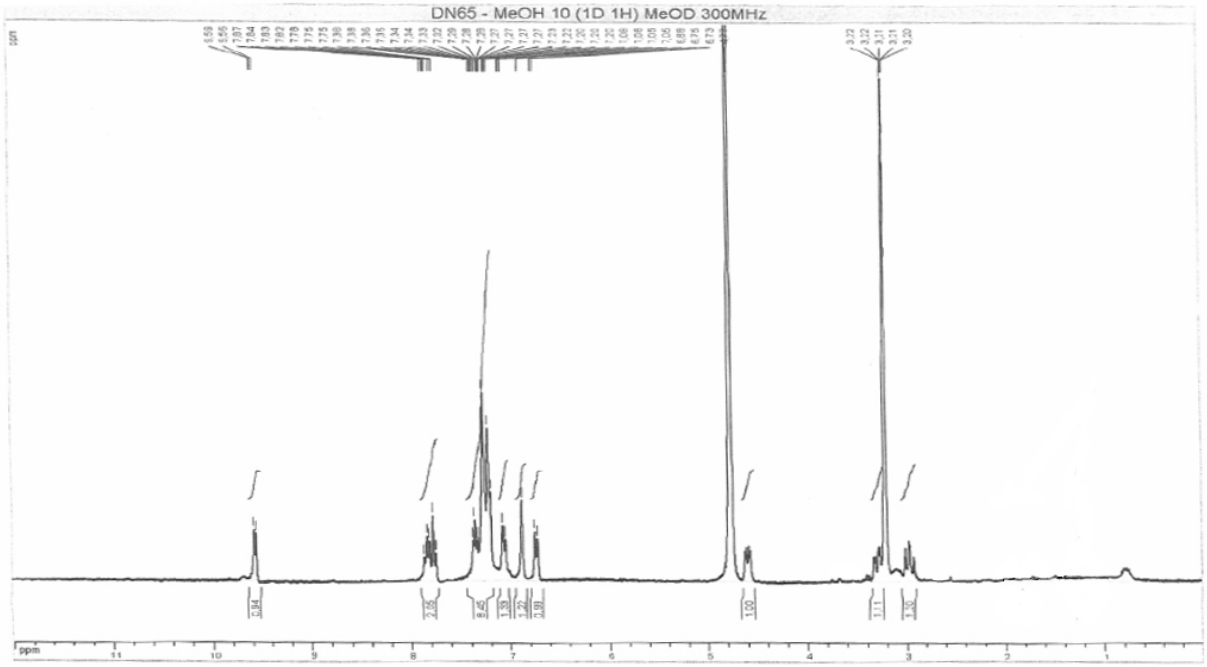

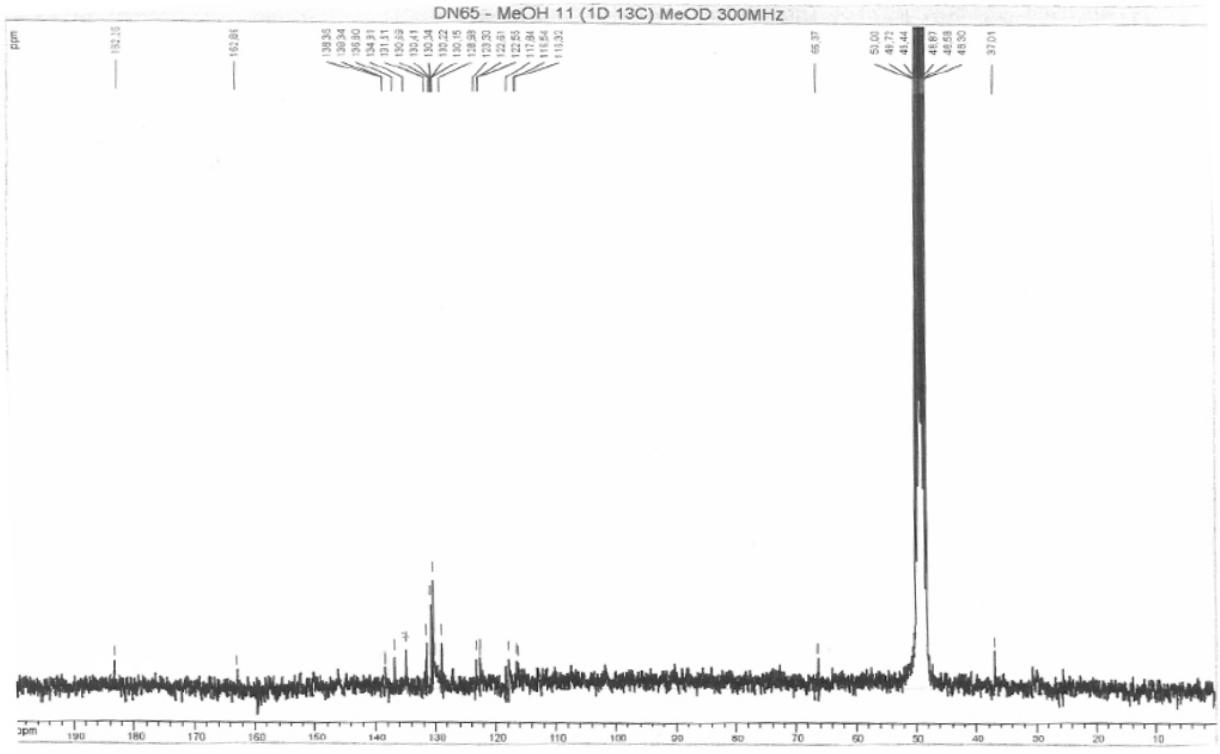

Compound **1z** (DMSO d_6, 300MHz)

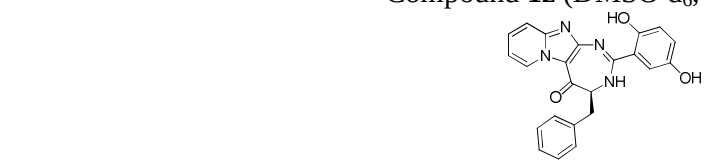

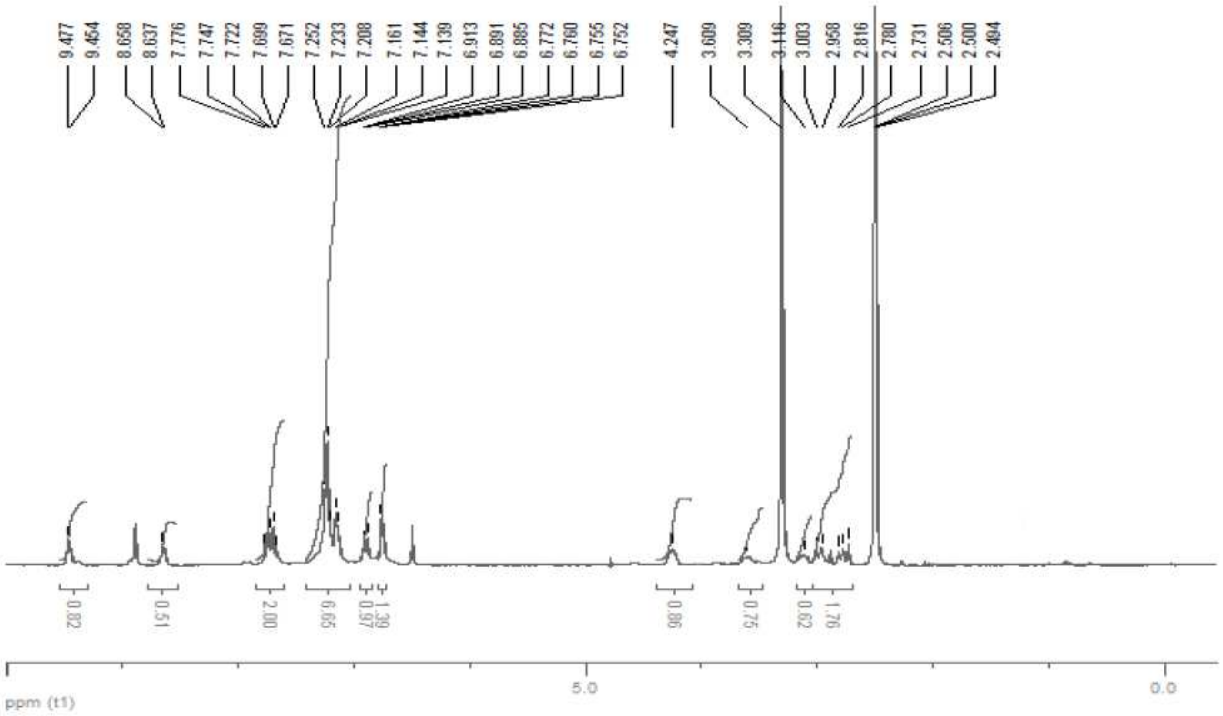

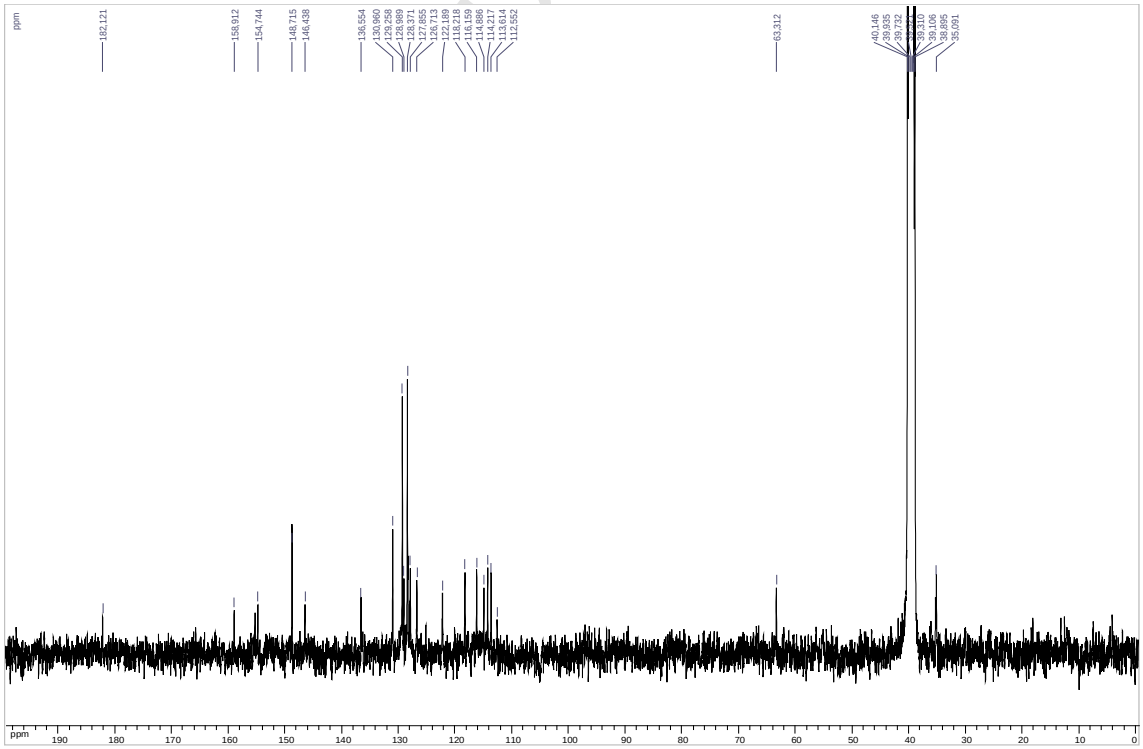

Compound **1ab** (DMSO d_6, 300MHz)

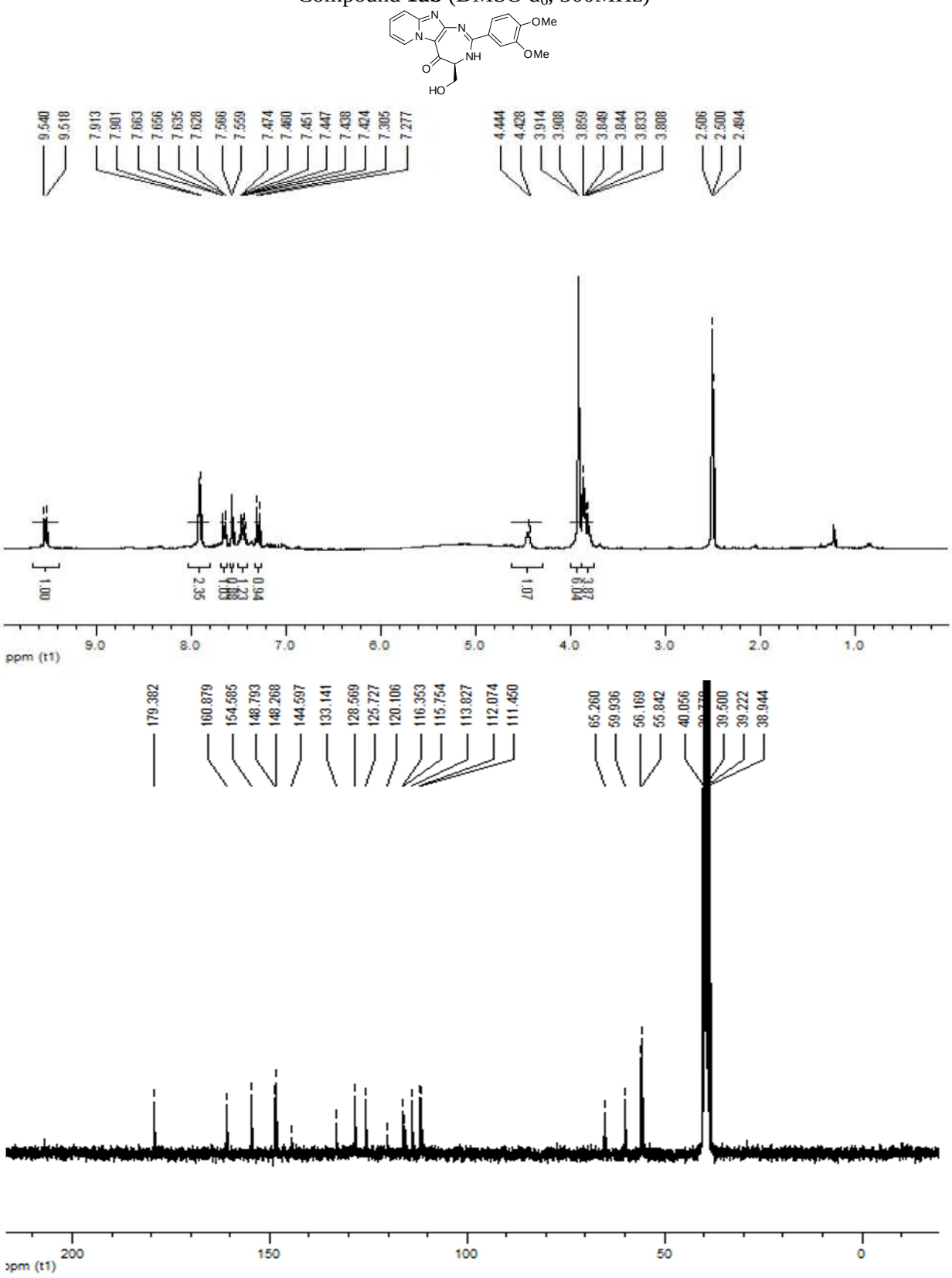

Compound **1ac** (DMSO d_6, 300MHz)

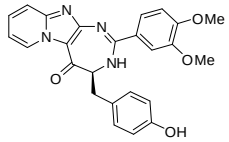

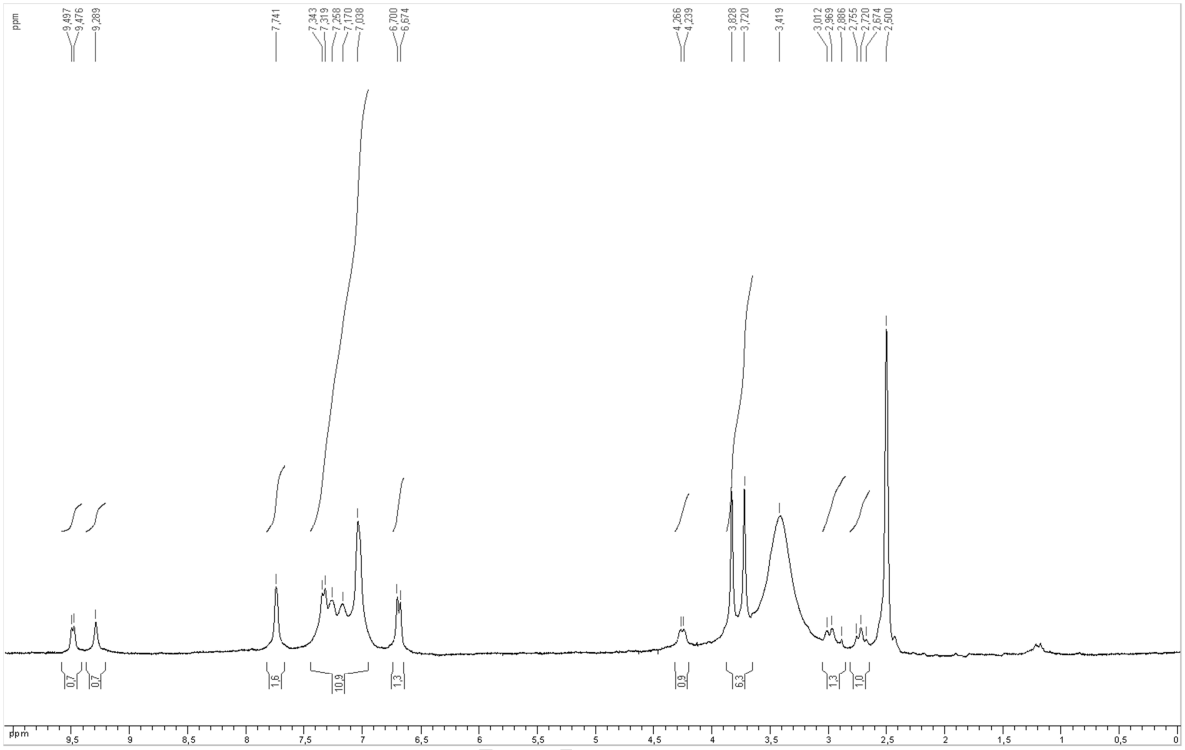

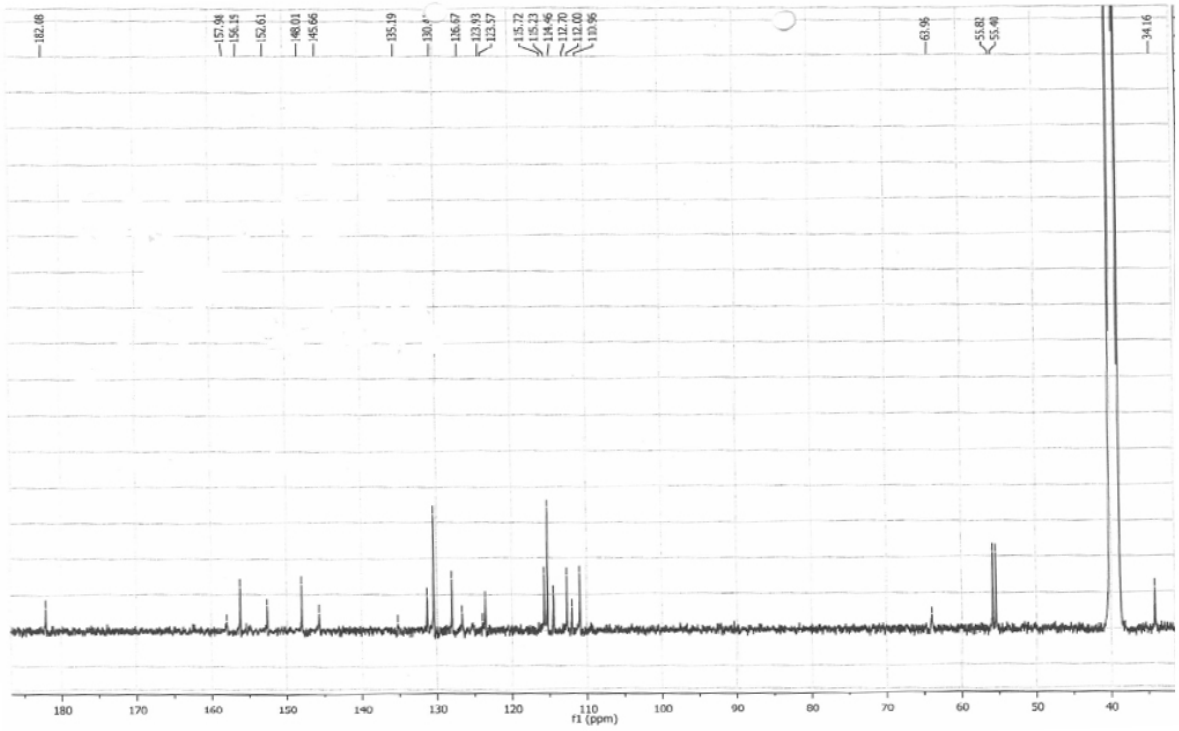

Compound **1ad** (DMSO d_6, 300MHz)

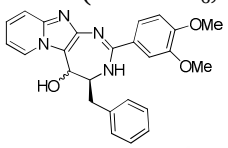

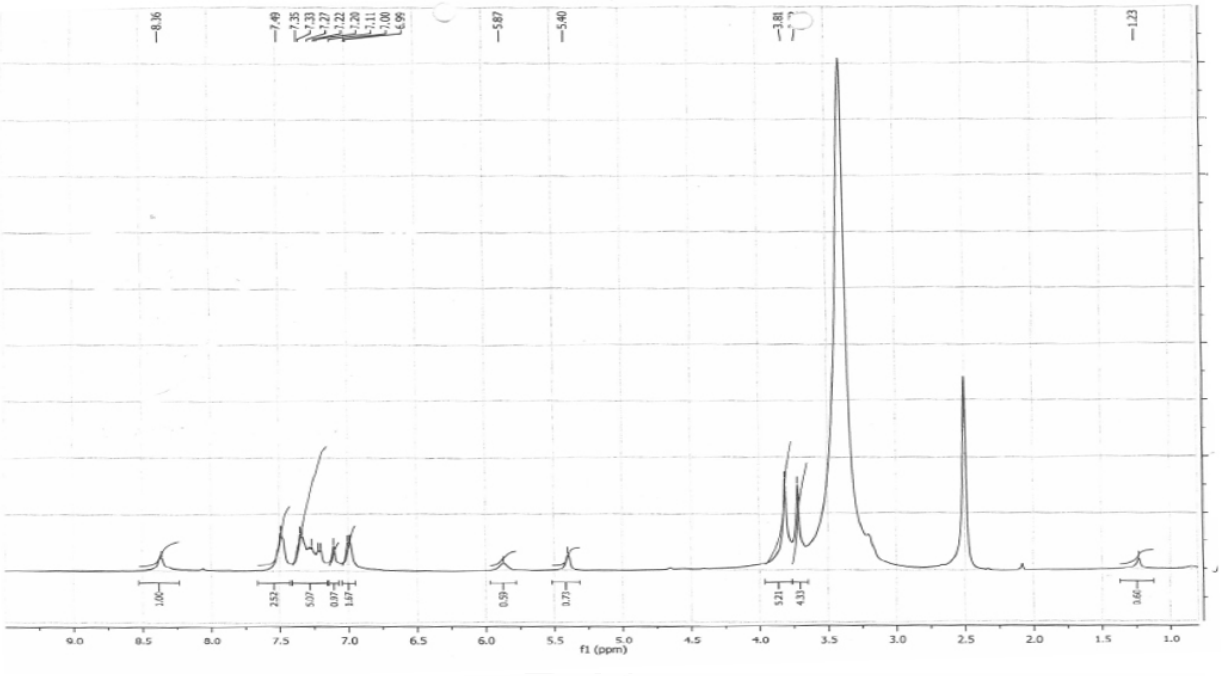

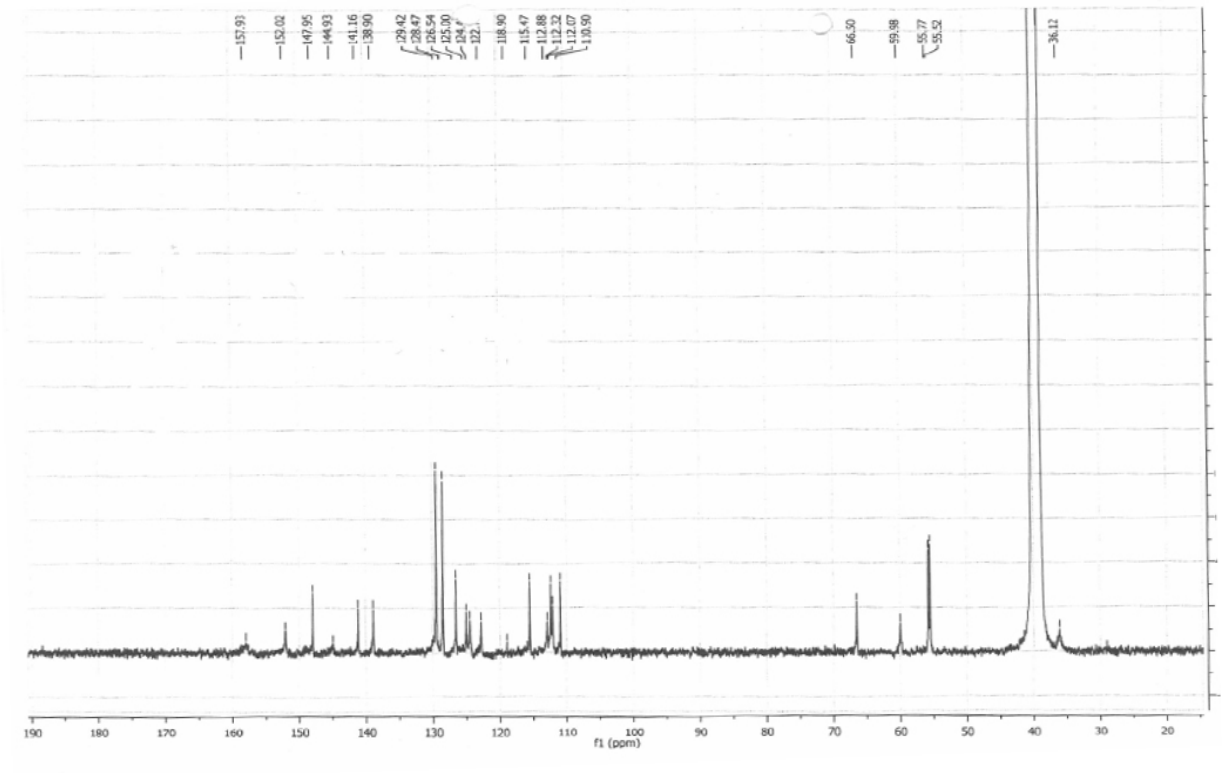

Compound **2a** ($CDCl_3$, 300MHz)

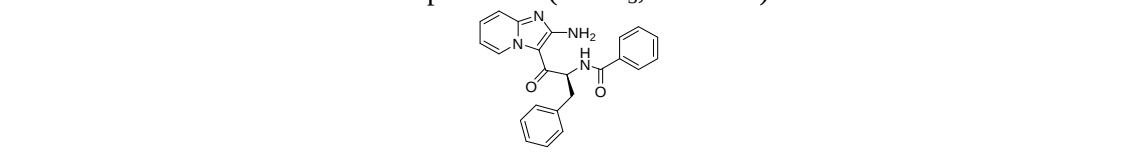

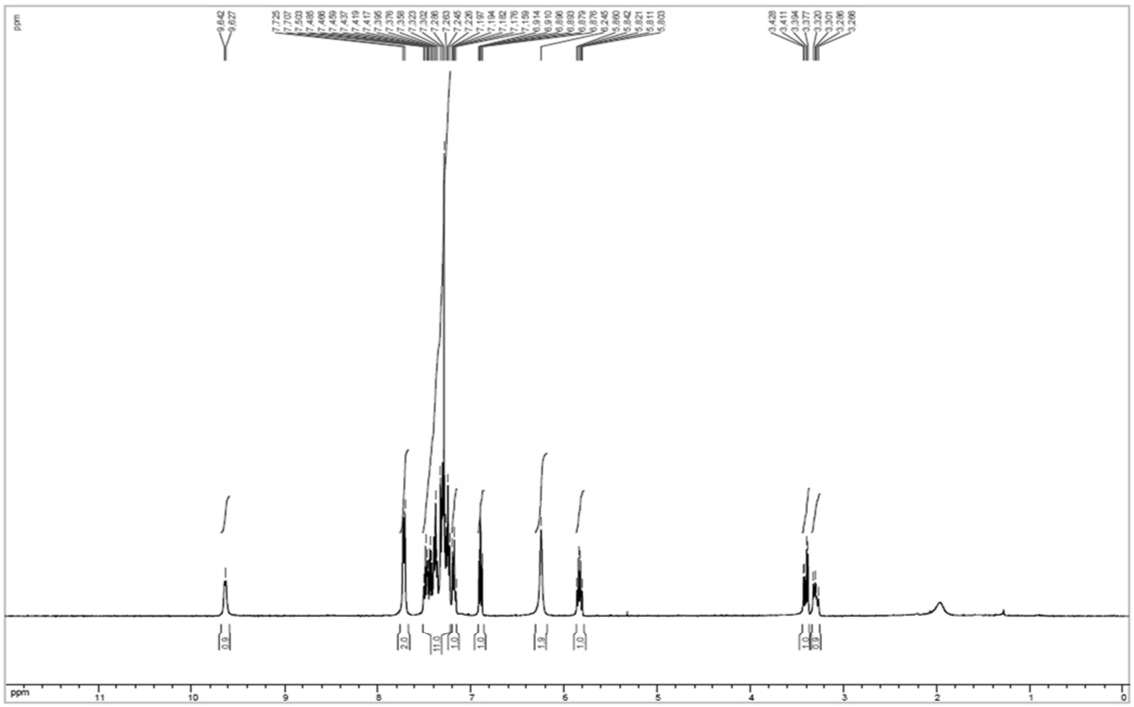

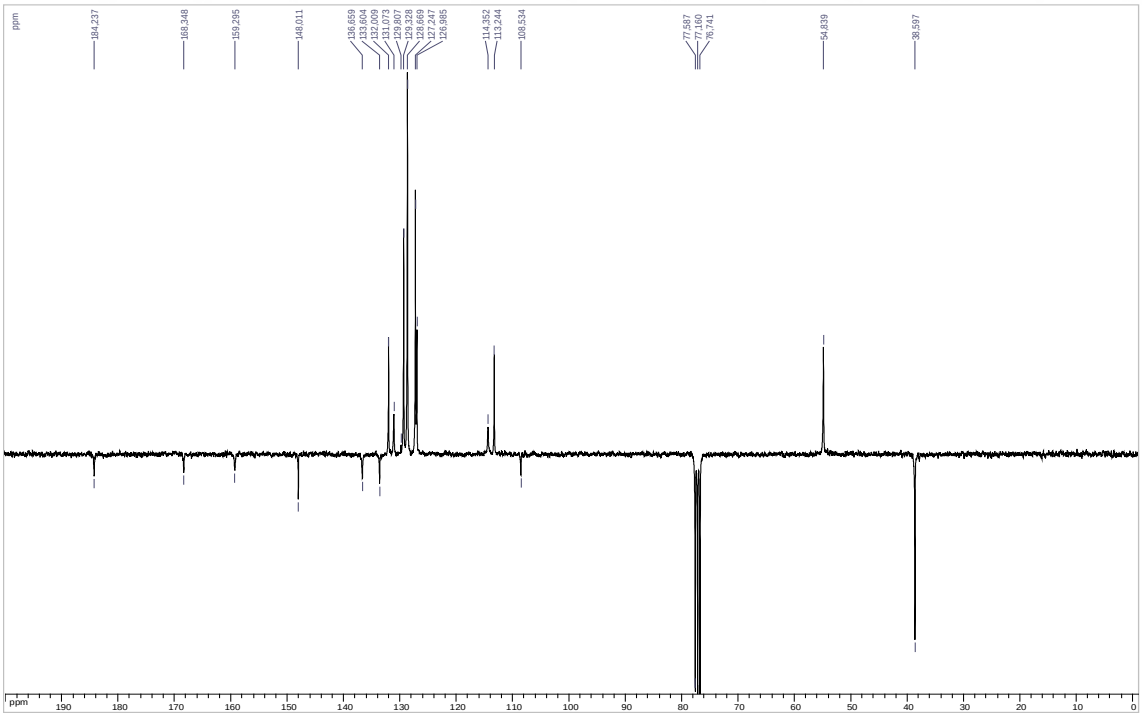

Compound **2b** ($CDCl_3$, 300MHz)

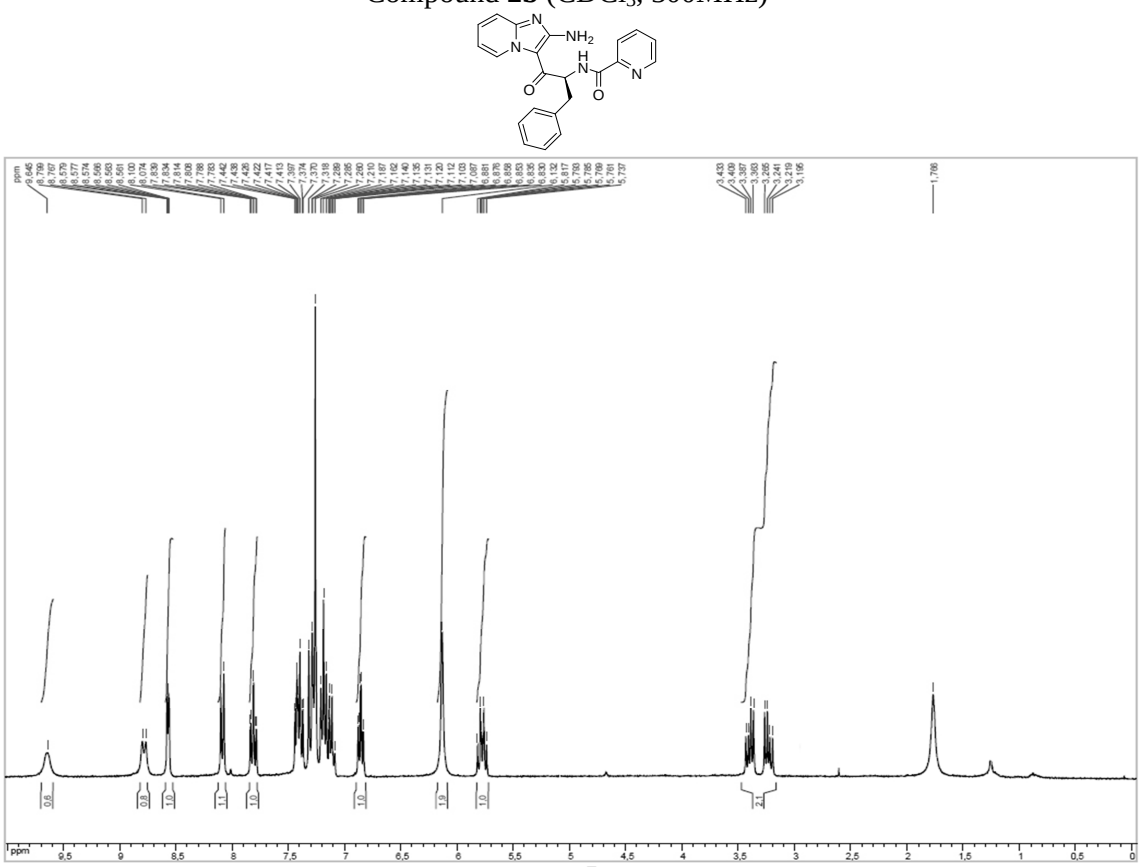

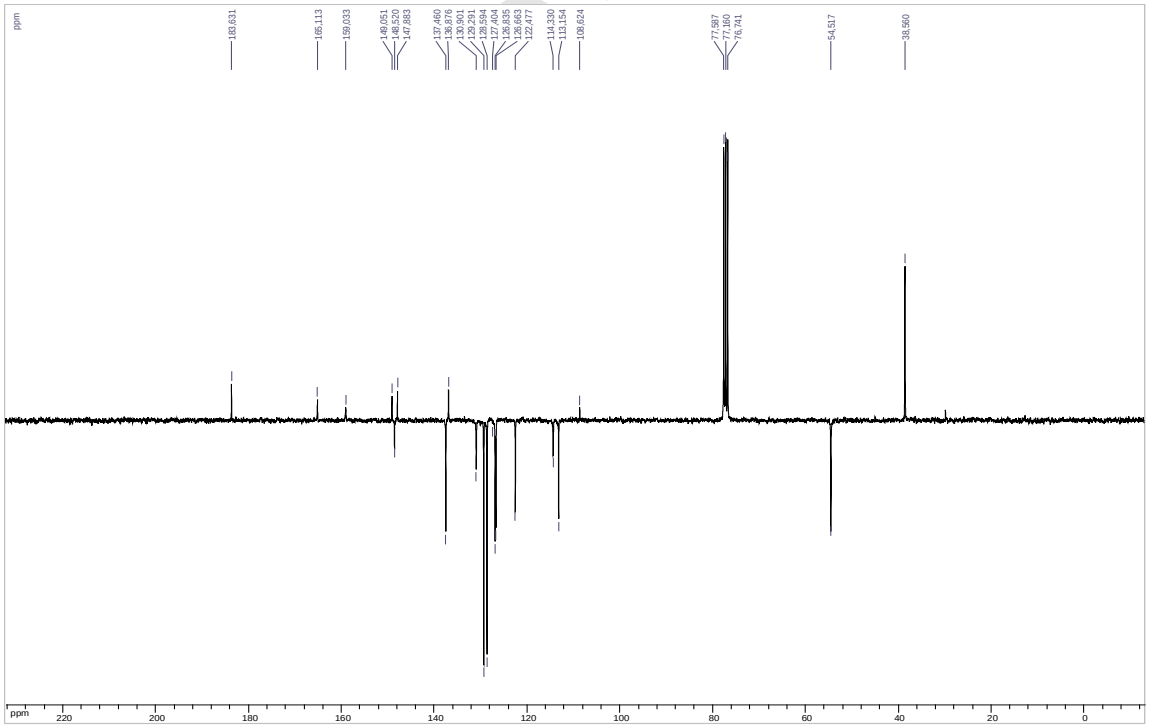

Compound **2c** ($CDCl_3$, 300MHz)

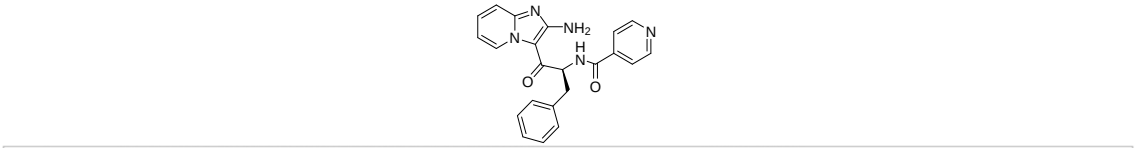

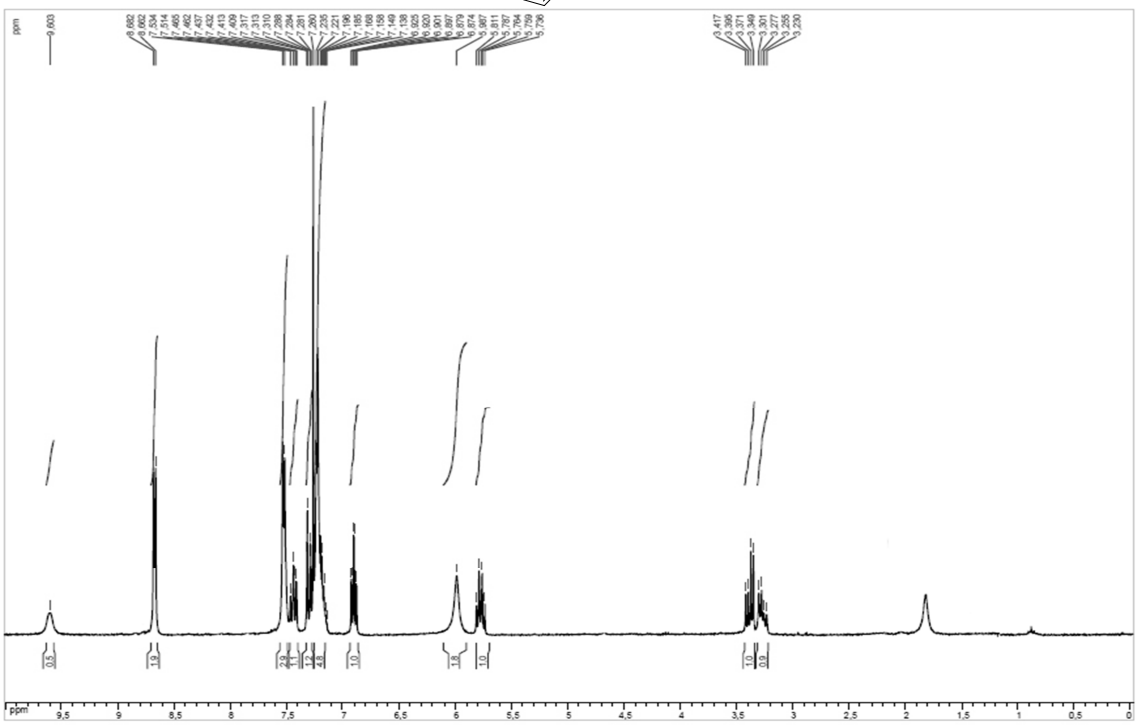

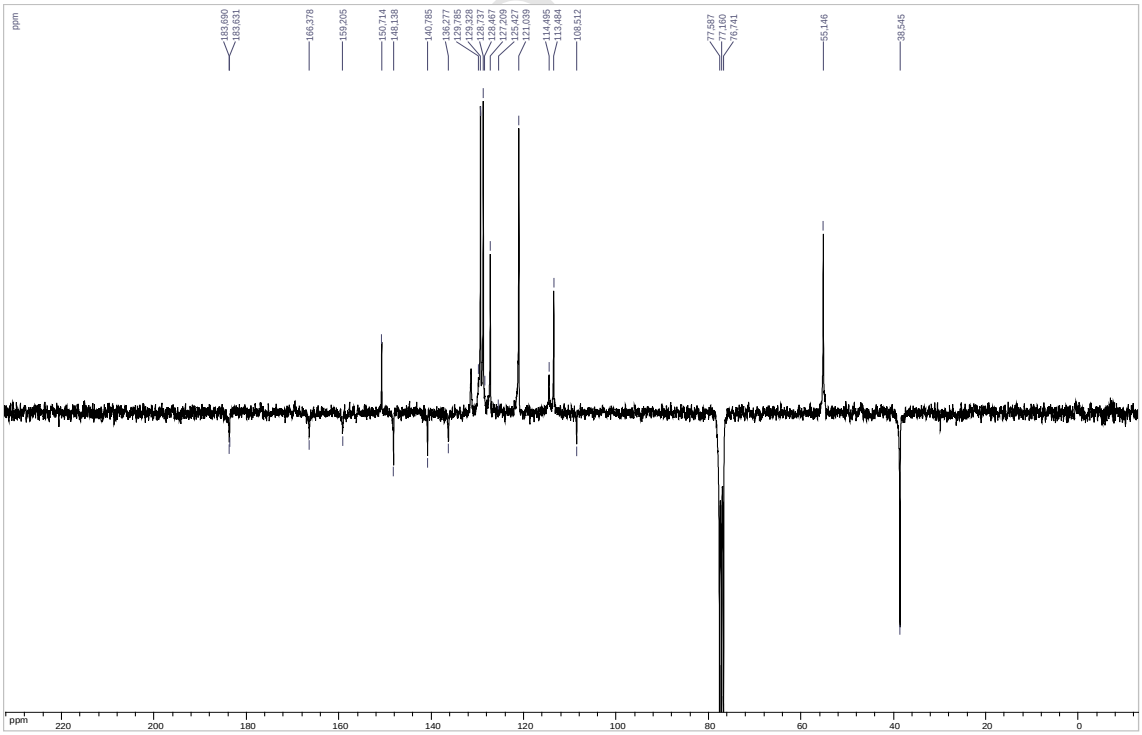

Compound **2d** (DMSO d_6, 300MHz)

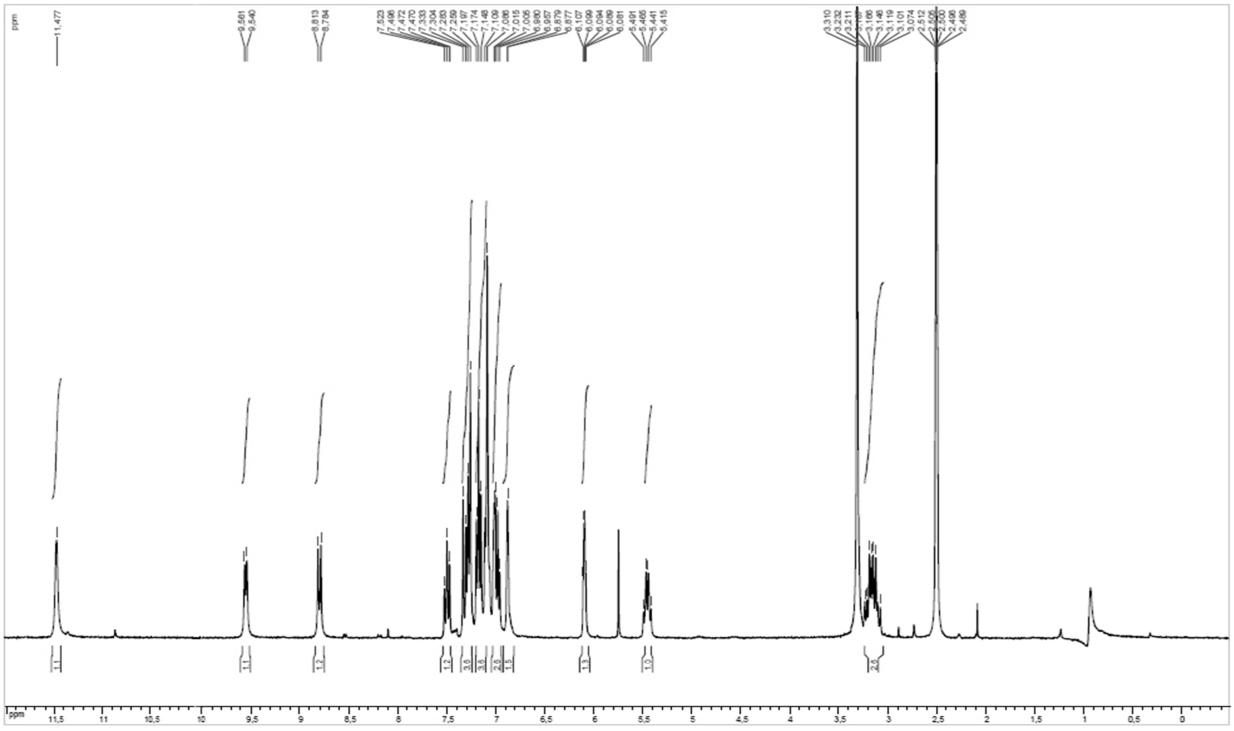

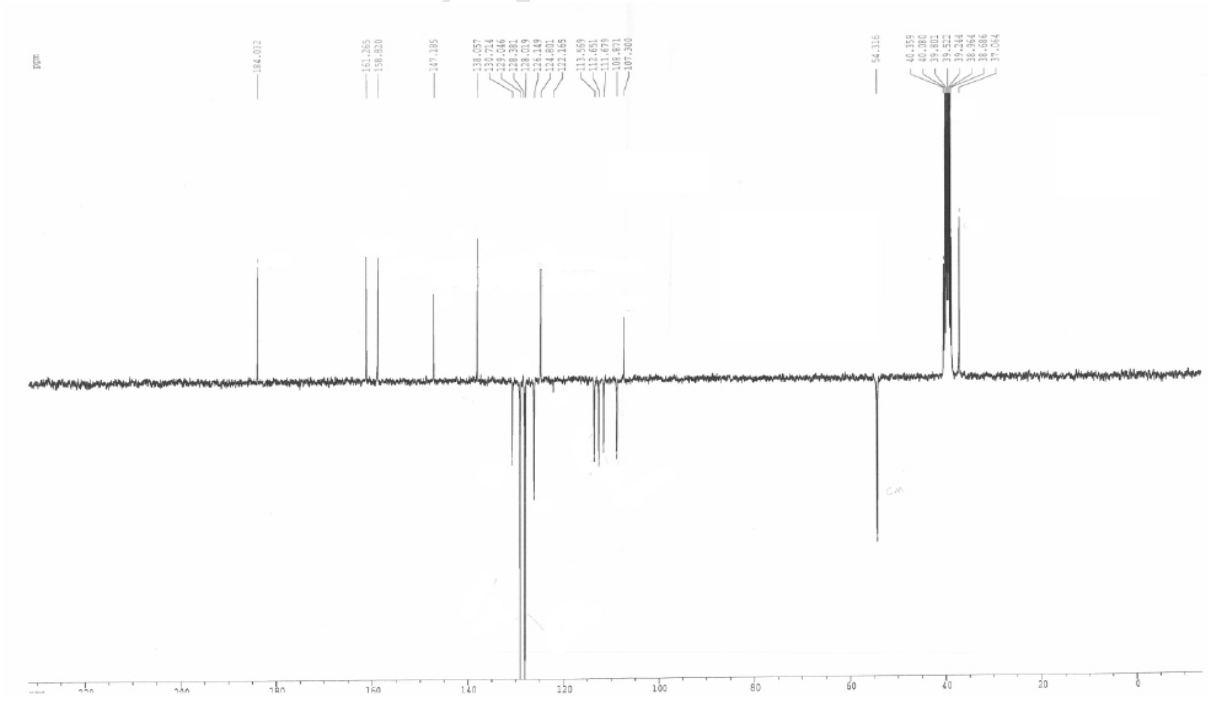

Compound **2e** ($CDCl_3$, 300MHz)

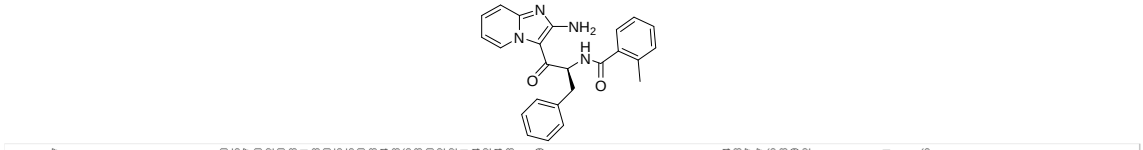

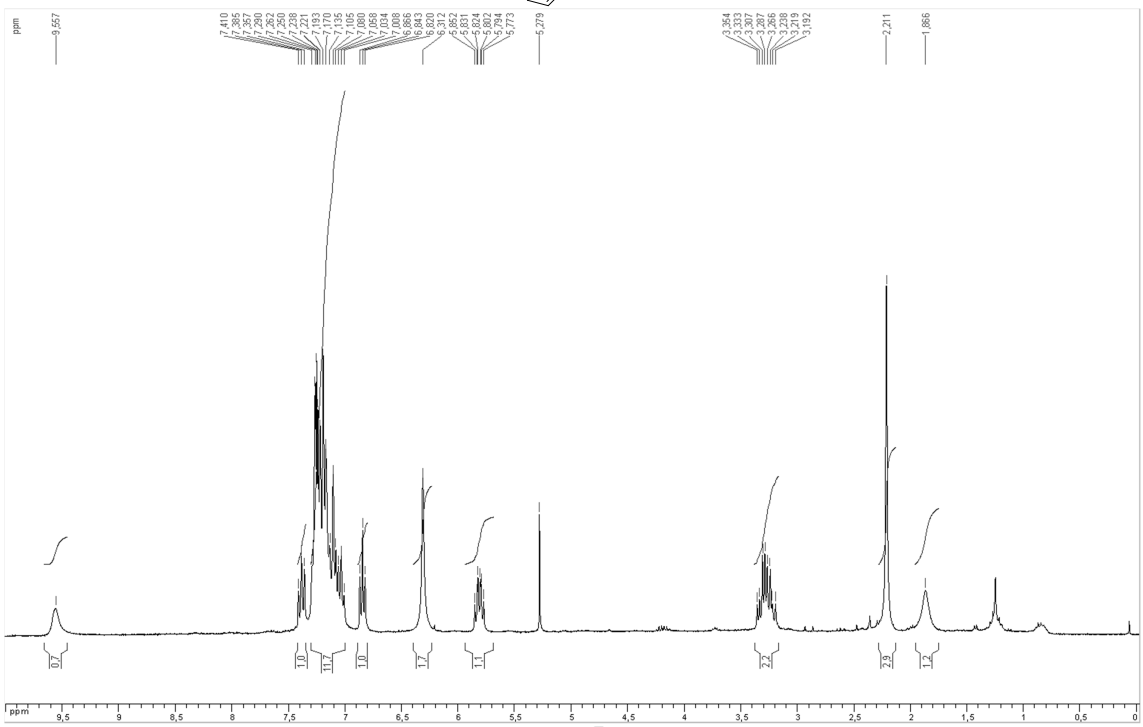

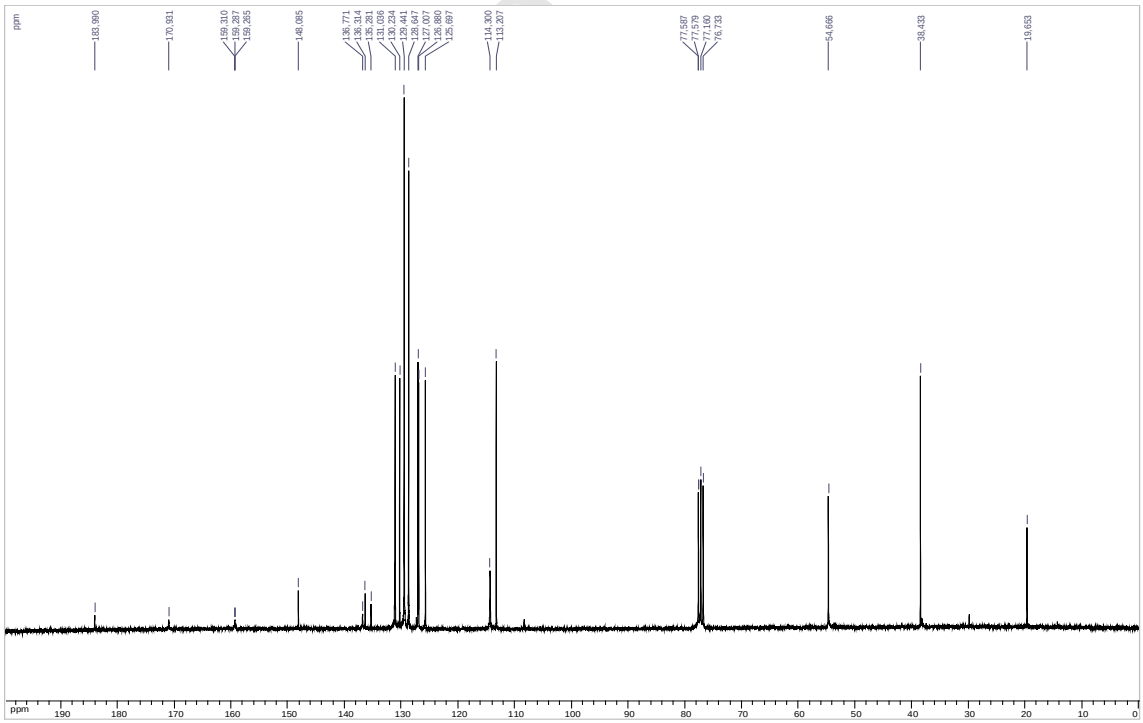

Compound **2f** ($CDCl_3$, 300MHz)

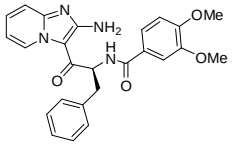

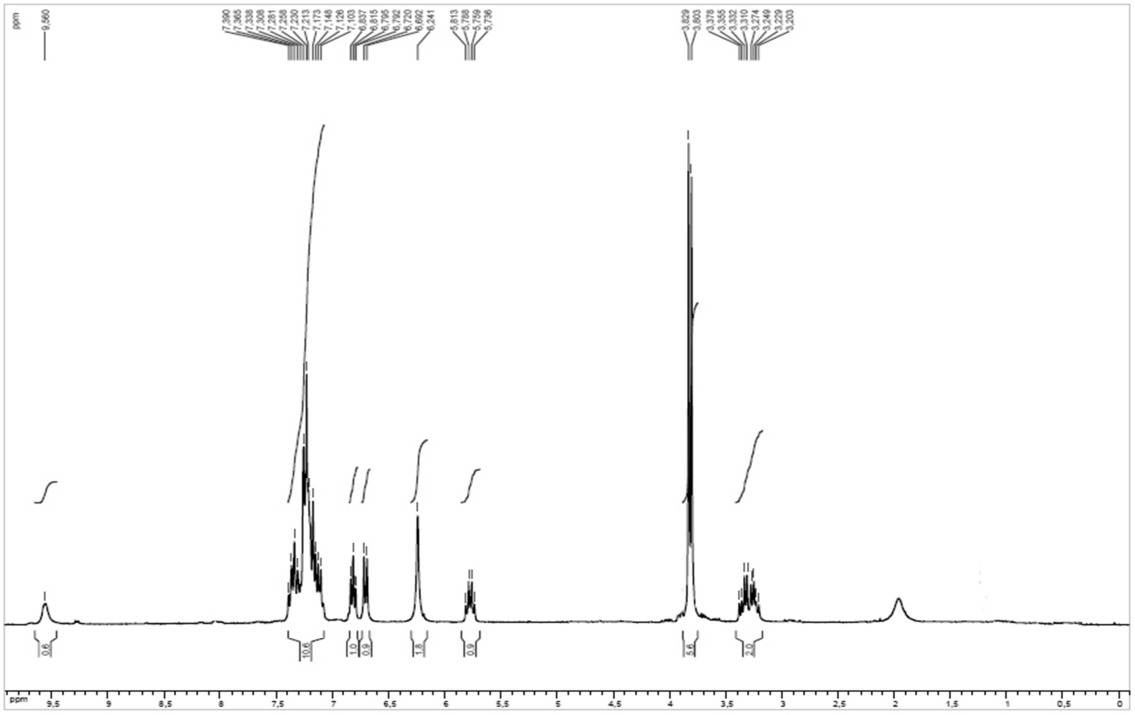

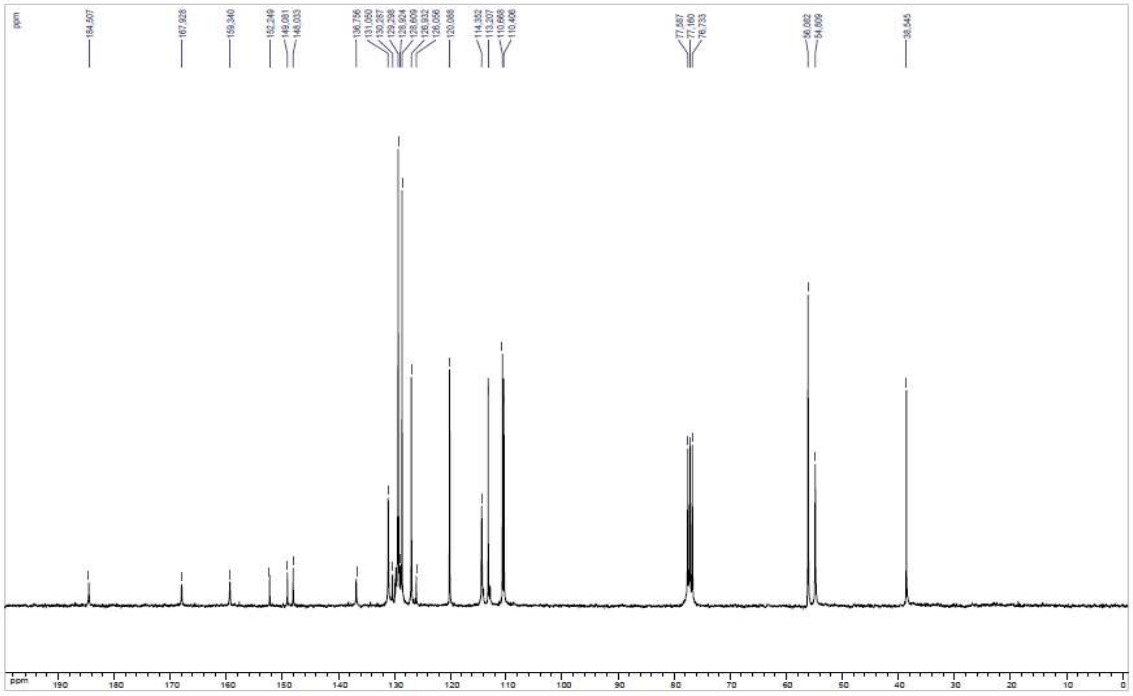

Compound **2g** (DMSO d_6, 300MHz)

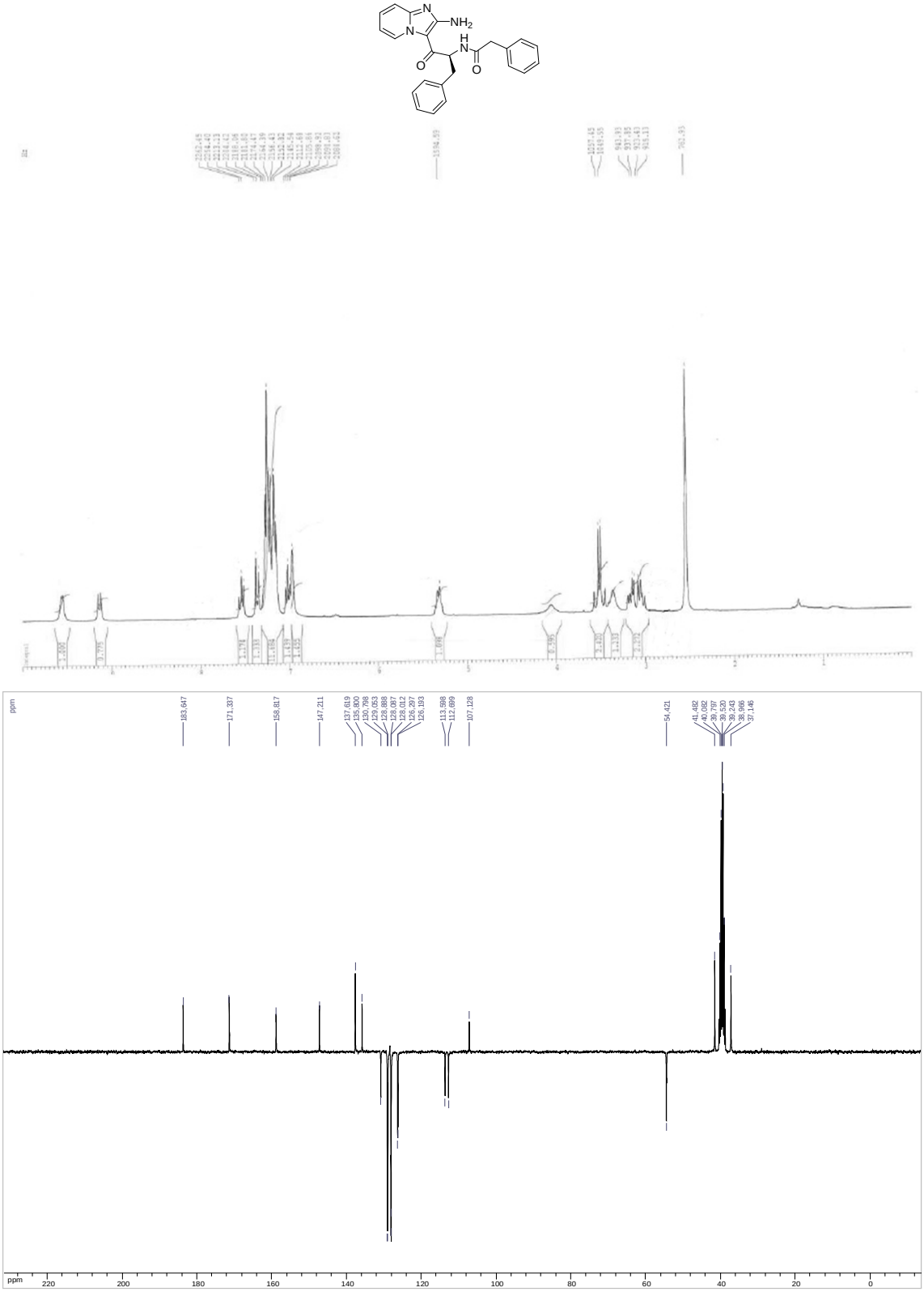

Compound **2h** ($CDCl_3$, 300MHz)

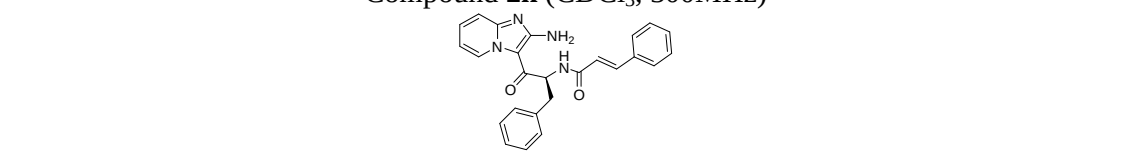

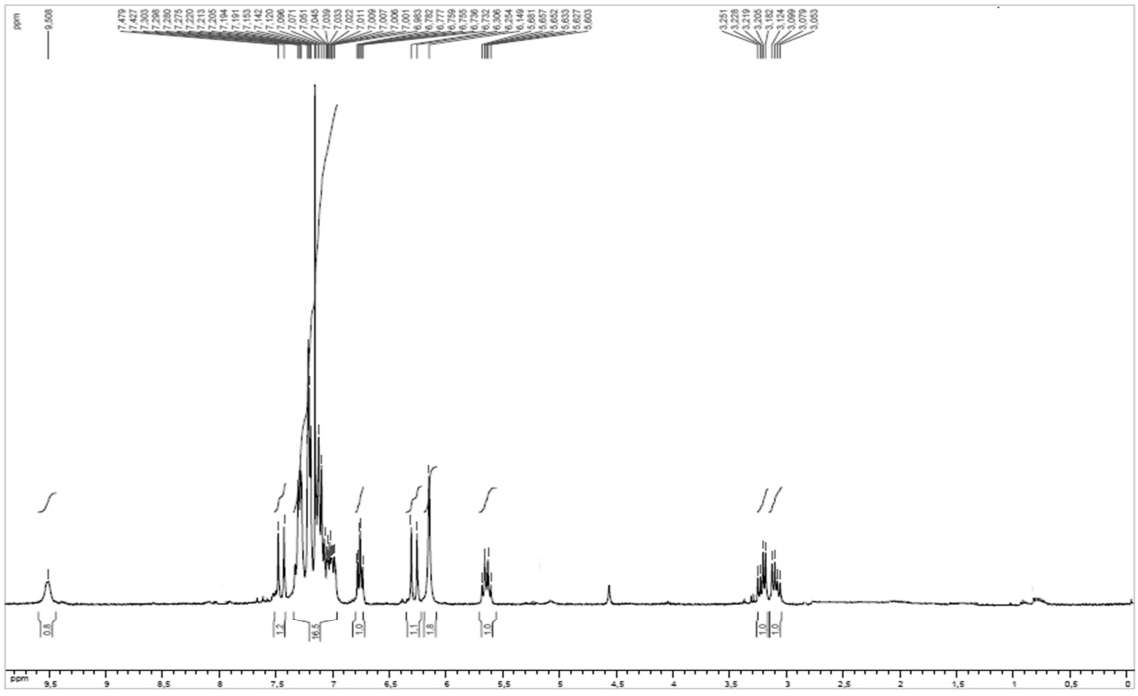

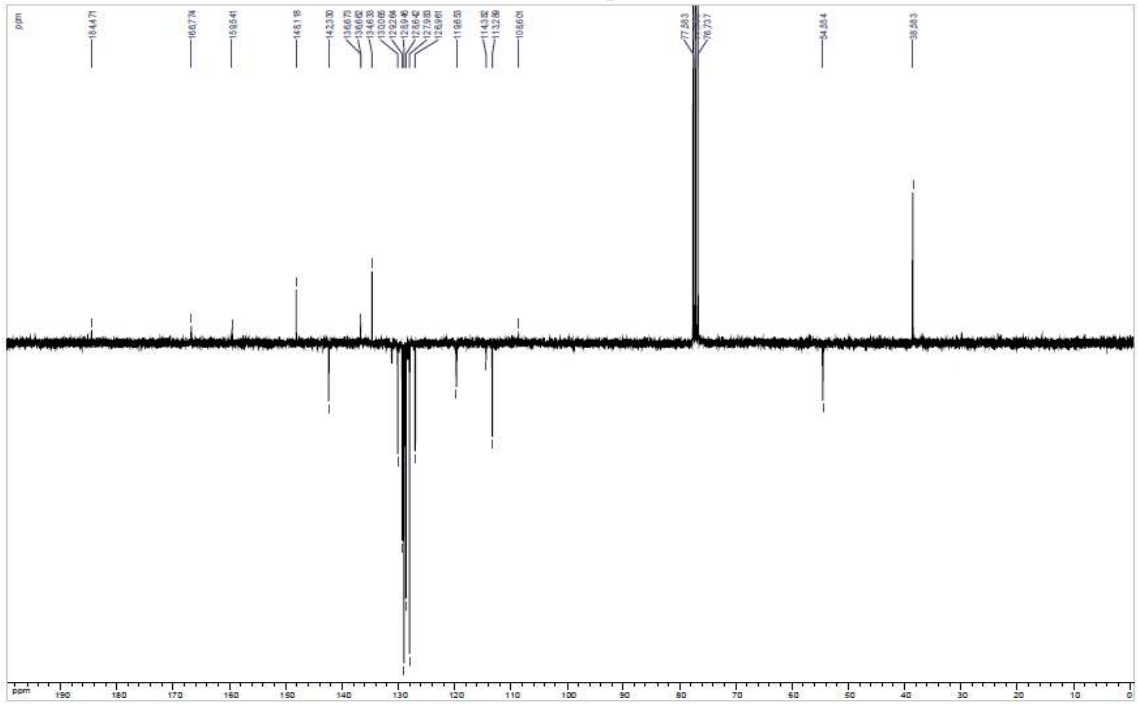

Compound **2i** ($CDCl_3$, 300MHz)